Technical specifications as recommendations for the design of the multi-fingered gripper

Deliverable 2.1

Deliverable Title	D2.1 Technical specifications as recommendations for the design of the multi-fingered gripper
Deliverable Lead:	CEA
Related Work Package:	WP2: Task-oriented dexterous manipulation
Related Task(s):	T2.1: Design guidelines based on human gesture analysis and taxonomy
Author(s):	Mathieu GROSSARD, Florian GOSSELIN, Jonatan ESCORCIA
Dissemination Level:	Public
Due Submission Date:	28/02/2022
Actual Submission:	28/02/2022
Project Number	101017089
Instrument:	Research and innovation action
Start Date of Project:	01.01.2021
Duration:	51 months
Abstract	The work reported in this deliverable aims at providing technical specifications for the to-be-developed gripper needed for the sterility testings.

Horizon 2020

TraceBOT receives funding from the European Union's H2020-EU.2.1.1. INDUSTRIAL LEADERSHIP programme (grant agreement No 101017089)

Versioning and Contribution History

Version	Date	Modified by	Modification reason
v.01	01.02.2022	Mathieu GROSSARD	Initial version of deliverable
v.02			
v.03	10.02.2022	Mathieu GROSSARD	Ready for internal revision
V.04	21.02.2022	Mathieu GROSSARD	Revised version read for submission

Horizon 2020

TraceBOT receives funding from the European Union's H2020-EU.2.1.1. INDUSTRIAL LEADERSHIP programme (grant agreement No 101017089)

Table of Contents

Versioning and Contribution History 2

Table of Contents 3

1 Executive Summary 5

2 Introduction 6

3 Overall human-centered gesture analysis 8

3.1 Overview of the proposed framework 8

3.2 Detailed presentation of the analysis methodology 9

4 Characterization of the use-case manual interaction patterns 13

4.1 Step 1: Identification and classification of manual interaction patterns 14

4.2 Step 02: Definition of hand-objects contact areas 18

4.3 Step 03: identification of the frequency of use of each pattern 23

4.4 Step 04: estimation of the efforts applied on the objects 25

4.5 Step 05: identification of the directions in which each area is solicited 26

5 Generation of interaction maps 27

6 Force-based grasp stability analysis 30

6.1 Theoretical approach for grasp stability 30

6.1.1 Recall about usual SoA contact models 31

6.1.2 Task-oriented grasp quality metric 32

6.2 Framework for grasp study 33

6.2.1 Overall architecture and workflow 33

6.2.2 Considerations about the human hand and object mapping 36

6.2.3 Considerations about external loads 44

6.3 Preliminary results about force human-related considerations 46

6.3.1 Data analysis 46

6.3.2 Recommendations for further analysis 49

6.4 Simplifying the human-inspired kinematics with respect to the task 50

Horizon 2020

TraceBOT receives funding from the European Union's H2020-EU.2.1.1. INDUSTRIAL LEADERSHIP programme (grant agreement No 101017089)

7 Robotic gripper-centered analysis 54

7.1 Design rules for a gripper architecture 54

7.2 Initial gripper configuration 56

7.3 Mapping from human grasps to robotic grasps 58

7.4 Alternative non human-inspired grasp strategies (for grasps requiring a huge amount of forces unavailable for the robotic gripper) 67

7.5 Hypotheses for the final kinematic design of the gripper 69

7.5.1 Palm configuration 1 69

7.5.2 Palm configuration 2 70

7.5.3 Palm configuration 3 71

7.5.4 Range of motion of fingers' phalanges 71

7.5.5 Gripper workspace analysis 73

7.6 Factorization of grasp patterns: from human hand to robotic gripper taxonomy 75

7.7 Replicating grasps for validating the final four-fingered gripper architecture 79

8 Conclusion 83

9 Appendix 86

10 References 90

Horizon 2020

TraceBOT receives funding from the European Union's H2020-EU.2.1.1. INDUSTRIAL LEADERSHIP programme (grant agreement No 101017089)

1 Executive Summary

The work performed in WP2 aims to deliver a multimodal manipulator with a level of complexity in terms of kinematics that is appropriate to the tasks requirements, and with all the actuation and sensing apparatus embedded in the system. The analysis of the existing solutions in the state-of-the-art emphasizes their poor effective dexterity, that is their limited functional capabilities and autonomy in executing operations in a human-oriented environment for life-critical tasks such as assembling and testing medical devices.

In relation with the requirements of the sterility testing use-case of TraceBot, CEA has developed a taxonomy-based human gesture analysis methodology, which aims to provide guidelines and specifications for the to-be-developed system. Key information, such as the large set of manual interactions involved in the sterility testing operations, the most frequently used hand areas or the estimation of the required level of efforts involved when grasping the objects, is deduced from an in-depth analysis of the TraceBot use-case. It serves as a core material in the perspective of designing the multifingered system: some specifications in terms of numbers of fingers, degrees-of-freedom, range of motions, tactile sensors placement, etc., are drawn for the hardware requirements in order it to be specifically tailored for the TraceBot use-case.

The work reported in the current deliverable will serve as a basis for the other tasks in WP2.

Horizon 2020

TraceBOT receives funding from the European Union's H2020-EU.2.1.1. INDUSTRIAL LEADERSHIP programme (grant agreement No 101017089)

2 Introduction

The work reported in this deliverable is intended to provide technical specifications for the to-be-developed gripping system needed for the TraceBot sterility testings. In the perspective of designing a versatile and dexterous gripper that is able to grasp and manipulate the various objects encountered in the use-case, CEA has developed a comprehensive global analysis of its required technical specifications. Such analysis fuses purely human-centered considerations about manual gestures together with theoretical stability tools to qualify each object's grasp as highlighted in TraceBot. Such analysis is based on an in-depth analysis of recorded videos of the use-case, as well as experimental investigations performed in lab environment at CEA.

The lessons learnt from this methodical analysis then help defining the most appropriate application-centered robotic gripper architecture, while guiding future WP2 developments towards an optimal compromise between manipulation capabilities and design complexity.

Briefly, CEA has developed and applied the following four-step task analysis methodology:

1. An in-depth observation and analysis of the human gestures seen in videos of the use-case is first performed in order to identify both typical manual interactions involved in the sterility testing operations, their frequency of use and the amplitude and directions of the efforts applied on the held objects and on the hand.
2. This information is used to compute the frequency of use of each area on the hand of the operator, both normal and tangential to the skin, allowing to quickly identify the most and less frequently used hand areas.
3. This methodology involves a complementary analysis of the grasps from an object-centered point of view, so as to study theoretically the influence of both the hand interaction areas and the required amount of effort on the stability of the grasps of the various objects involved in the use-case.
4. The previously generated data leads finally to the synthesis of a proposed gripper architecture (kinematics, required tactile sensors instrumentation, together with a theoretical estimation of the required amount of effort to be produced by the actuation system).

This work will serve as a basis for the other tasks in WP2. Its outputs will be extensively used by CEA as guidelines in an effort to promote an optimal compromise between manipulation capabilities and design complexity.

Horizon 2020

TraceBOT receives funding from the European Union's H2020-EU.2.1.1. INDUSTRIAL LEADERSHIP programme (grant agreement No 101017089)

The deliverable is organized as follows. In section 3, the overall human-centered analysis method as developed and applied by CEA is described. In section 4, we focus on the observation of the large set of manual interactions involved in the use-case and on the gathering of complete information about them (type of manual interaction patterns, associated hand areas, frequencies of use, effort on the held objects, direction of the efforts on the hand) (1). In section 5, we present how we use this information to obtain directional manual interaction maps (2). Such maps inform the designer on the most used hand areas, where tactile sensors are the most useful, and on the less used areas that do not deserve to be reproduced in a robotic gripper if one wants to simplify its design. In section 6, a focus on the developed force-based stability analysis methodology (3) is detailed. Such object-centered grasp analysis tool accounts for the mechanical ability of the contacts to hold still the TraceBot objects, while facing the external perturbations imposed by the use-case. In other words, this study brings a complementary approach on the forces that need to be guaranteed by the hand to ensure a stable grip of the various objects. Then section 7 is devoted to the proposition of design guidelines for the to-be-developed robotic gripper, with a focus on the study of a grid allowing to anticipate gripper's capabilities and versatility as a function of its design complexity (4). It relies on previous data coming from the pure human-centered analysis (2) together with theoretical estimated level of forces (3). Technical specifications, such as the appropriate number of gripper-objects interaction areas, the number of required degrees-of-freedoms (to interact naturally with objects such as canisters, flexible tubings, etc.), the needed workspace (reached by the fingers with respect to the palm) and the force capability, as well as the required area of interest for embedding tactile sensors into the gripper, are investigated. Finally, technical specifications as recommendations for the design of the multifingered gripper are summarized in the conclusion.

Horizon 2020

TraceBOT receives funding from the European Union's H2020-EU.2.1.1. INDUSTRIAL LEADERSHIP programme (grant agreement No 101017089)

3 Overall human-centered gesture analysis

3.1 Overview of the proposed framework

The analysis method presented in this deliverable follows a multi-step process as shown on Figure 3.1. While some steps focus on a pure human-centered point of view and rely on a methodic identification and analysis of the grasp types and manual interaction patterns observed when considering a set of tasks performed by a human operator[1], other steps provide complementary information on the forces applied on the hand obtained from the use of theoretical grasp analysis tools usually employed in robotics. Thus, the overall methodology presented hereafter is completely original with respect to the state-of-the-art relating to the field of taxonomy-based design of multi-fingered grippers.

The principle is the following: we first look at use-case videos to identify the objects of interest and the grasps and interactions patterns used by human operators. We also note their durations. Then we draw regions on the surface of the hand representing the contact areas associated with the interaction patterns. Finally, we identify the directions in which efforts are applied on these areas, based on considerations on the objects the operator is manipulating and the efforts applied on those objects.

This information is exploited in two ways:

- First, the interaction surfaces are weighted by their frequencies of use and displayed on maps that allow to quickly isolate the hand areas that are most frequently used in the different directions, given a certain set of tasks. This information is valuable both for guiding the integration of tactile sensors where they are the most useful and for guiding potential simplifications of the robotic gripper kinematics regarding the less used areas.
- Second, the grasp types and forces applied on the objects are used to estimate the forces that have to be applied on the different hand-objects interaction surfaces to guaranty stable grasps. These computations are performed considering both human-like grasps inspired by the operator, and simplified grasps suggested by the interaction maps' most and less used areas.

[1] The first steps are partly inspired by the work presented in [Gonzalez et al. 2013] [Gonzalez et al. 2014] and [Chabrier et al. 2015] which focused on hand exoskeleton design. However, they are used in a completely different way for the case of gripper design, for which several analysis steps have been removed in favour of new task- and robotics-oriented steps.

Horizon 2020

TraceBOT receives funding from the European Union's H2020-EU.2.1.1. INDUSTRIAL LEADERSHIP programme (grant agreement No 101017089)

The goal is to estimate both the maximum number of grasps and the amount of force required on each finger as a function of the number and position of the contacts between the dexterous robotic gripper and the manipulated objects. This methodology informs the designer on the available grips given a set of contact surfaces and forces that can be controlled. In other words, it gives an indication on the versatility of the device as a function of the gripper complexity. This methodology allows to maximize the theoretical compromise between grasping and manipulation capabilities and design complexity (thus cost).

The last step consists in comparing these theoretical results with the real capabilities of different robotic gripper designs. Therefore, we consider candidate preliminary CAD designs inspired by the results of our analysis and test whether they can reproduce the recommended simplified grasps. This last step further allows some simplification and factorization of the grasps, as well as alternative strategies proposed to decrease the required amount of force.

3.2 Detailed presentation of the analysis methodology

As shown on Figure 3.1, nine successive steps (some being themselves composed of several substeps, see below) are required to analyze the way humans perform dexterous tasks and how a robotic gripper could reproduce them at best:

1. We first look at videos from the use-case in order to identify the grasps and interaction patterns used to perform the associated tasks. These gestures are classified as either canonical grasps and interaction patterns found in common existing taxonomies [Cutkosky 1989] [Feix et al. 2009] [Jones and Lederman 2006] [Lederman and Klatzky 2009] or as use-case specific grasps.
2. Each interaction pattern is then associated with a specific contact area on the hand, and those areas are superimposed in order to split the hand in elementary contact areas.
3. Each interaction pattern is also associated with a frequency of use, as first proposed in [Zheng et al. 2001] for housework requiring mostly power grasps and rough manipulation and for shop floor work emphasizing more precise tasks and fine manipulation and extended in [Gonzalez et al. 2014] to blind exploration. These frequencies of use are reported on all the elementary areas the interaction patterns are composed of objects' properties.
4. The previous information is complemented with additional data including the objects' weight, as well as the external forces they are submitted to during the completion of the use-case.

Horizon 2020

TraceBOT receives funding from the European Union's H2020-EU.2.1.1. INDUSTRIAL LEADERSHIP programme (grant agreement No 101017089)

5. The collected data is also used to identify the directions in which forces are applied on each elementary contact area involved in the interaction patterns.
6. By combining the solicitations associated with each interaction pattern on each elementary area, we get interaction maps showing the percentage of time each elementary contact area on the hand is solicited when performing the tasks involved in the use-case. This information is very valuable for guiding the integration of tactile sensors where they are the most useful. It can also be used to identify the less used areas that do not deserve to be reproduced in a robotic gripper as they would make the design much more complex without high gain in terms of possible grasps. In other terms, it can be used for guiding potential simplifications of a robotic gripper's kinematics regarding the less used areas.
7. Then we use a model of the grasps coming from the robotics literature to compute the forces that need to be applied on the different hand areas to hold stably the objects involved in the use-case. Therefore, we use the objects' CAD and mesh models and reproduce at best the number and location of contact points as observed in the previously identified grasp patterns. We further make use of theoretical tools relative to grasp stability framework to quantify the required amount of efforts at each elementary area.
8. These tools are further used to study the influence of the shift from a purely human-like hand to the simplified designs suggested by the interaction maps. This study allows to compare the efforts required when a simpler design is chosen, typically with a fewer number of fingers, or with less phalanges involved.
9. The last step consists in trying to reproduce the use-case grasps using gripper designs inspired from the previous simplification hypotheses. After an analysis of the grasping of the different objects, some simplifications and factorizations are proposed in order to reduce the library of proposed robotics grasps, and the ability of the proposed designs to perform those grasps is verified.

These different steps can be grouped into five categories detailed in the next sections. Steps 1 to 5 cover a comprehensive collection of information on the use-case, as performed by an expert human operator. Step 6 consists in a statistical analysis of the use of the different hand areas. Steps 7 and 8 give additional information on the forces required to grasp the objects. Finally, step 9 allows to verify the feasibility of the grasps with a robotic gripper derived from previous analysis.

Horizon 2020

TraceBOT receives funding from the European Union's H2020-EU.2.1.1. INDUSTRIAL LEADERSHIP programme (grant agreement No 101017089)

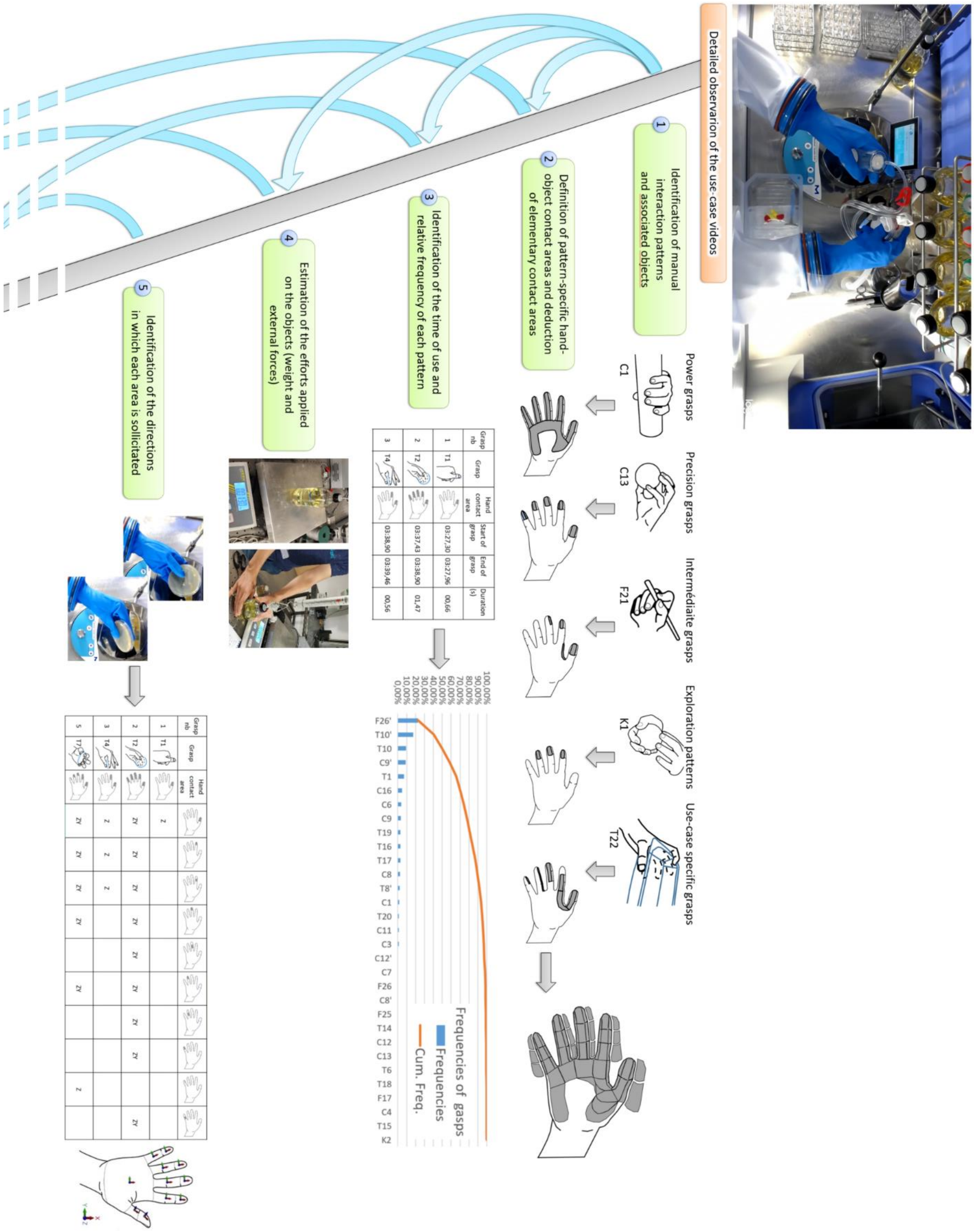

(a) Steps 1-5

Horizon 2020

TraceBOT receives funding from the European Union's H2020-EU.2.1.1. INDUSTRIAL LEADERSHIP programme (grant agreement No 101017089)

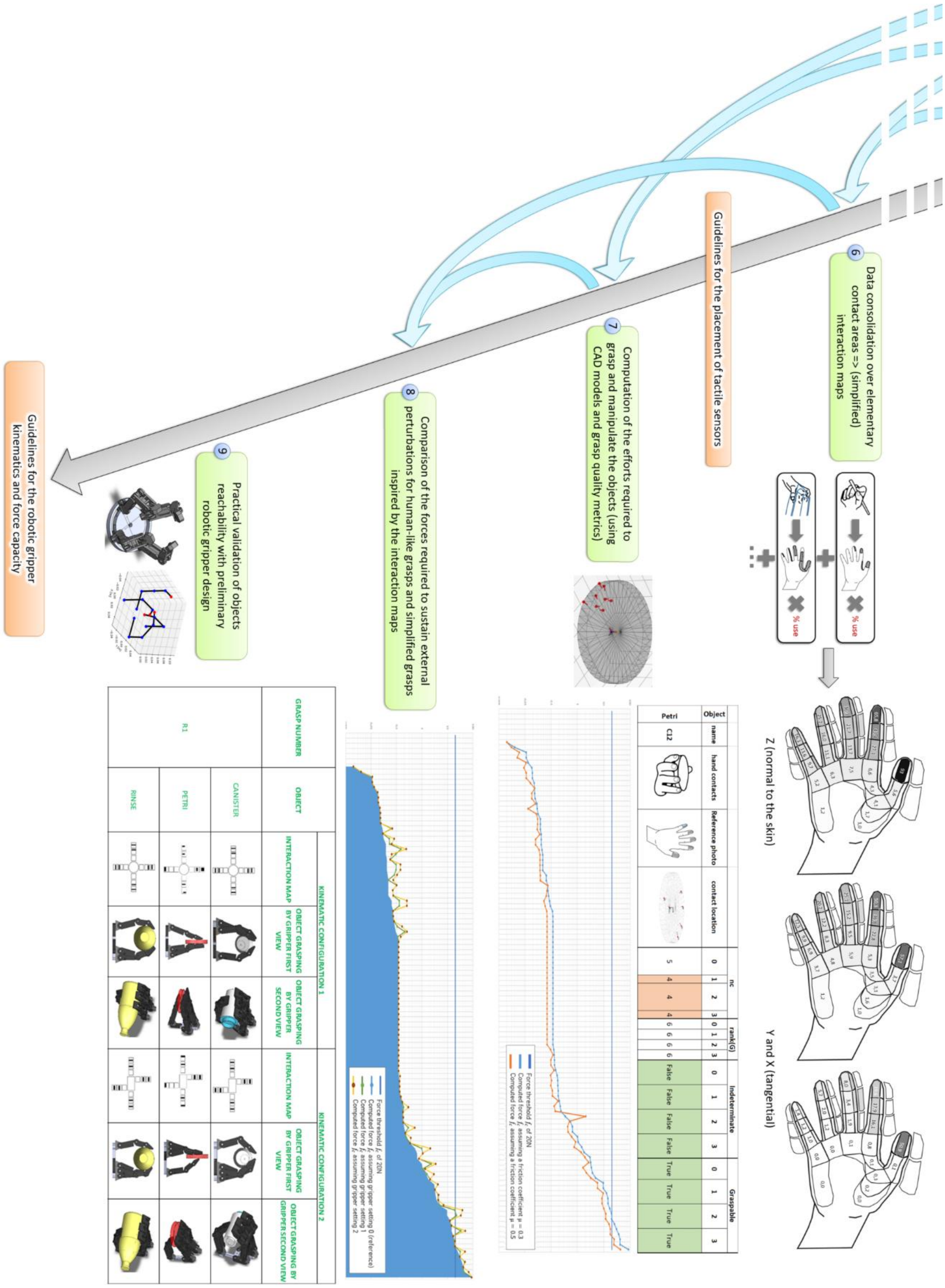

(b) Steps 6-9

Figure 3.1: Human-centered gesture analysis methodology.

Horizon 2020

TraceBOT receives funding from the European Union's H2020-EU.2.1.1. INDUSTRIAL LEADERSHIP programme (grant agreement No 101017089)

4 Characterization of the use-case manual interaction patterns

The characterization of the manual interaction patterns involved in the use-case is based on an analysis of the 15 videos provided by INVITE. These videos show the use of a Steritest pump in a glove box. Each video was edited with the Windows video editor, allowing to play it frame by frame. The aim of this review, performed by several people as proposed in [Zheng et al., 2011] in order to double validate all information, is to identify the successive grasps used by the operator, and for each grasp to record in an Excel sheet the following information:

- The current grasp, which can be a usual grasp as found in the Cutkosky's and Feix et al.'s taxonomies, a canonical exploration gesture as found in Lederman and Klatzky's reference article, or a TraceBot specific interaction pattern. The grasps are named C_i (for Cutkosky), F_i (for Feix), K_i (for Klatzky) or T_i (for TraceBot) according to the category they belong to (the latter are named according to their order of appearance, considering both left and right hands);
- The hand that performed the grasp (L or R, of L+R if both hands are used);
- Its start time and end time, allowing to determine its duration;
- The object being manipulated;
- The type of the grasp: static, regrasping or manipulation.

As shown in Figure 4.1, additional information are reported in the tables:

- A picture of the grasp;
- A picture of the hand-object contact area;
- The name of the video the grasp belongs to;
- The name of the associated atomic task, as proposed by the project's partners.

Grasp number	Start of the grasp	End of grasp	Dura-tion (s)	Grasps		Hand contact area	Hand	Object	Original Video	Recut Video	Static / manipulation	Atomic task	Task categorie
17	00:00,00	00:01,40	01,40	T26			L	Canister	4 : Fit Canister to drain	03 : Kit mounting	Regrasping avec suivant	move canister over drain	install canister
18	00:01,40	00:03,80	02,40	T2			L	Canister	4 : Fit Canister to drain	03 : Kit mounting	In-hand manipulation	Insert canister into drain	install canister
19	00:04,23	00:04,73	00,50	T28			L	Tube	4 : Fit Canister to drain	3 : Kit mounting	Static	grab tube	install canister

Figure 4.1: information gathered during the analysis of the use-case videos (left hand, a similar analysis is made for the right hand).

Horizon 2020

TraceBOT receives funding from the European Union's H2020-EU.2.1.1. INDUSTRIAL LEADERSHIP programme (grant agreement No 101017089)

4.1 Step 1: Identification and classification of manual interaction patterns

As previously mentioned, human grasps are traditionally organized in taxonomies. The most commonly used is the one proposed by Cutkosky [Cutkosky 1989], which is widely used for robotic and prosthetic hands designs. This taxonomy depicts 16 different patterns using task dexterity and precision as discriminants. Some usual grasps as e.g. holding a pen are however missing in this classification. Feix et al. proposed a more complete grid which includes intermediate grasps and is designed with respect to the posture of the hand [Feix et al. 2009]. The combined taxonomy obtained when merging both authors' work is displayed below. Each pattern is called C_i (with $i \in [1;16]$) or F_j (with $j \in [17;34]$) whether it is part of the Cutkosky or Feix et al. taxonomy respectively. This classification is easily readable and provides a wide overview of grasping as it takes into account non prehensile, power, intermediate and precision grasps.

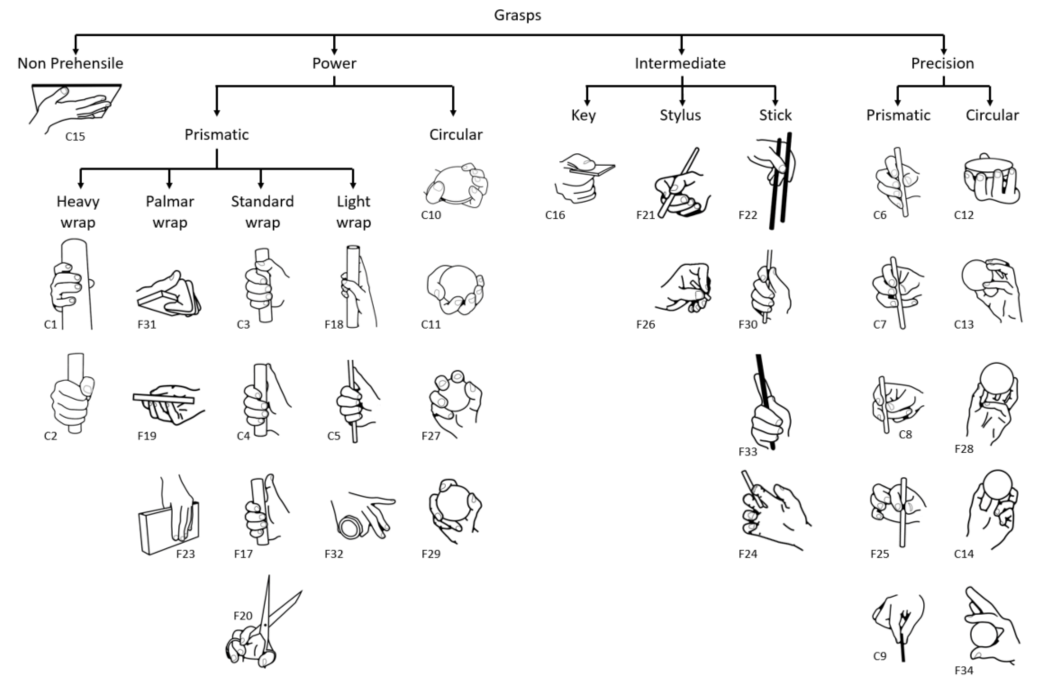

Non Prehensile & Power				Intermediate		Precision	
Label	Grasp	Label	Grasp	Label	Grasp	Label	Grasp
C_1	Large Diameter	F_{19}	Extension Type	C_{16}	Lateral Pinch	C_6	Thumb-4 Finger
C_2	Small Diameter	F_{20}	Distal Type	F_{21}	Writing Tripod	C_7	Thumb-3 Finger
C_3	Medium Wrap	F_{23}	Parallel Extension	F_{22}	Tripod Variation	C_8	Thumb-2 Finger
C_4	Adducted Thumb	F_{27}	Sphere-4 Finger	F_{24}	Adduction Grip	C_9	Thumb-Index Finger
C_5	Light Tool	F_{29}	Sphere-3 Finger	F_{26}	Lateral Tripod	C_{12}	(Precision) Disk
C_{10}	(Power) Disk	F_{31}	Palmar	F_{30}	Stick	C_{13}	(Precision) Sphere
C_{11}	(Power) Sphere	F_{32}	Ring	F_{33}	Ventral	C_{14}	Tripod
C_{15}	Hook, Platform Push					F_{25}	Tip Pinch
F_{17}	Fixed Hook					F_{28}	Quadpod
F_{18}	Index Finger Extension					F_{34}	Inferior Pincer

Figure 4.2: The Cutkosky and Feix grasp taxonomies.

Horizon 2020

TraceBOT receives funding from the European Union's H2020-EU.2.1.1. INDUSTRIAL LEADERSHIP programme (grant agreement No 101017089)

Researchers also seem to agree that some stereotyped behaviors are used in order to evaluate the physical characteristics of an object or a material. These gestures are usually classified according to the taxonomies proposed in [Jones and Lederman 2006] and [Lederman and Klatzky 2009], which group them in six exploratory procedures, each one being optimal to a certain kind of information. These procedures are named K_i (with $i \in [1;6]$) in the following.

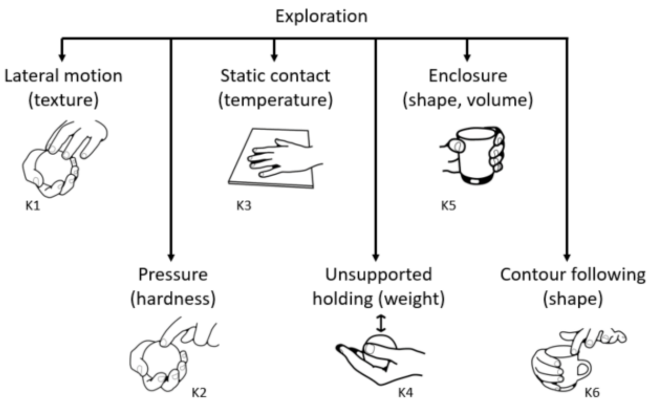

Figure 4.3: The exploratory gestures' taxonomy derived from the work of Lederman and Klatzky.

Previous work however only refers to situations as typically encountered when manipulating 'classical' objects such as tools (e.g. hammers, screwdrivers) or household objects (e.g. glass, plates). They are not sufficient to describe the way expert operators manipulate the Steritest kit in a glove box. This task indeed involves the manipulation of flexible objects (e.g. flexible tubes) which are not covered in usual taxonomies. Also, operators make use of non-typical grasps in order to grasp difficult to access objects, and they tend to grasp several objects at the same time. To cope with these grasps, we introduced a novel grasp category called T_i. In practice, we identified 80 of those grasps (hence $i \in [1;80]$). To describe them, we first drew schematic representations of each of them.

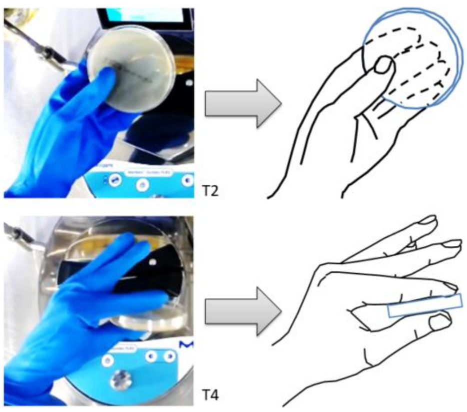

Figure 4.4: schematic representations of the TraceBot specific grasps (ex. of T2 and T4).

Horizon 2020
TraceBOT receives funding from the European Union's H2020-EU.2.1.1. INDUSTRIAL LEADERSHIP programme (grant agreement No 101017089)

The TraceBot grasps are displayed in the taxonomy presented below, with non prehensile, power, intermediate and precision grasps similarly as in Cutkosky and Feix' work. These grasps are mostly positioned as a function of their number. However, the grasps used to grab the same object are repositioned close to each other.

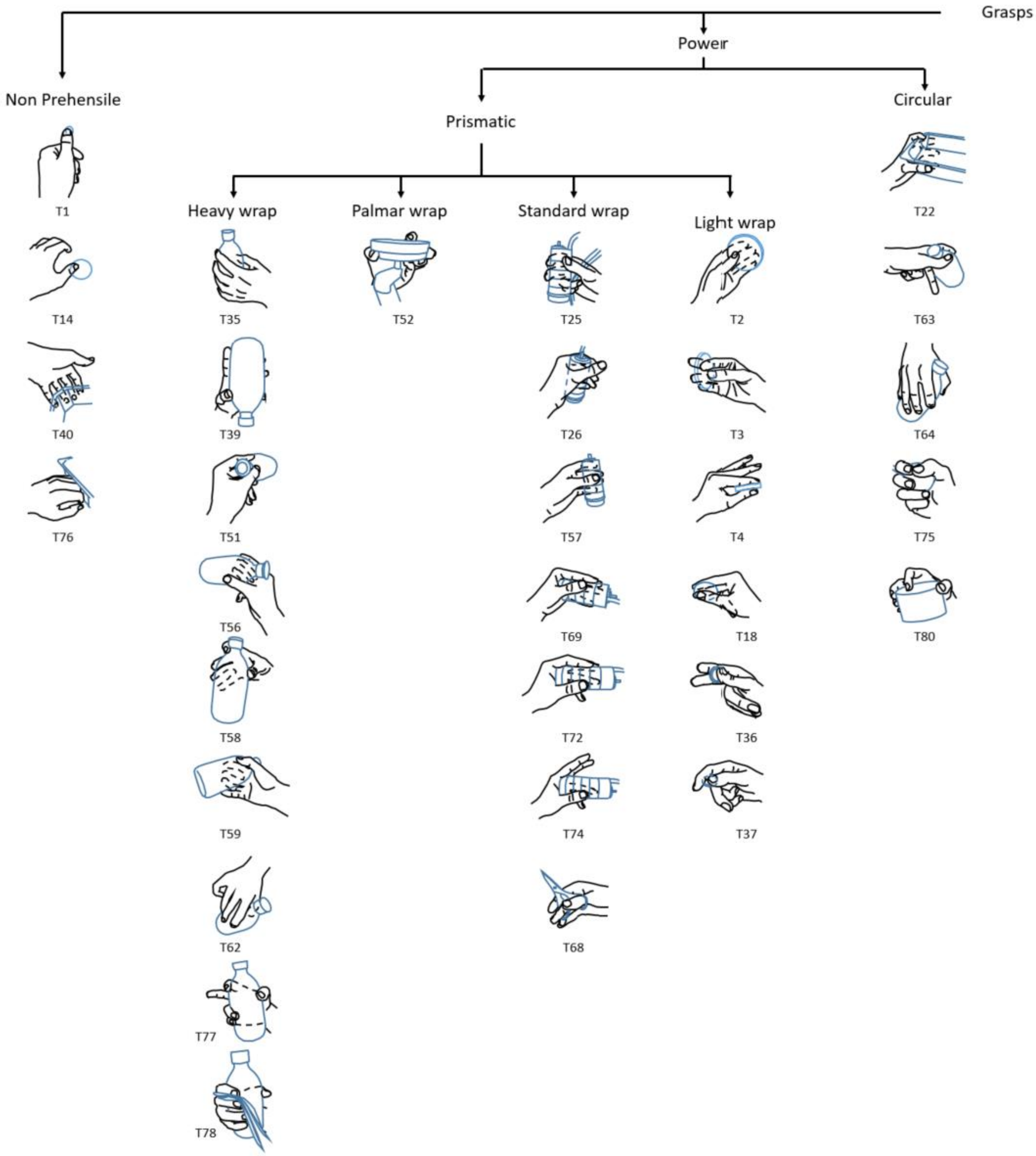

Figure 4.5: TraceBot specific grasps' taxonomy (part 1/2: non prehensile and power grasps).

Horizon 2020

TraceBOT receives funding from the European Union's H2020-EU.2.1.1. INDUSTRIAL LEADERSHIP programme (grant agreement No 101017089)

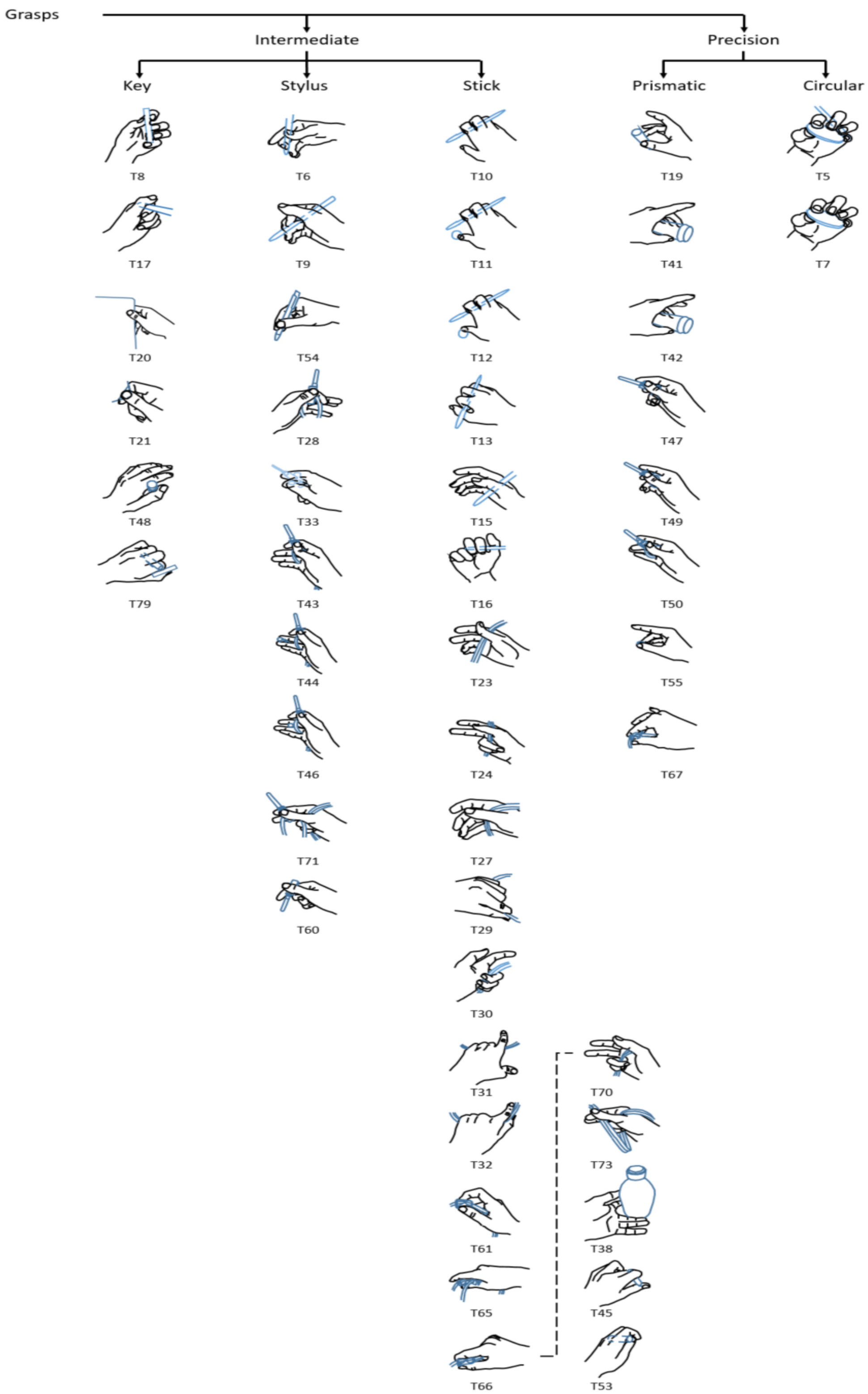

Figure 4.6: TraceBot specific grasps' taxonomy (part 2/2: intermediate and precision grasps).

Horizon 2020

TraceBOT receives funding from the European Union's H2020-EU.2.1.1. INDUSTRIAL LEADERSHIP programme (grant agreement No 101017089)

4.2 Step 02: Definition of hand-objects contact areas

The second step consists in identifying, for each interaction pattern, the hand-object contact area. For standard grasps types and exploratory movements, we refined the characterization of the contact areas compared to [Gonzalez et al. 2013] [Gonzalez et al. 2014] and [Chabrier et al. 2015]. Indeed, in previous studies reported in the literature, the palm is considered as fully involved in most power grasps, while in practice the palmar arch prevents contact with the center of the palm for most objects. We thus decided to refine the characterization of the contact area for all grasps and interaction patterns. Therefore, we took in hand objects representative of the different usual grasps and we tried to insert a thin metal sheet between the hand and the object. We considered that the skin is in contact with the object only when we were not able to insert this tool between their surfaces. The result is reported in the pictures below. As in practice the contact surface may vary according to the size of the grasped objects, we tried to grasp objects of different sizes. The contact surfaces in blue below represent this variability.

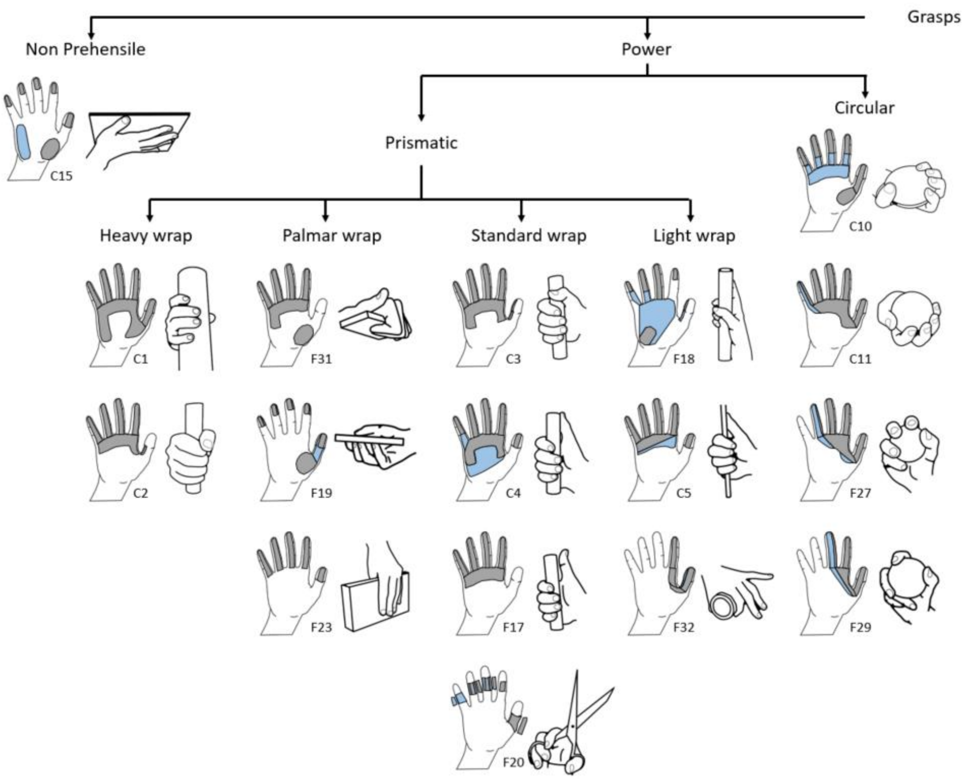

Figure 4.7: Hand-object contact surfaces for the usual grasps from Cutkosky and Feix' taxonomy (part 1/2: non prehensile and power grasps).

Horizon 2020

TraceBOT receives funding from the European Union's H2020-EU.2.1.1. INDUSTRIAL LEADERSHIP programme (grant agreement No 101017089)

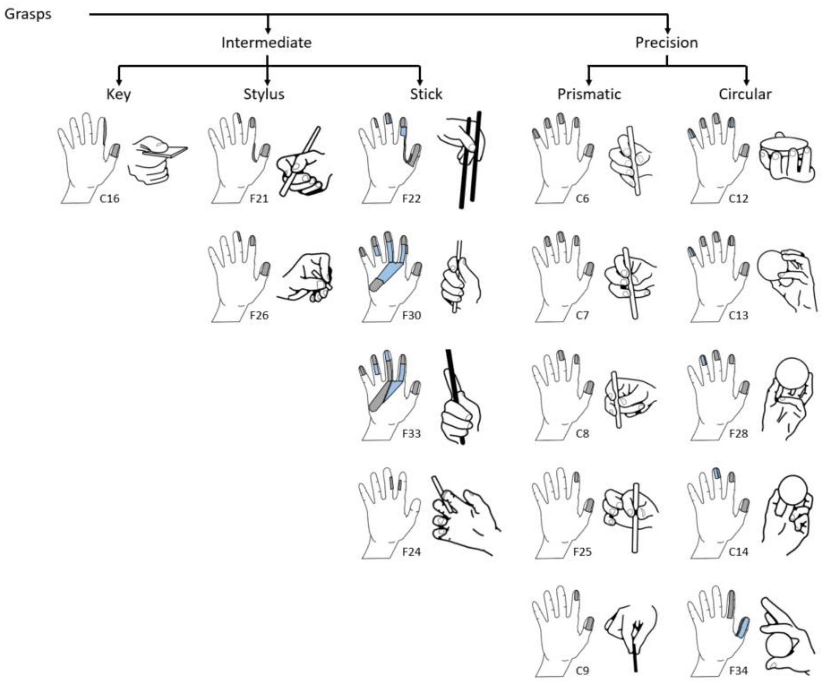

Figure 4.8: Hand-object contact surfaces for the usual grasps from Cutkosky and Feix' taxonomy (part 2/2: intermediate and precision grasps).

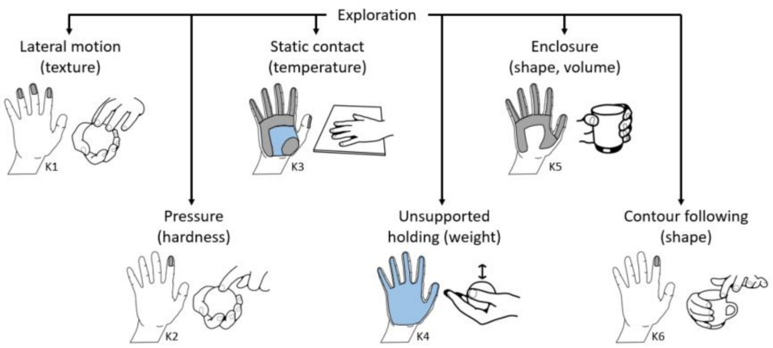

Figure 4.9: Hand-object contact surfaces for the canonical exploratory gestures.

For the specific TraceBot interaction patterns also, we tried to identify the hand-objects contact surfaces' as precisely as possible. As the gloves used by the operator do not always allow a clear vision of the way the objects are held, we reproduced the grasps with bare hands. Also, we took into account the information gathered during the whole duration of the grasp and not only at the time the picture was extracted (for most grasps, the user moves the held object from an initial to a final configuration which have different orientations, allowing to better see how the fingers are placed on the objects). The results of this analysis are reported below. For some grasps, we distinguish hand support areas

Horizon 2020

TraceBOT receives funding from the European Union's H2020-EU.2.1.1. INDUSTRIAL LEADERSHIP programme (grant agreement No 101017089)

(in red below) and functional areas (in grey). Supports are useful for humans but they are not required for robots. Red areas will thus not be considered in the remaining of the process.

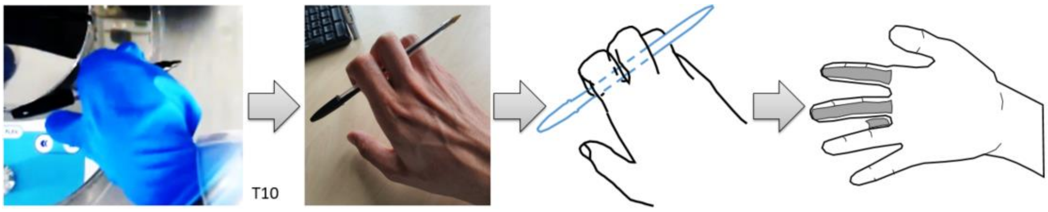

Figure 4.10: Determination of the TraceBot specific grasps' hand-object contact surfaces.

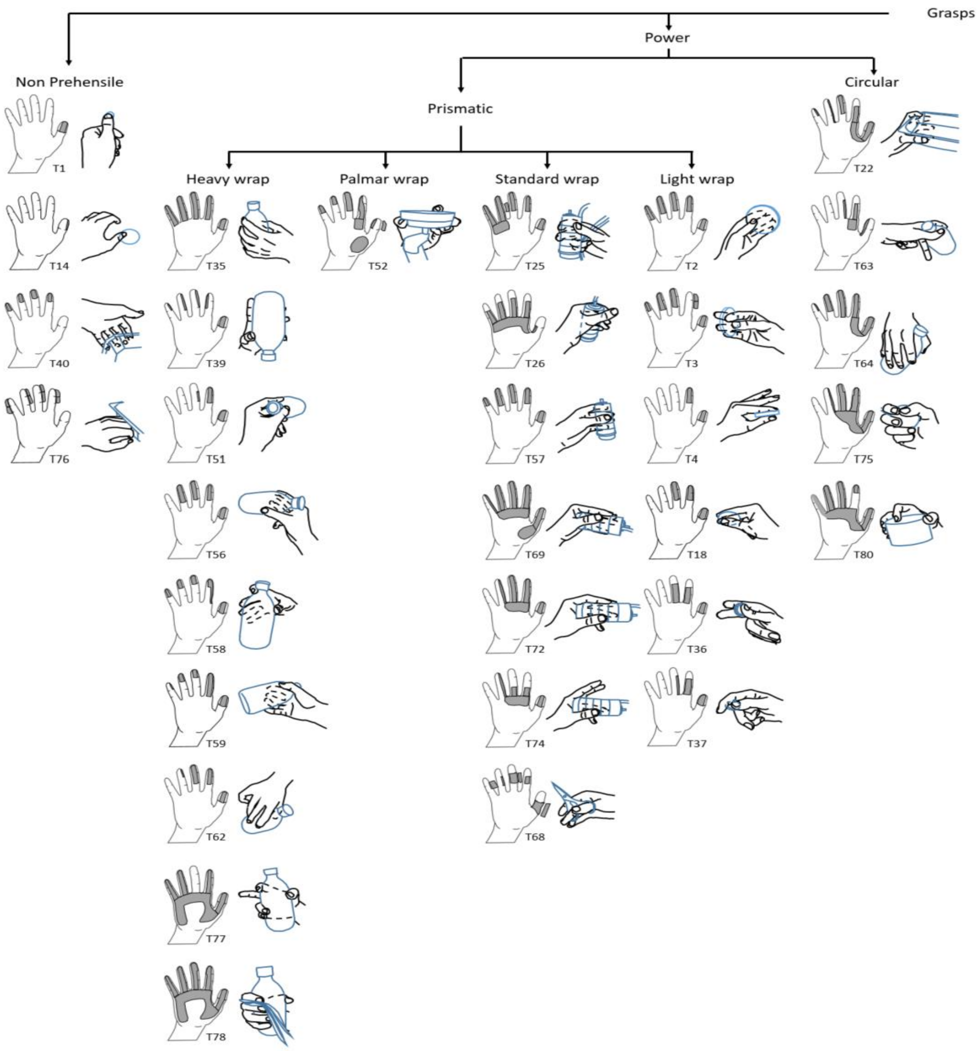

Figure 4.11: Hand-object contact surfaces for the TraceBot specific grasps
(part 1/2: non prehensile and power grasps).

Horizon 2020

TraceBOT receives funding from the European Union's H2020-EU.2.1.1. INDUSTRIAL LEADERSHIP programme (grant agreement No 101017089)

Figure 4.12: Hand-object contact surfaces for the TraceBot specific grasps (part 2/2: intermediate and precision grasps).

Horizon 2020

TraceBOT receives funding from the European Union's H2020-EU.2.1.1. INDUSTRIAL LEADERSHIP programme (grant agreement No 101017089)

These hand contact surfaces are then used to generate interaction maps composed of elementary contact areas obtained by superimposing them. Compared to previous work, it was necessary here to refine the hand surface decomposition. Indeed, a lot of the TraceBot grasps involve the sides of the fingers (in the Cutkosky and Feix' taxonomy on the contrary, it is only the case of few grasps like for example the adduction grip used to grab a cigarette). Since using finger edges is common in this study, it was chosen to standardize all fingers by placing an edge on each side of each phalanx. Moreover, as some of the TraceBot grasps use the back of some fingers, we also added the dorsal side of each phalanx (the representation of the dorsal areas is done by adding a small area next to the fingers). Thus, each phalanx of each finger is divided according to its four faces: palmar face, radial face, ulnar face, and dorsal face. To allow representing the thumb similarly as the other fingers, we introduce an offset angle so that these four faces are also visible for this finger. This results in the hand surface decomposition below (the palm division is also refined compared to previous work).

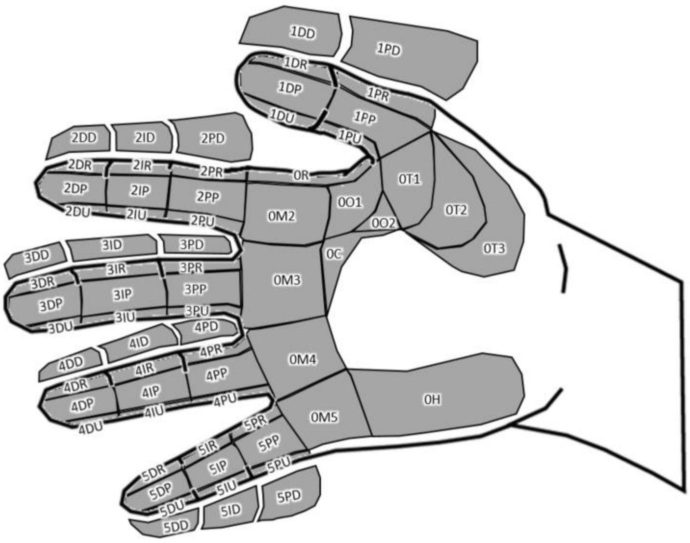

Figure 4.13: Labelling of the elementary contact areas.

The labels used to describe the elementary contact areas obey the following logic:

- The labels of the finger areas have 1 digit and 2 letters:
  - The digit is used to designate the finger: 1 for the thumb, 2 for the index, 3 for the middle, 4 for the ring and 5 for the little.
  - The first letter is used to designate the phalanx: P for proximal, I for intermediate and D for distal.
  - The second letter corresponds to the face of the finger: P for palmar, R for radial, U for ulnar and D for dorsal.

Horizon 2020

TraceBOT receives funding from the European Union's H2020-EU.2.1.1. INDUSTRIAL LEADERSHIP programme (grant agreement No 101017089)

- The palm is referred to as 0, and the associated labels have 1 additional letter and digit:
    - The digit 0 indicates the palm.
    - The letter is used to indicate the palm subdivision: T for the Thenar, O for the Opposition, H for the Hypothenar, M for the Metacarpal areas and C for the Central triangular.
    - The last digit allows to differentiate the palm subareas.

4.3 Step 03: identification of the frequency of use of each pattern

As previously explained, the frequency of use of each interaction pattern is obtained from a video analysis of the operators' gestures. As proposed in [Zheng et al. 2011], several observers carefully look at the videos and identify the interaction patterns used by the operators. As shown in the example video analysis displayed in Figure 4.1 and reproduced below, we note for each grasp the time it begins and the time it ends to be used. By subtracting the former from the latter, we get the grasp duration.

Grasp number	Start of the grasp	End of grasp	Duration (s)	Grasps		Hand contact area	Hand	Object	Original Video	Recut Video	Static / manipulation	Atomic task	Task categorie
17	00:00,00	00:01,40	01,40	T26			L	Canister	4 : Fit Canister to drain	03 : Kit mounting	Regrasping avec suivant	move canister over drain	install canister
18	00:01,40	00:03,80	02,40	T2			L	Canister	4 : Fit Canister to drain	03 : Kit mounting	In-hand manipulation	Insert canister into drain	install canister
19	00:04,23	00:04,73	00,50	T28			L	Tube	4 : Fit Canister to drain	3 : Kit mounting	Static	grab tube	install canister

Figure 4.14: Computation of the grasp durations.

It is worth noting that in practice, some grasps are used several times and/or with both hands. In such cases, we cumulate the times they are used over the whole process in order to get the total amount of time each grasp is used. These durations are further used to compute the relative frequency of use of the different grasps and interaction patterns, that is the duration of a given grasp divided by the duration of all grasps. This time consuming work is mandatory. It allows identifying the total time as well as the relative frequency (i.e. the percentage of time) each pattern is used. The results obtained

Horizon 2020

TraceBOT receives funding from the European Union's H2020-EU.2.1.1. INDUSTRIAL LEADERSHIP programme (grant agreement No 101017089)

for the INVITE use-case are displayed below, considering both all grasps and the 10 most frequent ones.

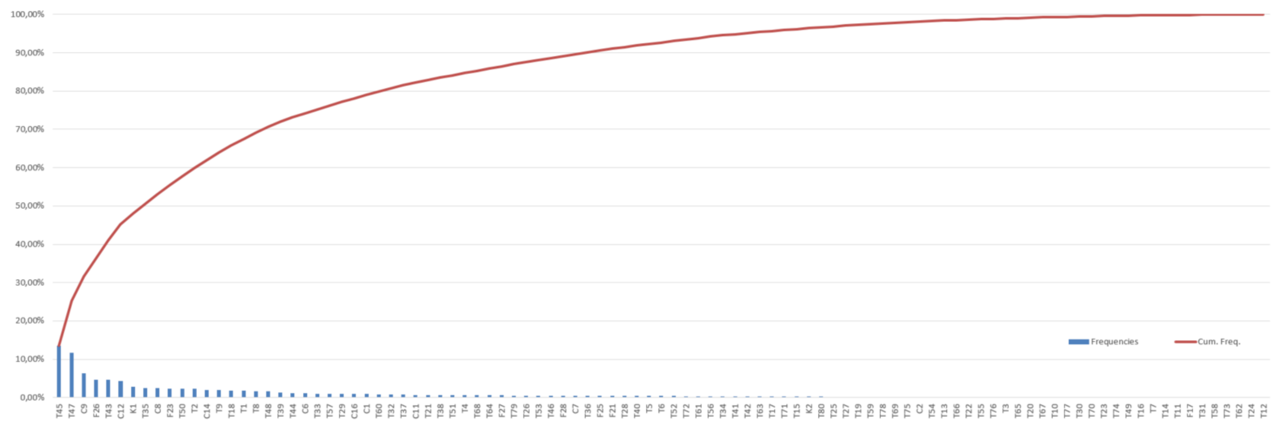

Figure 4.15: frequencies of use of the different grasps used in the INVITE use-case presented in descending order, and cumulated frequencies.

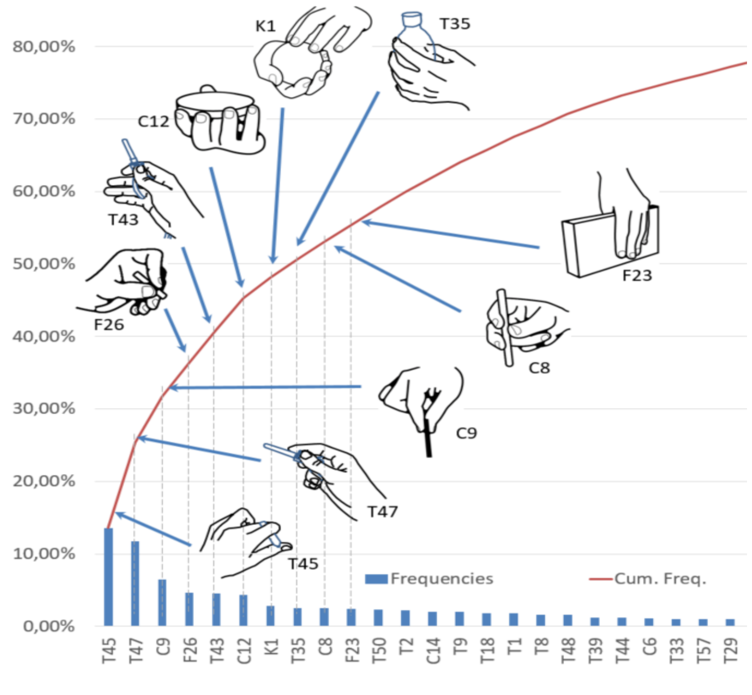

Figure 4.16: illustration of the 10 most frequent grasps.

Horizon 2020

TraceBOT receives funding from the European Union's H2020-EU.2.1.1. INDUSTRIAL LEADERSHIP programme (grant agreement No 101017089)

4.4 Step 04: estimation of the efforts applied on the objects

The observation of the videos allows to identify the grasped objects along with the grasps themselves. A sample of each of these objects provided by INVITE is weighted with a scale and the interactions seen in the video are reproduced in lab environment at CEA and measured. The example of the insertion and extraction of the needle in and from the cap of the rinse glass is illustrated in the figure below. The insertion and extraction efforts are measured with dynamometers.

Figure 4.17: Identification of the efforts applied on the manipulated objects when replicating use-case manual gestures using a laboratory balance and dynamometers at CEA.

The data for all objects and interactions are gathered in the table below, obtained either from voluntary pessimistic upper bound estimations of such efforts or from direct measurements using the experimental test bench at CEA.

Table 4.1. Summary of estimated efforts applied on the manipulated objects.

Object	Weight (in N)	External disturbances Direction-dependent perturbations applied to the object (in N)										
	HOLD	WRITE	UNCAP	RECAP	OPEN	INSERT	REMOVE	PIERCE	UNPIERCE	CLAMP	UNCLAMP	CUT
Petri dish	0.20	2.5	N.A.	N.A.	N.A.	N.A.	N.A.	N.A.	N.A.	N.A.	N.A.	N.A.
Marker	0.10	2.47	23.0	34.4	N.A.	N.A.	N.A.	N.A.	N.A.	N.A.	N.A.	N.A.
Marker cap	0.02	N.A.	23.0	34.4	N.A.	N.A.	N.A.	N.A.	N.A.	N.A.	N.A.	N.A.
Kit	1.70	N.A.	N.A.	N.A.	20.0	N.A.	N.A.	N.A.	N.A.	N.A.	N.A.	N.A.
Kit tab	0.004	N.A.	N.A.	N.A.	20.0	N.A.	N.A.	N.A.	N.A.	N.A.	N.A.	N.A.
Canister	0.04	N.A.	N.A.	N.A.	N.A.	87.2	110.0	N.A.	N.A.	N.A.	N.A.	N.A.
Tube	0.30	N.A.	N.A.	N.A.	N.A.	45.7	N.A.	N.A.	N.A.	N.A.	N.A.	N.A.
Needle	0.10	N.A.	9.4	N.A.	N.A.	N.A.	N.A.	23.4	11.0	N.A.	N.A.	N.A.
Needle cap	0.01	N.A.	9.4	N.A.	N.A.	N.A.	N.A.	N.A.	N.A.	N.A.	N.A.	N.A.

Horizon 2020

TraceBOT receives funding from the European Union's H2020-EU.2.1.1. INDUSTRIAL LEADERSHIP programme (grant agreement No 101017089)

Rinse glass	5.51	N.A.	N.A.	N.A.	N.A.	N.A.	N.A.	N.A.	N.A.	N.A.	N.A.	N.A.
Red plug	0.01	N.A.	N.A.	N.A.	N.A.	35.9	23.0	N.A.	N.A.	N.A.	N.A.	N.A.
Glass vial	0.15	N.A.	N.A.	N.A.	30.0	N.A.	N.A.	N.A.	N.A.	N.A.	N.A.	N.A.
Yellow plug	0.01	N.A.	N.A.	N.A.	N.A.	2.3	N.A.	N.A.	N.A.	N.A.	N.A.	N.A.
Tube clamp	0.04	N.A.	N.A.	N.A.	N.A.	N.A.	N.A.	N.A.	N.A.	40.8	3.1	N.A.
Scissors	0.59	N.A.	N.A.	N.A.	N.A.	N.A.	N.A.	N.A.	N.A.	N.A.	N.A.	55.0

4.5 Step 05: identification of the directions in which each area is solicited

During the analysis of the videos, we also try to identify the directions in which forces are applied on the hand. This analysis has to be made on each of the elementary hand areas as all areas may not be solicited similarly during a given manual interaction.

The first step consists in setting a Cartesian frame on every phalanx (distal, intermediate and proximal) and on each area on the palm (see simplified figure below). Then several observers evaluate the direction(s) in which each area is solicited.

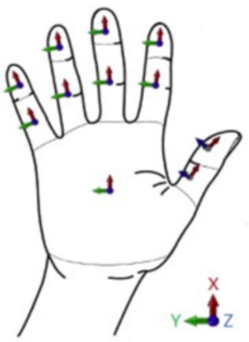

Grasp nb	Grasp	Hand contact area										
1	T1		Z									
2	T2		ZY	ZY	ZY	ZY	ZY	ZY	ZY	ZY		ZY
3	T4		Z	Z	Z							
5	T7		ZY	ZY	ZY	ZY		ZY			Z	

Figure 4.18: Example directional force analysis.

It is worth noting that when coming in contact with an object to interact with it or grasp it, forces are first applied in the Z direction. Then depending on the forces exerted on the object, forces may also appear in the Y and/or X directions. As a result, the Z direction is the most used direction when manipulating objects, followed by the Y and X directions.

Horizon 2020

TraceBOT receives funding from the European Union's H2020-EU.2.1.1. INDUSTRIAL LEADERSHIP programme (grant agreement No 101017089)

5 Generation of interaction maps

By associating the inner surface of the hand used to execute a given grasp or gesture with its frequency of use, we can get the frequency of use of each of the elementary interaction areas it is composed of in each direction. By overlapping the results associated with the different grasp types, it is possible to draw interaction maps. As shown in the figure below, the accumulated frequency of use on a given elementary contact area in a given direction is computed as the sum of the frequencies of use of all grasps requiring this elementary contact surface in this direction.

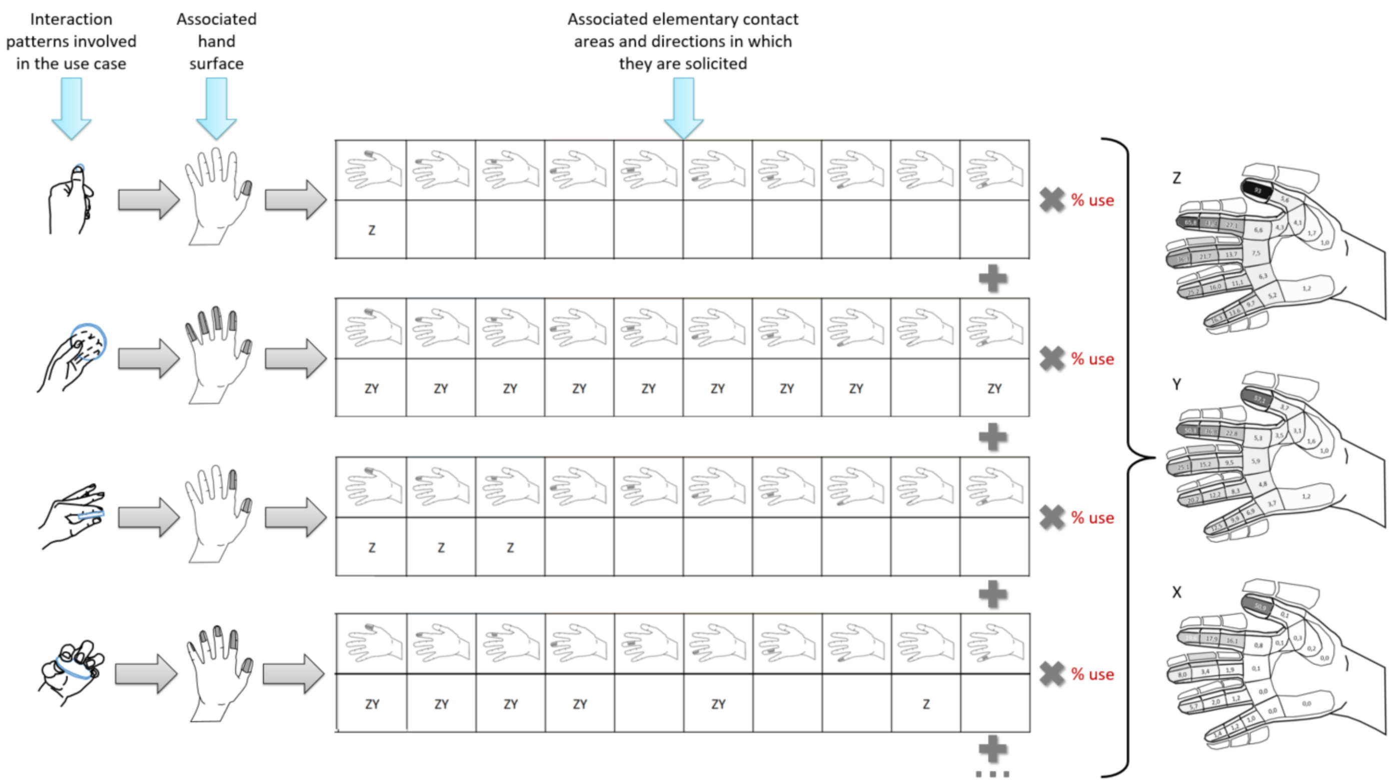

Figure 5.1: Generation of the interaction maps.

Interaction maps in the Z (normal to the skin), Y and X (tangential to the skin) are given below. They give an overview of the way the hand is excited while performing the use-case dexterous activities.

Horizon 2020
TraceBOT receives funding from the European Union's H2020-EU.2.1.1. INDUSTRIAL LEADERSHIP programme (grant agreement No 101017089)

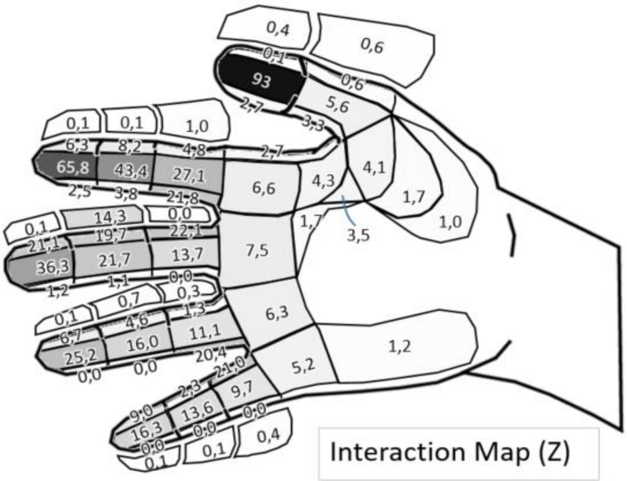

Figure 5.2: Interaction map normal to the skin (z – direction).

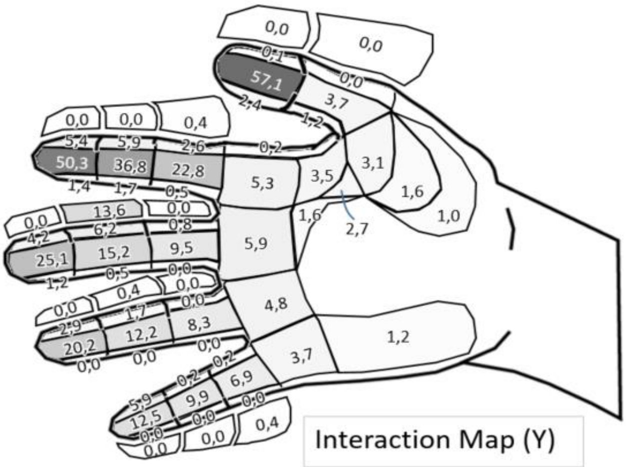

Figure 5.3: interaction map tangential to the skin and normal to the fingers (Y – direction).

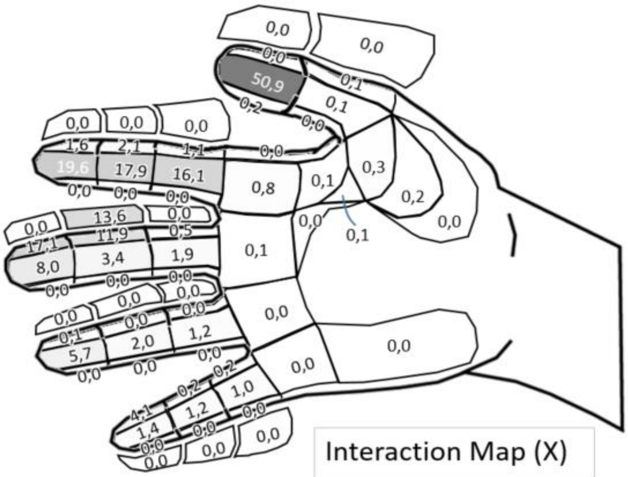

Figure 5.4: interaction map tangential to the skin in the direction of the fingers (X – direction).

Horizon 2020

TraceBOT receives funding from the European Union's H2020-EU.2.1.1. INDUSTRIAL LEADERSHIP programme (grant agreement No 101017089)

From these interaction maps, we deduce that the fingers' palmar side are the most solicited areas, followed by the ulnar and radial sides of only few phalanges. The ulnar and radial sides of most fingers are much less used, as the dorsal side of the fingers and the palm. This tends to guide the placement of tactile sensors on the palmar side of the fingers, especially on their distal phalanges which are the most frequently used areas.

Regarding the directions, we can see that the hand is mostly solicited in Z (i.e. normal to the skin). This highlights the primary importance of the fingers' flexion movements which should be considered with care in the gripper's design.

Finally, we can conclude that the most used finger is the thumb, followed by the index, the middle, the ring and the little. The latter is the less used. If a simplification of the design is sought, it is surely this finger that should be removed, provided it does not compromise the grasps stability nor increase the forces required on each finger.

Horizon 2020

TraceBOT receives funding from the European Union's H2020-EU.2.1.1. INDUSTRIAL LEADERSHIP programme (grant agreement No 101017089)

6 Force-based grasp stability analysis

This section focuses on the details related to the force-based grasp stability analysis, as it appears in the seventh and eighth steps of the previously presented overall analysis framework. A specifically developed complementary object-centered grasp analysis is addressed in these steps through its most basic, yet crucial, assets: the contact modeling hypothesis and the grasp quality evaluation.

- Based on a reconstructed CAD and meshed model of all objects involved in the use-case, we infer the location and number of the contact points applied on the object envelope. Then, using state-of-the-art results related to object grasping with multifingered robot gripper, we take advantage of the usual friction-based mechanical contact modeling at the phalanx/object interface to represent the distribution of static wrenches applied to each object. This step is realized for each pair made of an object and a previously identified grasp pattern taken from the previously introduced taxonomy. Thus, a mapping between these contact points given in an object-centered reference and the identified elementary contact area of the human hand is deduced.
- Then, we make use of theoretical tools to quantify the required amount of efforts at each elementary areas, in order to ensure grasp stability of the object held within the hand. Task-oriented grasp quality metrics, conveniently adjusted to the TraceBot use-case, define the grasp analysis aspect of the framework. The proposed grasp analysis tool accounts for the mechanical ability of the contacts to hold still objects, while facing the external perturbations as imposed by the TraceBot use-case. The main considered external perturbations applied to the objects are related to inertia and gravity effects, as well as mechanical interaction forces that may occur between two objects during certain subtasks (e.g. insertion or assembly).

In the following, we provide more practical details about how such methodology helps us to generate quantitative task-oriented data to be served as a basis for extracting design rules related to the robotic gripper (section 7).

6.1 Theoretical approach for grasp stability

This subsection is dedicated to the brief description of the mathematical model of contact for grasping, which will be referred to in the following subsections. The adopted notations are widely inspired by [Prattichizzo et al. 2008].

Horizon 2020

TraceBOT receives funding from the European Union's H2020-EU.2.1.1. INDUSTRIAL LEADERSHIP programme (grant agreement No 101017089)

6.1.1 Recall about usual SoA contact models

Assuming an unique, well-defined, tangent plane at each contact point C_i between the finger and the grasped object, we can define a contact frame $\{C_i, o_i, t_i, n_i\}$, with n_i defining the contact normal, directed towards the object. The contact efforts locally transmitted at C_i will then be denoted by the static wrench f_{c_i}. The following notations will also be adopted : $f_{c_{n_i}}$ denotes the normal component of the transmitted contact forces, $f_{c_{t_i}}$ and $f_{c_{o_i}}$ the tangential ones.

Among the main contact types in grasping, we adopted the Hard Finger (HF) one in our study, assuming that normal and tangential components are transmitted at the contact point location from the phalanx to the object. In such a case, contact forces are transmitted in the contact tangent plane following the inequality constraints:

$$\begin{cases} f_{c_{n_i}} & \geq & 0 \\ \sqrt{f_{c_{o_i}}^2 + f_{c_{t_i}}^2} & \leq & \mu f_{c_{n_i}} \end{cases}$$

where μ defines the tangential friction coefficient between the finger and the grasped object, which may vary depending on several contact characteristics.

The above standard sets of inequality constraints form a *friction cone*, that can be approximated by a polyhedral cone for an appropriate formatting for optimization, defined by a *local friction cone matrix* F_i in the following way (Figure 6.1):

$$\mathrm{F}_i = \{ f_{c_i} \text{ s.t. } F_i f_{c_i} \geq 0 \}.$$

In the following sections, such approximation will be referenced to through the *global friction cone matrix* $F = \mathrm{blockdiag}(F_1, \ldots F_{n_c})$, which allows to easily test the respect of contact types for all contact points n_c at once, through the following linear inequality :

$$F f_c \geq 0.$$

Horizon 2020

TraceBOT receives funding from the European Union's H2020-EU.2.1.1. INDUSTRIAL LEADERSHIP programme (grant agreement No 101017089)

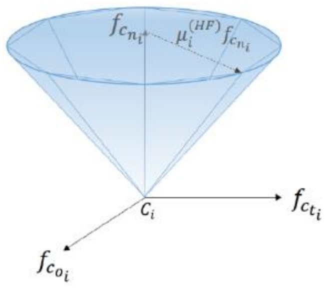

Figure 6.1: Representation and approximation of a spatial friction cone with vertices in the case of *HF* contact modeling.

6.1.2 Task-oriented grasp quality metric

A specifically tailored task-oriented approach for grasp quality assessment is proposed as a new metric adapted to our class of problem. This subsection is dedicated to the brief description of the mathematical formulation of the considered metrics, which will be referred to in the following sections. Focus has been put on the mechanical ability of the human hand to hold still the object, while facing the external perturbations imposed by the use-case. This point of view is depicted as *the magnitude of forces required at the hand-object contact locations required to counter an external effort exerted at the center of the object frame*.

One interest of this metric lies in its ability to provide insight on the to-be-designed gripper ability to counter given external perturbations. It provides, for each identified object and each external effort considered in the TraceBot use-case, an estimation of the grasp force necessary to hold still the object.

In practice, we denote by $d_{W_{ext}}$ the fixed direction of the studied external effort and α its variable magnitude, such that:

$$g = \alpha d_{W_{Ext}}$$

reports for both forces and torques applied to the object, the last three components of $d_{W_{ext}}$ will be normalized according to a characteristic length L of the grasped object.

The magnitude metric is computed by resolving the following problem (P):

$$\boxed{\begin{array}{llll} (P) & & \min \| f_c \| & \\ & s.t. & G f_c + \alpha d_{W_{Ext}} = 0 & \text{(Static equilibrium)} \\ & & F f_c \geq 0 & \text{(Friction cone)} \end{array}}$$

Horizon 2020

TraceBOT receives funding from the European Union's H2020-EU.2.1.1. INDUSTRIAL LEADERSHIP programme (grant agreement No 101017089)

where the grasp matrix G maps the contact wrench given in their local frames onto the object frame. The proposed problem (P) roughly embodies the mechanical limitations of the gripper actuators and helps finding the minimal requirement about the maximal force upper bound $f < f_{c_{max}}$.

6.2 Framework for grasp study

A specifically developed grasp analysis, based on the above constructed grasp analysis tools together with a mapping of the grasping fingers layout on the considered TraceBot objects, is thereafter detailed. The global outline of the proposed analysis is summarized in Figure 6.2.

6.2.1 Overall architecture and workflow

The main analysis rationale is briefly introduced below.

- **Specifications**
  The grasp synthesis takes as inputs a batch of parameters, which help formulating the mathematical problem.
    - Firstly, a whole set of *object data* deals with the geometry, the inertial properties of the to-be-grasped object, as well as its eventual restricted areas (i.e. areas where a contact point has to be avoided, either for safety or practical reasons).
    - A second set of data comprises the identified *external disturbances* (seen as external wrenches from a mechanical point of view) applied to each object involved in the task. This last feature is task-oriented, since it aims at documenting the perturbations applied to each object as imposed by the TraceBot use-case. These are related to inertia and gravity effects, as well as mechanical interaction forces that may occur between two objects during certain tasks (e.g. insertion or assembly).
    - Finally, a third set of parameters, also known as *grasp type settings*, describe useful characteristics of the human or gripper grasp pattern: the number of fingers (including the palm) and the number of contacts (the contact type being chosen as HF for all fingers) as defined by each grasp pattern from the taxonomy.

Horizon 2020

TraceBOT receives funding from the European Union's H2020-EU.2.1.1. INDUSTRIAL LEADERSHIP programme (grant agreement No 101017089)

- **Mapping between human hand/gripper and object**
  First, a reconstructed meshed version of each object to be grasped is done. Then, the issue of finding the appropriate positioning of each finger and palm on the object's envelope is solved according to the identified grasp pattern from the taxonomy-based human-gesture analysis (from step one to five in section 4). For each pair of *grasp type settings* and *object data*, the selection procedure computes a collection of *contact positions*, which maps the identified elementary contact area of the human hand or gripper to the object. All associated elements form a *ready-to-analyse grasp*.

- **Grasp stability analysis tool**
  A comparative tool is built: it is able to hold the *grasp quality metric* scores computed from (P) for each *ready-to-analyze grasp*. The tool takes into account a multi-parametric analysis that includes all the combinatorial combinations of parameters (*object data*, *grasp type settings* and *external perturbations*). Let note that, prior to solve (P), each *ready-to-analyze grasp* is classified as "indeterminate or not" and as "graspable or not". It is based on the mathematical study of the grasp matrix G computed for each *ready-to-analyze grasp*: the analysis of the rank of the null space of G and G^T helps us understanding, from a control point of view, if the considered grasp allows to control all internal object forces and twists.

- **Extraction of solution and conception guidelines derivation**
  The previously obtained analysis tool is post-processed to identify a satisfactory level of required forces threshold $f_{c_{max}}$ at contact points. The list of obtained metric values, computed from an object-centered point of view, happens to hold interesting insights concerning the required maximal force capability to be produced by the to-be-designed gripper considering a specific pair of *object data* & *grasp type settings*. Finally, according to scores from grasp quality metric, a specific ordering between the proceed grasps can be derived.

The above grasp analysis methodology has been applied to the study of the TraceBot use-case. The hypothesis and modeling background relative to the use-case are reported in the following subsections.

Horizon 2020

TraceBOT receives funding from the European Union's H2020-EU.2.1.1. INDUSTRIAL LEADERSHIP programme (grant agreement No 101017089)

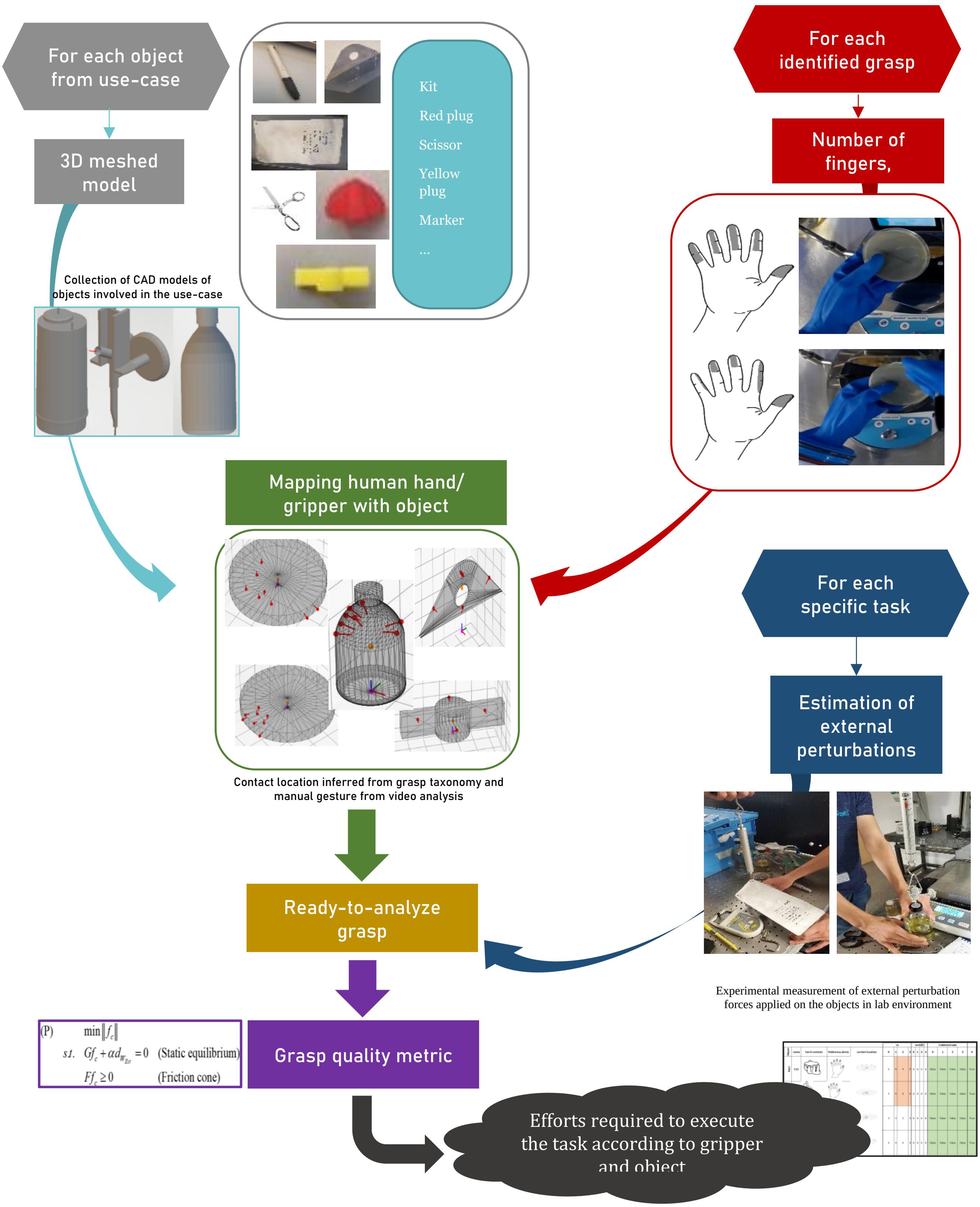

Figure 6.2: Global outline for grasp analysis methodology.

Horizon 2020
TraceBOT receives funding from the European Union's H2020-EU.2.1.1. INDUSTRIAL LEADERSHIP programme (grant agreement No 101017089)

6.2.2 Considerations about the human hand and object mapping

An in-depth analysis of the whole use-case has led to the documentation of all the pairs that combine objects and grasp types extracted from the TraceBot taxonomy. These pairs are summarized in the Table below, some pair being subjected to several perturbation loads as explained in the next subsection.

Table 6.1: List of combinations between grasps and perturbations considered in the use-case

Objects	**Grasps type identified from taxonomy**	**Perturbations**
Petri dish	C6, C8, C12, F28, T2, T3, T4, T7, T8, T18	HOLD, WRITE
Marker	C8, F26, F28, T9, T10, T13, T16, T18	HOLD, UNCAP, RECAP, WRITE
Marker cap	C16, T17, T53	HOLD, UNCAP, RECAP
Kit	C6, C7, C8, C11, F28, T22, T35	HOLD, OPEN
Kit tab	T21	HOLD, OPEN
Canister	C1, C6, C8, T2, T18, T26, T57	HOLD, INSERT, REMOVE
Tube	C2, C6, C7, C8, F17, F26, T4, T17, T23, T24, T27, T28, T29, T30, T70	HOLD, INSERT
Needle	C8, T21, T28, T33, T60	UNCAP, HOLD, PIERCE, UNPIERCE
Needle cap	C14, T4, T28	UNCAP
Rinse glass	C6, C12, T2, T18, T34, T35, T38, T39, T51, T58, T69	HOLD
Red plug	F26, T21	HOLD, INSERT, REMOVE
Glass vial	T45	HOLD, OPEN
Yellow plug	T21	HOLD, INSERT
Tube clamp	C16, T28, T65	HOLD, CLAMP, UNCLAMP
Scissors	C8, C16, T68, T68_	HOLD, CUT

Number of pairs {objects, grasp types}	**81**

For each pair made of one object and one grasp type, the procedure infers a collection of theoretical *contact positions*, which maps the elementary contact areas of the human hand involved in the current grasp type to the meshed CAD of the current object. From a mathematical point of view, one elementary contact area from the human hand (as sketched in section 4) is assumed to be modelled as one punctual Hard Finger (HF) contact model with *Coulombs* friction property. In short, at the interface between the phalanx/palm and the object, only normal and tangential force components are transmitted at the contact points locations.

The exhaustive list of available pairs for the entire use-case is reported in Table 6.2 below, showing the diversity and the complexity of the human gesture as involved in the use-case.

Horizon 2020

TraceBOT receives funding from the European Union's H2020-EU.2.1.1. INDUSTRIAL LEADERSHIP programme (grant agreement No 101017089)

Table 6.2. List of all mappings between object and human hand grasps involved in the use-case

Object —	Grasp name	Object grasped by human hand: Object grasp as shown in INVITE use-case videos	Object grasped by human hand: Replicated object grasp in lab at CEA by human hand	Hand grasp model	Hand contacts involved in the grasp	Meshed object with inferred contact points
PETRI	T2					
CANISTER	T2					
RINSE GLASS K	T2					
PETRI	T3	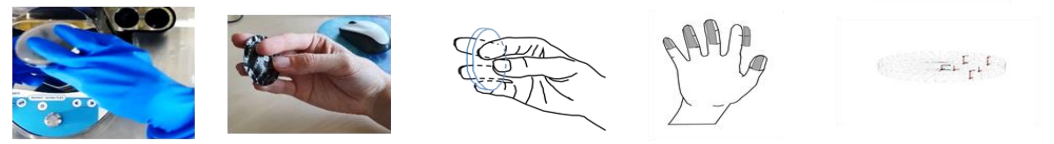				
PETRI	T4	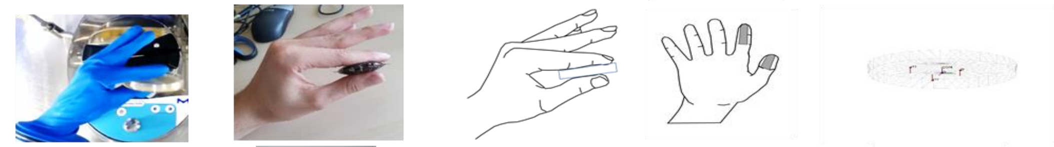				
TUBE	T4					
NEEDLE CAP	T4	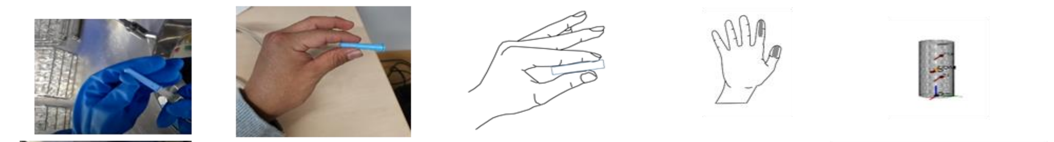				
PETRI	T7					
PETRI	T8	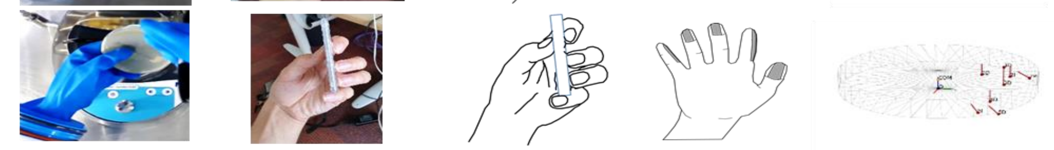				
MARKER	T9	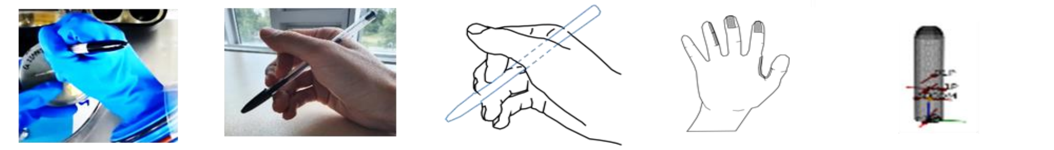				

Horizon 2020

TraceBOT receives funding from the European Union's H2020-EU.2.1.1. INDUSTRIAL LEADERSHIP programme (grant agreement No 101017089)

MARKER	T10	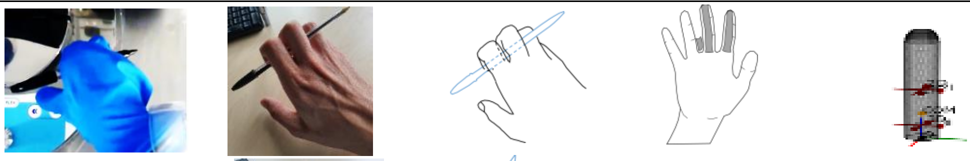
MARKER	T13	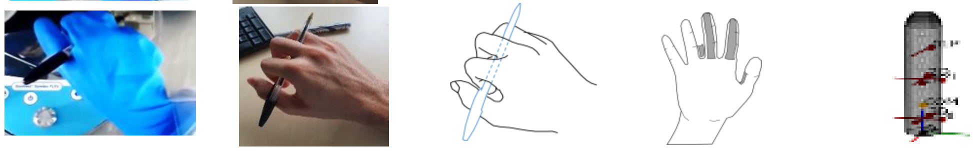
MARKER	T16	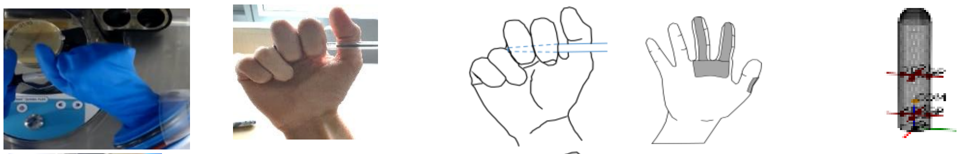
MARKER CAP	T17	
TUBE	T17	
PETRI	T18	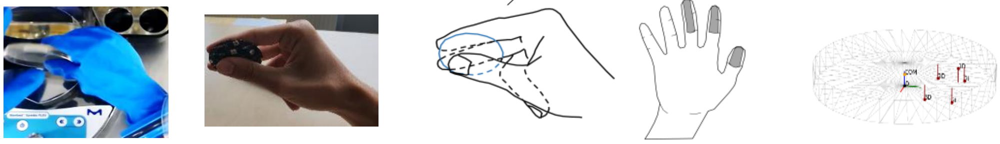
MARKER	T18	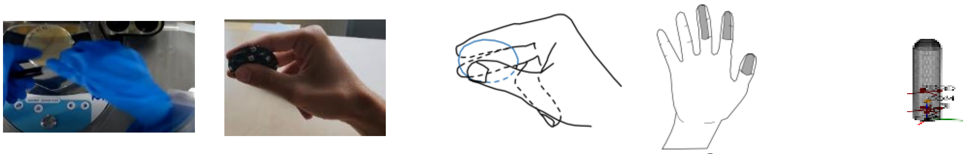
CANISTER	T18	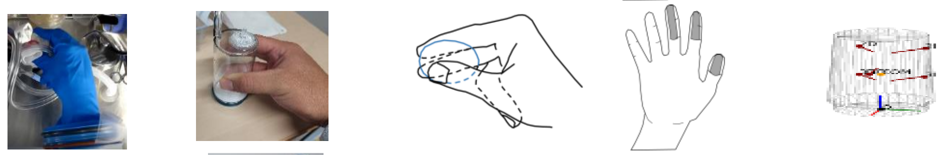
RINSE GLASS K	T18	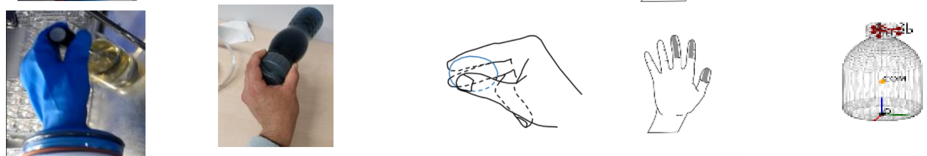
KIT TAB	T21	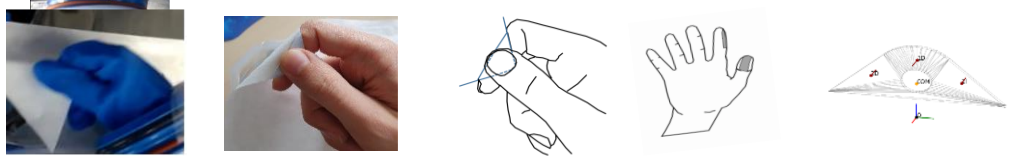
NEEDLE	T21	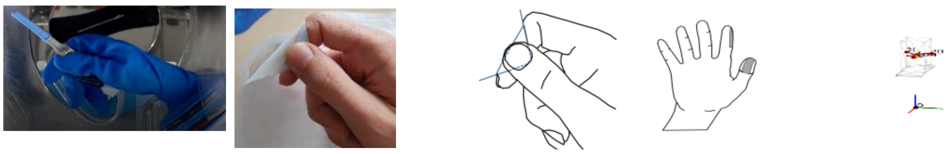

Horizon 2020

TraceBOT receives funding from the European Union's H2020-EU.2.1.1. INDUSTRIAL LEADERSHIP programme (grant agreement No 101017089)

YELLOW PLUG	T21	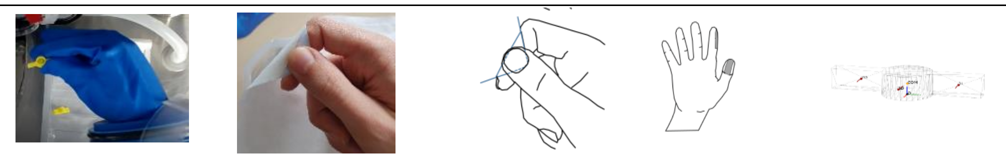
RED PLUG	T21	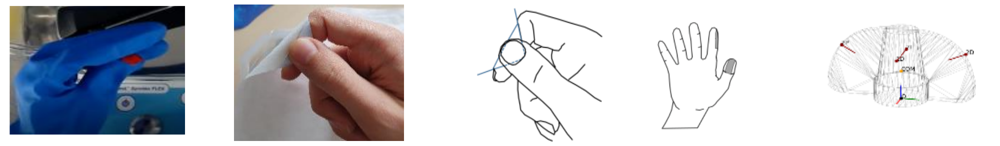
KIT	T22	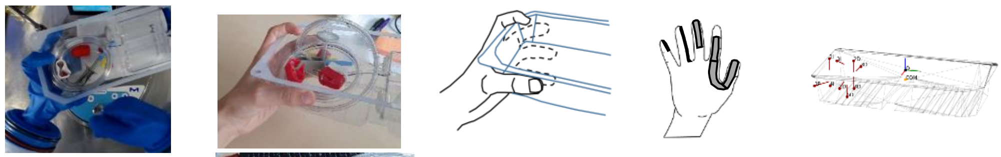
TUBE	T23	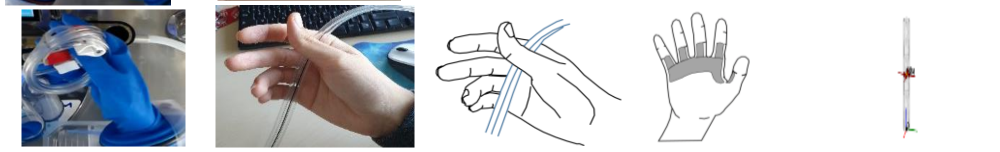
TUBE	T24	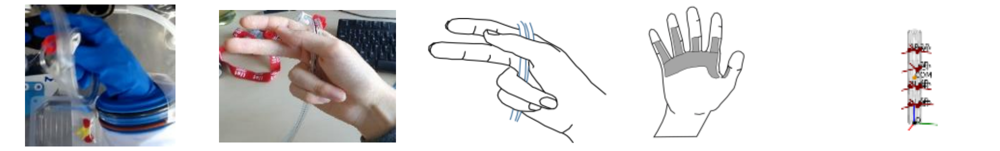
CANISTER	T26	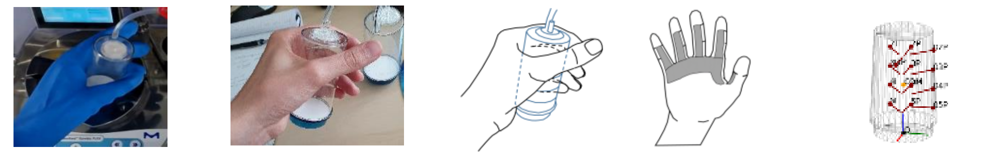
TUBE	T27	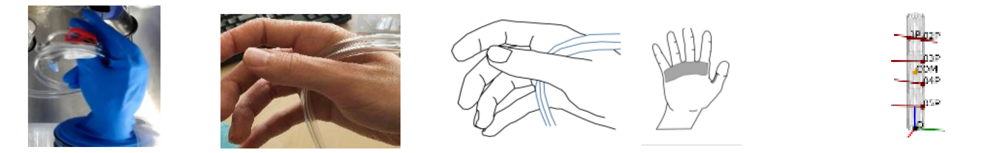
TUBE	T28	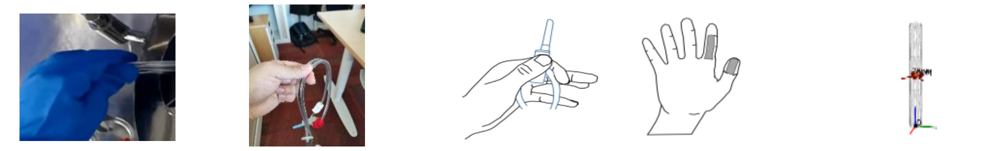
NEEDLE	T28	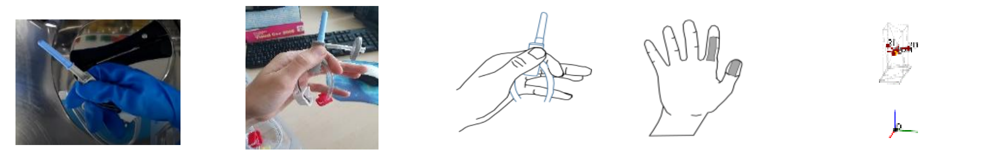
NEEDLE CAP	T28	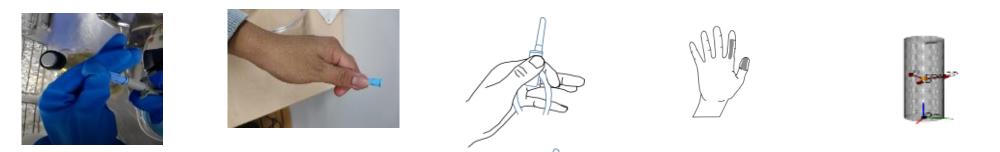
TUBE CLAMP	T28	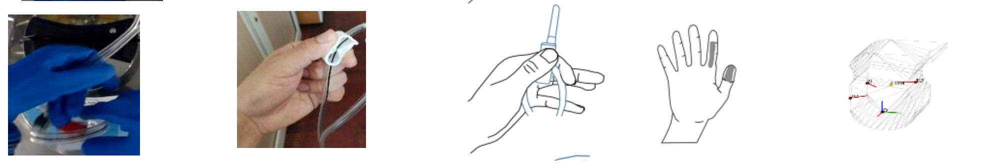

Horizon 2020

TraceBOT receives funding from the European Union's H2020-EU.2.1.1. INDUSTRIAL LEADERSHIP programme (grant agreement No 101017089)

TUBE	T29	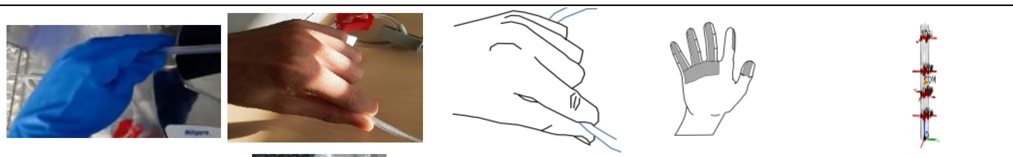
TUBE	T30	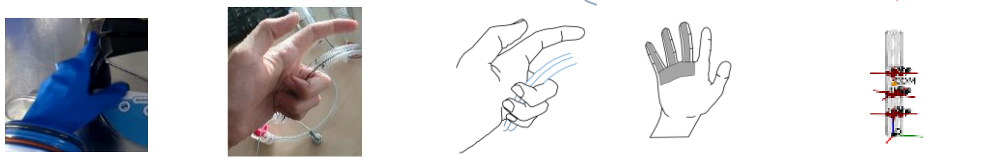
NEEDLE	T33	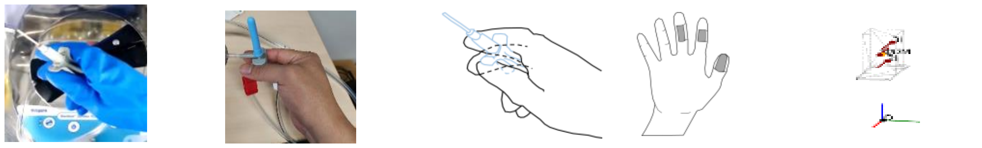
RINSE GLASS K	T34	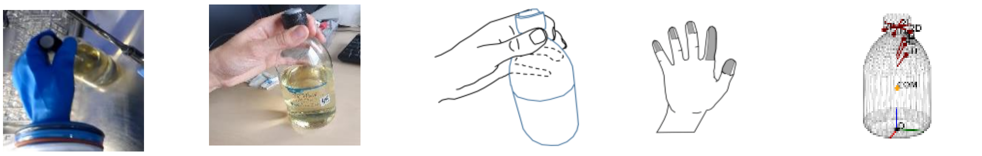
KIT	T35	
RINSE GLASS K	T35	
RINSE GLASS K	T38	
RINSE GLASS A	T39	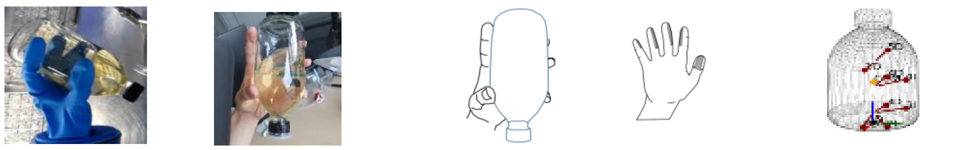
GLASS VIAL	T45	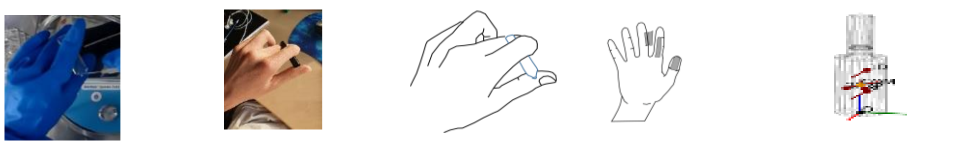
RINSE GLASS	T51	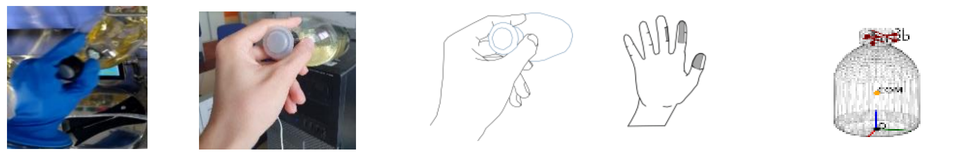
MARKER CAP	T53	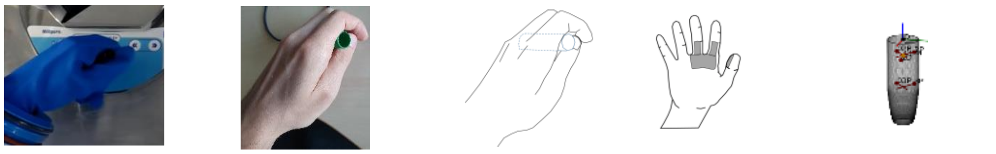

Horizon 2020

TraceBOT receives funding from the European Union's H2020-EU.2.1.1. INDUSTRIAL LEADERSHIP programme (grant agreement No 101017089)

CANISTER	T57	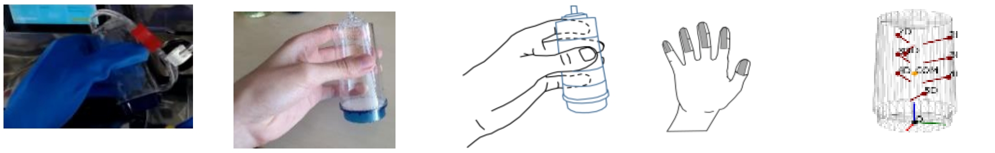
RINSE GLASS	T58	
NEEDLE	T60	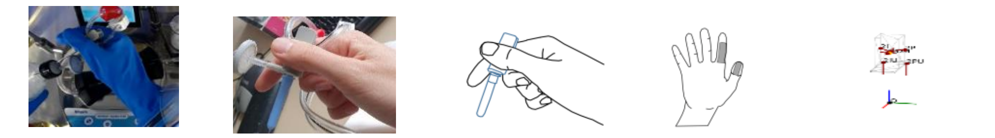
TUBE CLAMP	T65	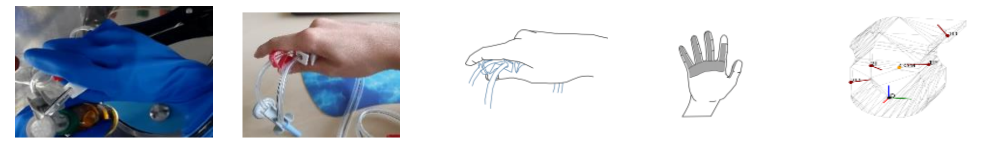
SCISSORS	T68	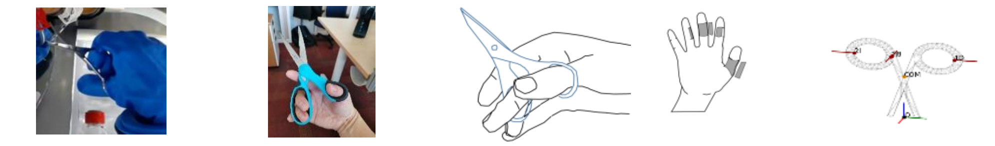
SCISSORS	T68_	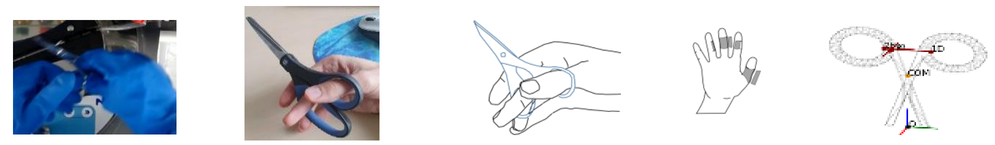
RINSE GLASS	T69	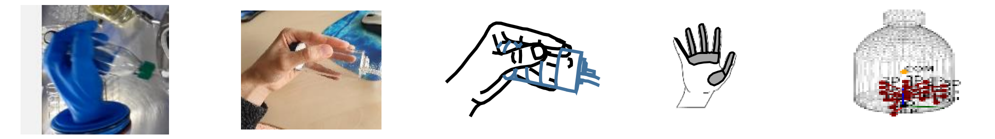
TUBE	T70	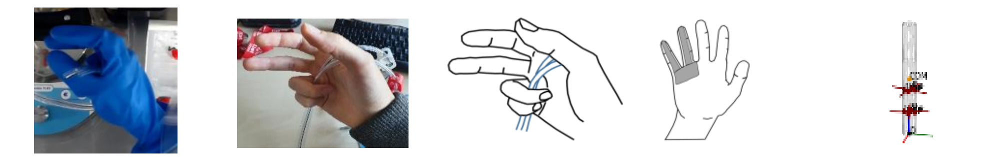
CANISTER	C1	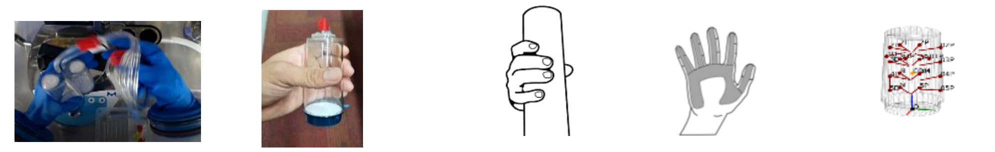
TUBE	C2	
PETRI	C6	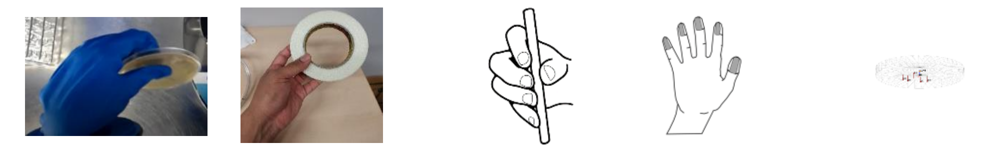

Horizon 2020

TraceBOT receives funding from the European Union's H2020-EU.2.1.1. INDUSTRIAL LEADERSHIP programme (grant agreement No 101017089)

KIT	C6	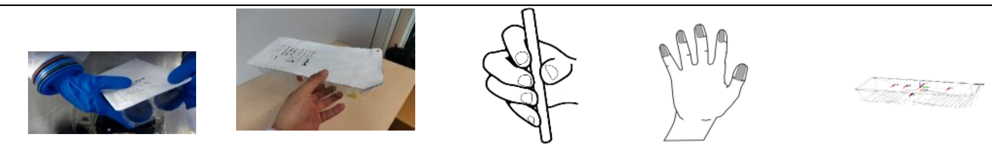
CANISTER	C6	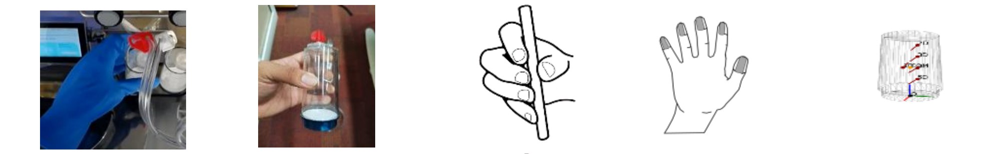
TUBE	C6	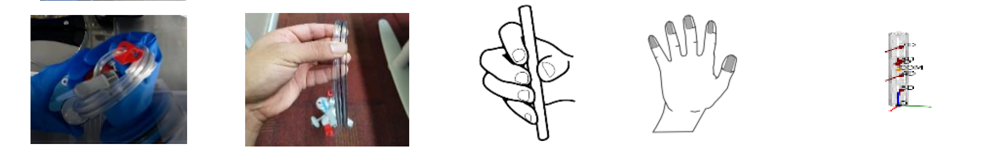
RINSE GLASS	C6	
KIT	C7	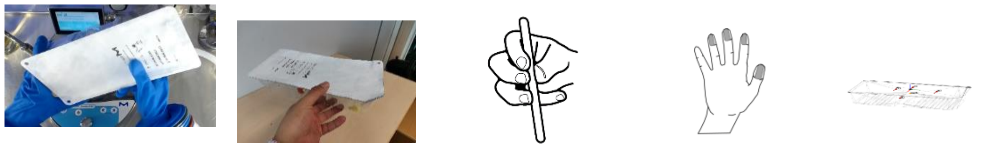
TUBE	C7	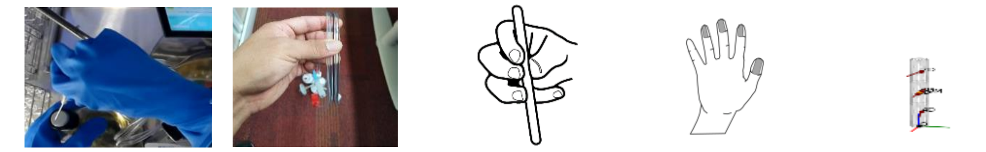
PETRI	C8	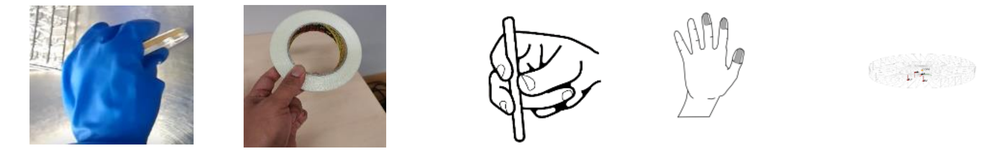
MARKER	C8	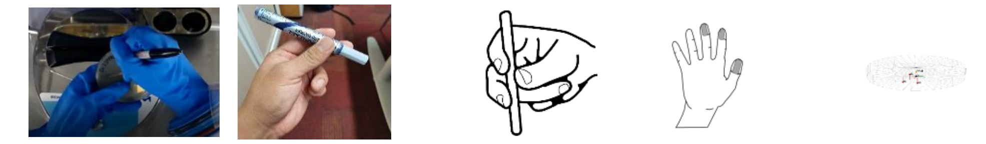
KIT	C8	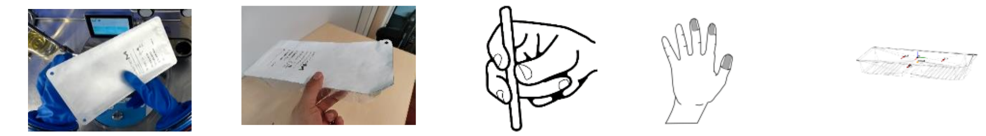
CANISTER	C8	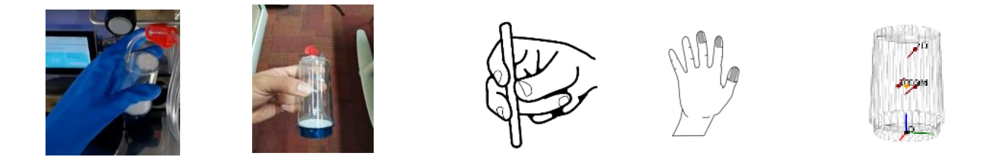
TUBE	C8	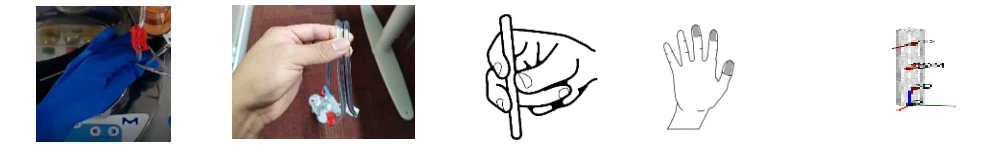

Horizon 2020
TraceBOT receives funding from the European Union's H2020-EU.2.1.1. INDUSTRIAL LEADERSHIP programme (grant agreement No 101017089)

NEEDLE	C8	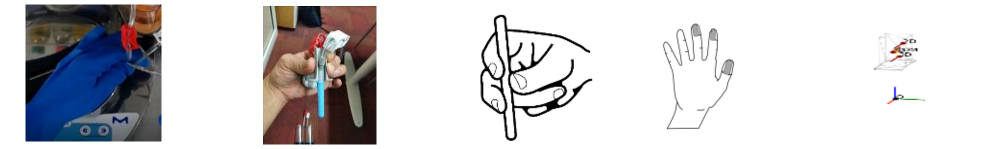
SCISSORS	C8	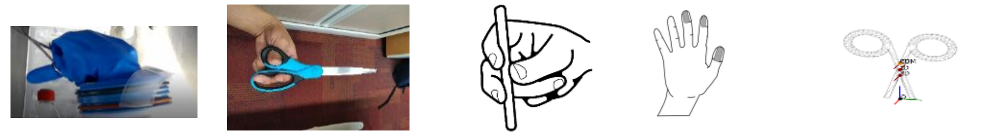
KIT	C11	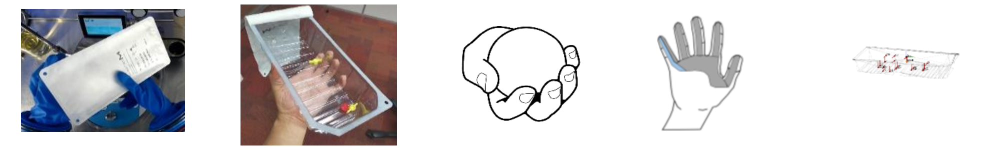
PETRI	C12	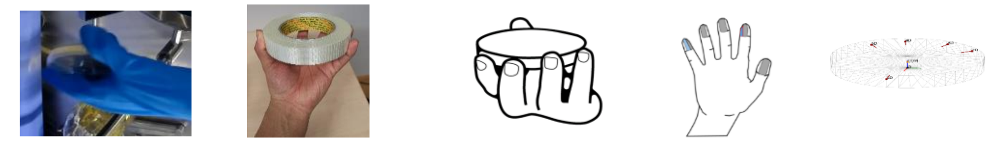
RINSE GLASS	C12	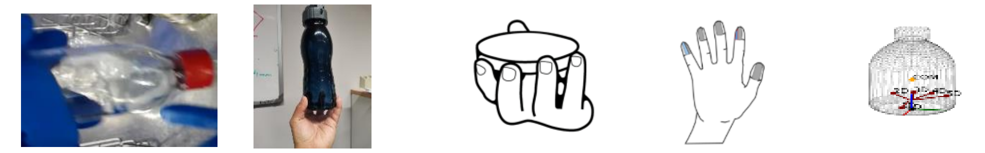
NEEDLE CAP	C14	
MARKER CAP	C16	
TUBE CLAMP	C16	
SCISSORS	C16	
TUBE	F17	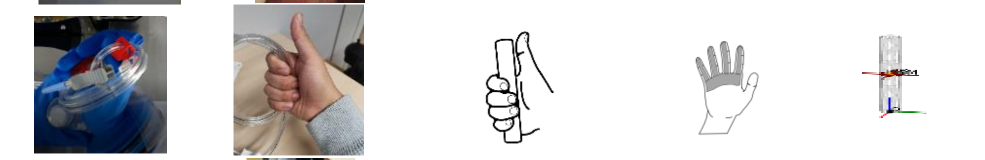
MARKER	F26	

Horizon 2020

TraceBOT receives funding from the European Union's H2020-EU.2.1.1. INDUSTRIAL LEADERSHIP programme (grant agreement No 101017089)

TUBE	F26					
RED PLUG	F26					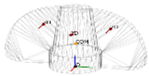
PETRI	F28	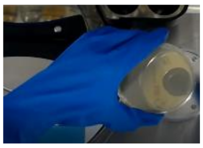				
MARKER	F28					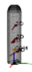
KIT	F28					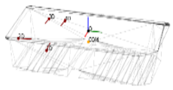

6.2.3 Considerations about external loads

One interest of the computation of stability equilibrium (P) lies in its ability to provide insight on the required level of effort to be applied at each contact points to counter *external disturbances*. The modeling hypothesis and numerical estimation of the *external disturbances* are then classified according to whether or not they are direction-dependent.

- The weight of the current object is seen as an *external disturbance* that is independent of the direction. Objects being grasped, lifted and manipulated over space randomly by the operator, gravitational effects can be directed along any axes of the object local frame. Thus, the required forces to be applied at contact points to withstand the object weight, action named “HOLD” in previous Table 6.1, are computed whatever the orientation of the object in space is.
- Other *external disturbances*, such as UNCAP, OPEN, INSERT, PIERCE, etc., have specific direction-dependent features: the assumed loads are caused by frictional forces to be overcome along certain privileged axes of the object frame, arising during the execution of certain tasks very specific to the use case (such as the insertion of the canister or the needle).

Horizon 2020

TraceBOT receives funding from the European Union's H2020-EU.2.1.1. INDUSTRIAL LEADERSHIP programme (grant agreement No 101017089)

Either voluntary pessimistic upper bound estimation of such effort or direct measurement using experimental test bench at CEA (Figure 6.3) have made possible the documentation of the loads magnitudes of efforts $\alpha d_{W_{ext}}$ in the problem formulation (P) for all objects (Table 4.1, reproduced below).

Table 6.3. Summary of estimated load magnitudes α^d of both direction-dependent and direction-independent external disturbances for all objects of the use-case.

Object	Weight (in N)	External disturbances										
		Direction-dependent perturbations applied to the object (in N)										
	HOLD	WRITE	UNCAP	RECAP	OPEN	INSERT	REMOVE	PIERCE	UNPIERCE	CLAMP	UNCLAMP	CUT
Petri dish	0.20	2.5	N.A.	N.A.	N.A.	N.A.	N.A.	N.A.	N.A.	N.A.	N.A.	N.A.
Marker	0.10	2.47	23.0	34.4	N.A.	N.A.	N.A.	N.A.	N.A.	N.A.	N.A.	N.A.
Marker cap	0.02	N.A.	23.0	34.4	N.A.	N.A.	N.A.	N.A.	N.A.	N.A.	N.A.	N.A.
Kit	1.70	N.A.	N.A.	N.A.	20.0	N.A.	N.A.	N.A.	N.A.	N.A.	N.A.	N.A.
Kit tab	0.004	N.A.	N.A.	N.A.	20.0	N.A.	N.A.	N.A.	N.A.	N.A.	N.A.	N.A.
Canister	0.04	N.A.	N.A.	N.A.	N.A.	87.2	110.0	N.A.	N.A.	N.A.	N.A.	N.A.
Tube	0.30	N.A.	N.A.	N.A.	N.A.	45.7	N.A.	N.A.	N.A.	N.A.	N.A.	N.A.
Needle	0.10	N.A.	9.4	N.A.	N.A.	N.A.	N.A.	23.4	11.0	N.A.	N.A.	N.A.
Needle cap	0.01	N.A.	9.4	N.A.	N.A.	N.A.	N.A.	N.A.	N.A.	N.A.	N.A.	N.A.
Rinse glass	5.51	N.A.	N.A.	N.A.	N.A.	N.A.	N.A.	N.A.	N.A.	N.A.	N.A.	N.A.
Red plug	0.01	N.A.	N.A.	N.A.	N.A.	35.9	23.0	N.A.	N.A.	N.A.	N.A.	N.A.
Glass vial	0.15	N.A.	N.A.	N.A.	30.0	N.A.	N.A.	N.A.	N.A.	N.A.	N.A.	N.A.
Yellow plug	0.01	N.A.	N.A.	N.A.	N.A.	2.3	N.A.	N.A.	N.A.	N.A.	N.A.	N.A.
Tube clamp	0.04	N.A.	N.A.	N.A.	N.A.	N.A.	N.A.	N.A.	N.A.	40.8	3.1	N.A.
Scissors	0.59	N.A.	N.A.	N.A.	N.A.	N.A.	N.A.	N.A.	N.A.	N.A.	N.A.	55.0

Figure 6.3: Identification of external disturbances magnitudes when replicating use-case manual gesture using force sensors and laboratory balance at CEA

Horizon 2020

TraceBOT receives funding from the European Union's H2020-EU.2.1.1. INDUSTRIAL LEADERSHIP programme (grant agreement No 101017089)

6.3 Preliminary results about force human-related considerations

In order to extract insights about human gesture capabilities, the previously presented grasp analysis methodology is carried out for all *ready-to-analyze grasp* using the metric (P).

6.3.1 Data analysis

A multi-parametric analysis that includes all the combinatorial combinations of parameters (*object data*, *grasp type settings* and *external perturbations*) is used to generate and store data for post-processing analysis. It helps better understanding the required theoretical levels of effort for achieving the use-case. Such task-centered grasp analysis is completed according to the following procedure.

Procedure for generating data analysis according to the use-case parameters

Inputs:
- meshed representation of the objects envelopes
- set of human hand grasp pattern from identified taxonomy
- set of objects identities
- parameters defining the external disturbances
Iterations:
for each meshed object :
    → Searching for grasp pattern used for grasping the current meshed object in the taxonomy (according to the video analysis);
    → Searching for external disturbances applied to the current meshed object (according to the video analysis and pre-computed estimated perturbation database);
    for each pair {object, grasp pattern}:
        → Identifying the number of contact points involved in the current grasp pattern;
        → Inferring a tuple of contact position on the objecs (according to the number of contacts as defined in the found grasp pattern);
        → Computing the grasp matrix G associated to each *ready-to-analyze grasp;*
        → Characterizing mathematical properties of the grasp matrix;
        for each external disturbances applied on the current meshed object:
            → Solving the optimization problem (P) ;
            → Storing the optimal values of f_c ;
        end
    end
end
Output:
- Multidimensional analysis matrix providing the optimal required efforts according to each combination of objects, grasps and external disturbances parameters

Horizon 2020

TraceBOT receives funding from the European Union's H2020-EU.2.1.1. INDUSTRIAL LEADERSHIP programme (grant agreement No 101017089)

Among the useful extracted information, the minimum required tightening force to be applied at contact points when holding the current object in order to perform the task (i.e. withstand the *external disturbances* applied on it) gives preliminary insights for further gripper design (Figure 6.4).

Comparing the required levels of effort between them highlights several analysis results.

- Realizing the tasks of the use-case involves a wide variety of effort levels to be produced, ranging from a few mN up to 80N;
- The majority of tasks (87%) that require moderate effort (less than 10N) deal with holding objects: these human hand grasps ensure to purely counterbalance the weight of the held object (i.e. HOLD) whatever the orientation of the object in space is;
- The tasks that require the highest levels of effort deal with specific use-case related operations that involve direction-dependent external disturbances (such as INSERT, PIERCE, etc.).

Among this last set of specific tasks, 5 tasks (or 6 tasks depending on the level of friction chosen for computing the object stability equilibrium, either pessimistic $\mu=0.3$ or optimistic $\mu=0.5$ level) require minimal human-based gesture force above 20N threshold. A focus on this limited set of tasks is summarized in Table 6.4:

- "*Red plug - INSERT*" corresponds to the action of plugging the object at the top of the canister;
- "*Canister - INSERT*" and "*Canister - REMOVE*" are to put and remove the canister from its holder;
- "*Needle - PIERCE*" is the action of inserting the needle into the rinse glass on the table;
- "*KIT- OPEN*" is the action of robustly holding the plastic kit box on one hand, while pulling on its tab with the second hand, in order to open it;
- "*Marker cap – RECAP*" and "*Marker cap – UNCAP*" are the actions of putting on and off the cap on the marker.

When dealing with compromise between force capabilities and mechanical compactness for multifingered gripper design, such force threshold value corresponds to a realistic upper bound of the physically reachable force value to be produced by a robotic gripper. Replicating these specific 5 (or 6) human-based gestures with a robotic multifingered gripper may not be effective in dealing with the disturbances experienced by the objects, and thus in successfully performing the tasks.

Horizon 2020

TraceBOT receives funding from the European Union's H2020-EU.2.1.1. INDUSTRIAL LEADERSHIP programme (grant agreement No 101017089)

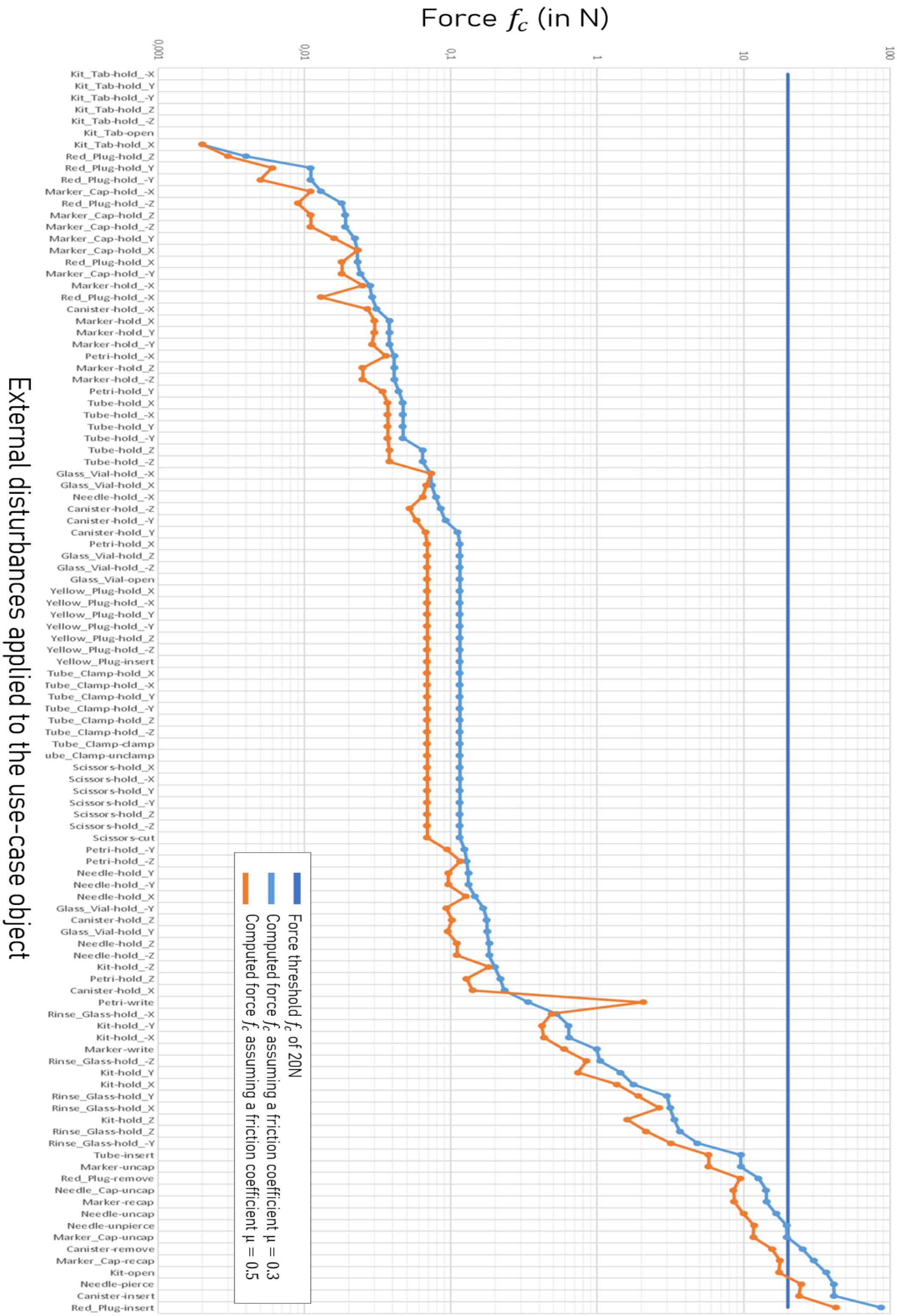

Figure 6.4: Theoretical required level of force to be applied at contact points of all objects as a function of external disturbances (computed forces assuming a pessimistic μ=0.3 and optimistic μ=0.5 friction coefficient in the HF contact modelling).

Horizon 2020

TraceBOT receives funding from the European Union's H2020-EU.2.1.1. INDUSTRIAL LEADERSHIP programme (grant agreement No 101017089)

Table 6.4. Set of tasks involving human-based grasps with generated force level above 20N threshold (let note that the last grasp involves force above 20N only in the case of pessimistic friction coefficient μ=0.3)

Object	**Grasp name**	**Object grasped by human hand**	**Hand grasp model**	**Hand contacts involved in the grasp**	**External disturbance**	**Theoretical level of effort $f_{c_{max}}$**
Red Plug	T21		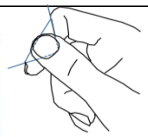		INSERT	81N
Canister	C1				INSERT	42N
Needle	T21	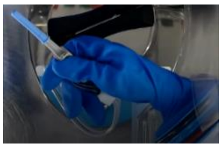			PIERCE	41N
Kit	C11		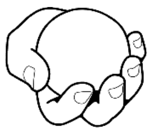		OPEN	37N
Marker Cap	C16	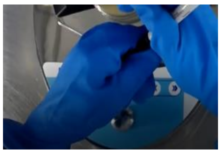			RECAP	30N
Canister	*C1*				*REMOVE*	*25N*

6.3.2 Recommendations for further analysis

This first insight tends to prove that considering a maximum amplitude of the force of 20N to be generated by the to-be-designed gripper is theoretically sufficient to counterbalance most of the external perturbations due to the own weight of the objects. Such contact forces that are applied either at the finger level or the palm authorize relatively significant stability margins when holding the objects. However, another lesson drawn from this analysis is that replicating human-like grasps with a purely anthropomorphic based gripper would require a huge amount of force (well above 20N) for

Horizon 2020

TraceBOT receives funding from the European Union's H2020-EU.2.1.1. INDUSTRIAL LEADERSHIP programme (grant agreement No 101017089)

certain tasks of the use-case, that remains excessive in view of the physical constraints of mechatronic design, in particular to actuation power.

Given the complexity of designing a human-like robotic gripper yet its inability to realize all tasks with a reasonably powerful actuation system, CEA decided to study the gain that could be obtained with a simpler design. These additional computations are presented in the next subsection.

6.4 Simplifying the human-inspired kinematics with respect to the task

An analysis has been made to reduce the complexity of human-like grasps kinematics, so as to converge to a streamlined mechatronic architecture for the gripper. This simplification finds its origin in the results of the previous study on the less used hand areas (see interaction maps in section 5). This study has shown that the little finger is less used than the other ones, suggesting that it could be removed if one wants to simplify the gripper design. Consequently, we decided to study the performance of a four-fingered device.

Indeed, one can choose to reduce the available contact areas, thus to tolerate a less significant range of grasp patterns, if it still allows to keep an acceptable stability margin when holding the objects. In a first approach, taking the previously studied full hand kinematics, along with its associated contact areas, grasp patterns and required force values as references, several simplified gripper parameters combinations have been successively evaluated:

0. Human-hand kinematics as reference, considering full 5 fingers made of distal (D), intermediate (I), proximal (P) phalanges, with the palm;
1. Gripper kinematics considering only 4 fingers made of two distal (D) and proximal (P) phalanges per finger, with the palm;
2. Gripper kinematics considering only 4 fingers made of one unique distal (D) phalange per finger with the palm, so as to restrict grasp patterns to distal ones and a limited set of power grasps.

The previous procedure for generating force analysis has been extended to take into account several batches of parameters related to the above gripper settings (0-1-2). Having reduced the number of phalanges in these configurations, let note that the resulting number of contact points has been re-evaluated accordingly for each gripper configuration.

Horizon 2020

TraceBOT receives funding from the European Union's H2020-EU.2.1.1. INDUSTRIAL LEADERSHIP programme (grant agreement No 101017089)

Modified procedure for generating data analysis according to the use-case parameters
Inputs: - meshed representation of the object envelops - set of human hand grasp pattern from identified taxonomy - set of object identities - parameters defining the external disturbances Iterations: for each meshed object : *for each tested gripper configuration chosen in the set of gripper parameters combinations :* → Searching for *gripper-dependent* grasp pattern used for grasping the current meshed object *while mimicking human-based grasp* from the taxonomy → Searching for external disturbances applied to the current meshed object (according to the video analysis and pre-computed estimated perturbation database) for each pair {object, grasp pattern}: → Identifying the number of contact points involved in the current grasp pattern → Inferring a tuple of contact position on the objects (according to the number of contacts as defined in the found grasp pattern) → Computing the grasp matrix G associated to each *ready-to-analyse grasp* for each external disturbances applied on the current meshed object: → Solving the optimization problem (P1) ; → Storing the optimal values of f_c ; end end *end* end Output: - Multidimensional analysis matrix providing the optimal required efforts according to each combination of *gripper configurations*, grasp parameters and external disturbances

Gripper settings with a high *number of contact* points are preferred (the maximum allowed in the study corresponding to the reference Human-hand kinematics) to increase grasp stability in face of external disturbances (Figure 6.5). As expected, reducing the *number of contact* points applied by the

Horizon 2020

TraceBOT receives funding from the European Union's H2020-EU.2.1.1. INDUSTRIAL LEADERSHIP programme (grant agreement No 101017089)

gripper on the objects tends to increase the required level of the contact forces to be generated by the gripper actuation system.

However, choosing 4 fingers instead of 5 fingers implies a very relative loss of stability margins and increase of the required tightening forces f_c ranging from 0% to 15% for all tasks. Most of the tasks implying such an increase of tightening forces level, when reducing the number of available contact areas (i.e. gripper settings 1 and 2), are still below the force threshold of 20N, and are thus acceptable.

Considering only 4 fingered gripper architectures leads to three additional tasks (namely “Marker – RECAP”, “Marker – UNCAP” and “Tube – INSERT”) that become above such force threshold, although at the cost of a price gain and a reduction in mechanical complexity in design (in particular, saving several actuators for controlling the motions associated to fifth finger). In the following, alternative non human-inspired grasp strategies using a four-fingered architecture comprising a palm will be investigated for accomplishing those tasks that require to deliver significant efforts at contact points.

Horizon 2020

TraceBOT receives funding from the European Union's H2020-EU.2.1.1. INDUSTRIAL LEADERSHIP programme (grant agreement No 101017089)

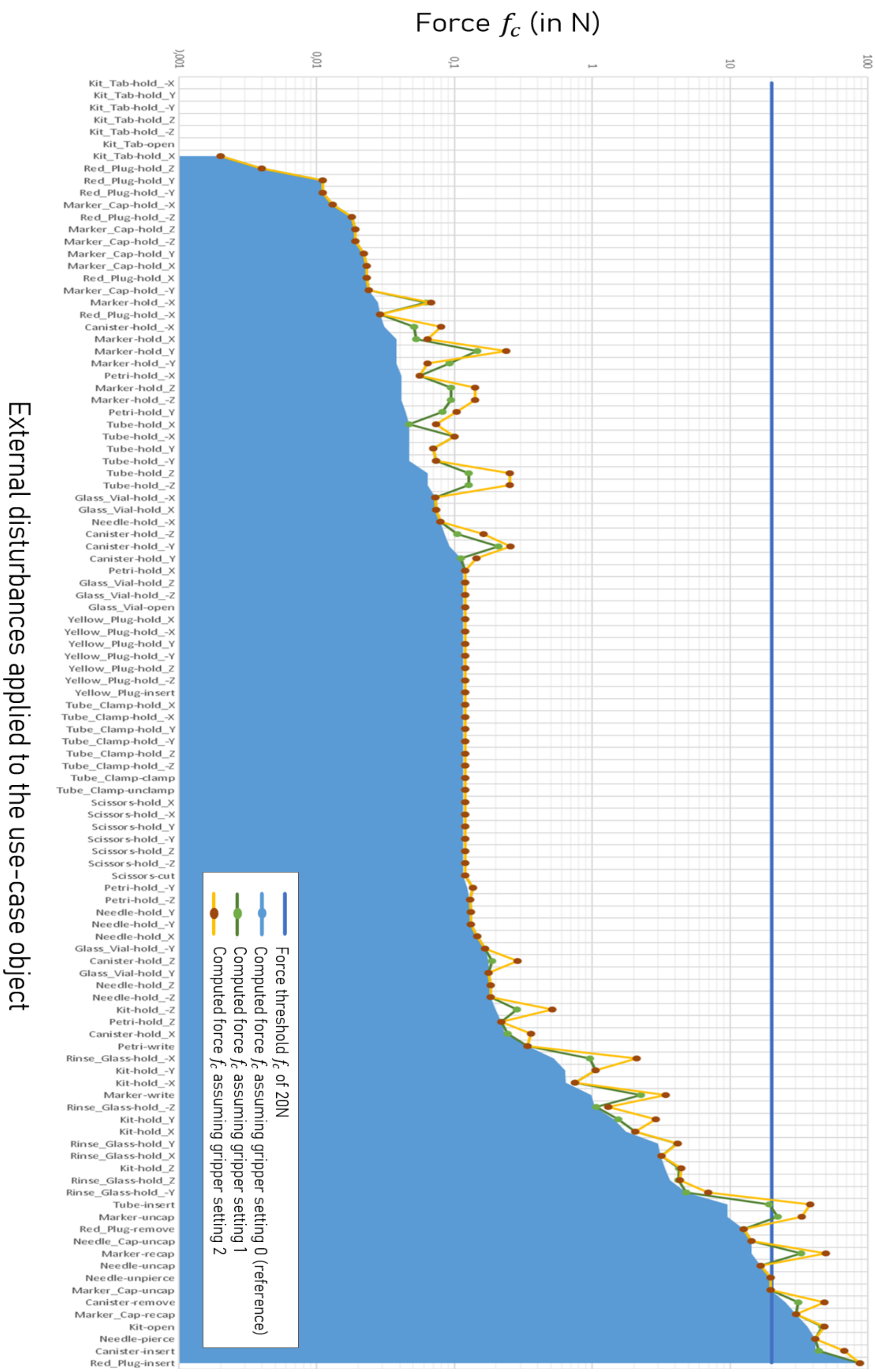

Figure 6.5. Comparing gripper settings with respect to theoretical required level of force to be applied at contact points (computed forces assuming a pessimistic μ=0.3 friction coefficient in the HF contact modelling)

Horizon 2020

TraceBOT receives funding from the European Union's H2020-EU.2.1.1. INDUSTRIAL LEADERSHIP programme (grant agreement No 101017089)

7 Robotic gripper-centered analysis

In this section, based on previous lessons from the theoretical use-case analysis, a robotic-centered design approach is adopted to get rid of the aforementioned limits. The data that have been generated so far according to considerations related to human gestures are crossed with practical considerations related to design constraints. Indeed, the above insights have to be studied / moderated in the light of the possibilities offered by the technological offer and the choice of certain components (such as actuators, etc.), the manufacturing and integration constraints (e.g. the size, weight of the system, etc.), the complexity and the cost resulting from the design (e.g. number actuated DoFs, etc.). Thus, depending on these practical constraints, a fine analysis of certain results (for example, the grasps to be authorized from the taxonomy) may allow the grasping requirements to be met via several alternative gripper architectures. The output of this section consists in providing feasible technical specifications related to the to-be-designed robotic gripper.

7.1 Design rules for a gripper architecture

Until now, the framework for grasp study has been centered on the human hand analysis, which is a fundamental aspect in the design of the gripper. According to [ElKoura et al. 2003], the human hand (including the wrist) has 27 degrees of freedom: four for index, middle, ring, and pinky fingers, five for the thumb, and, six for the wrist. This complex kinematics allows the human hand to perform dexterous and fine manipulation that may require a high amount of force.

Since the gripper is intended to be used in the sterility test process, which is performed by human hands, the most obvious solution would be to design a gripper with the same characteristics as the human hand. However, in practice, the design and construction of the gripper would be complex due to the number of degrees of freedom and the actuation system. Considering the information provided by Figure 6.1 on section 6, we can observe that the gripper must be capable to provide more than 20 N to resist perturbations presented on the TraceBot use-case. Therefore, designing a gripper able to provide such an amount of force will lead to the integration of robust transmissions, which will considerably increase the mass and volume of the gripper; consequently, it may be necessary to use a bigger and more expensive robot arm. For these reasons, it is necessary to realize a gripper with a simpler kinematics than the human hand but capable of performing the tasks described in Table 6.2.

Horizon 2020

TraceBOT receives funding from the European Union's H2020-EU.2.1.1. INDUSTRIAL LEADERSHIP programme (grant agreement No 101017089)

To obtain a suitable gripper kinematic architecture we follow the following steps:

1. Define a provisional architecture for the gripper.
2. Using such defined preliminary gripper design, attempt to replicate human grasp patterns of the TraceBot use-case (Table 6.2).
3. Propose alternative non-human-based grasp patterns for the grasp where the amount of force exceeds 20N.
4. Analyze the joint positions of the fingers of the preliminary gripper in order to suggest simpler kinematic architectures for the final gripper design.
5. Examine the resulting grasps obtained by the preliminary gripper factorizing similar grasp patterns.
6. Using the alternative non-human-based grasps and the factorized ones, propose a new grasp classification (i.e. a robotic-type taxonomy).
7. Replicate the proposed robotic grasp patterns with the suggested simpler kinematic architectures.

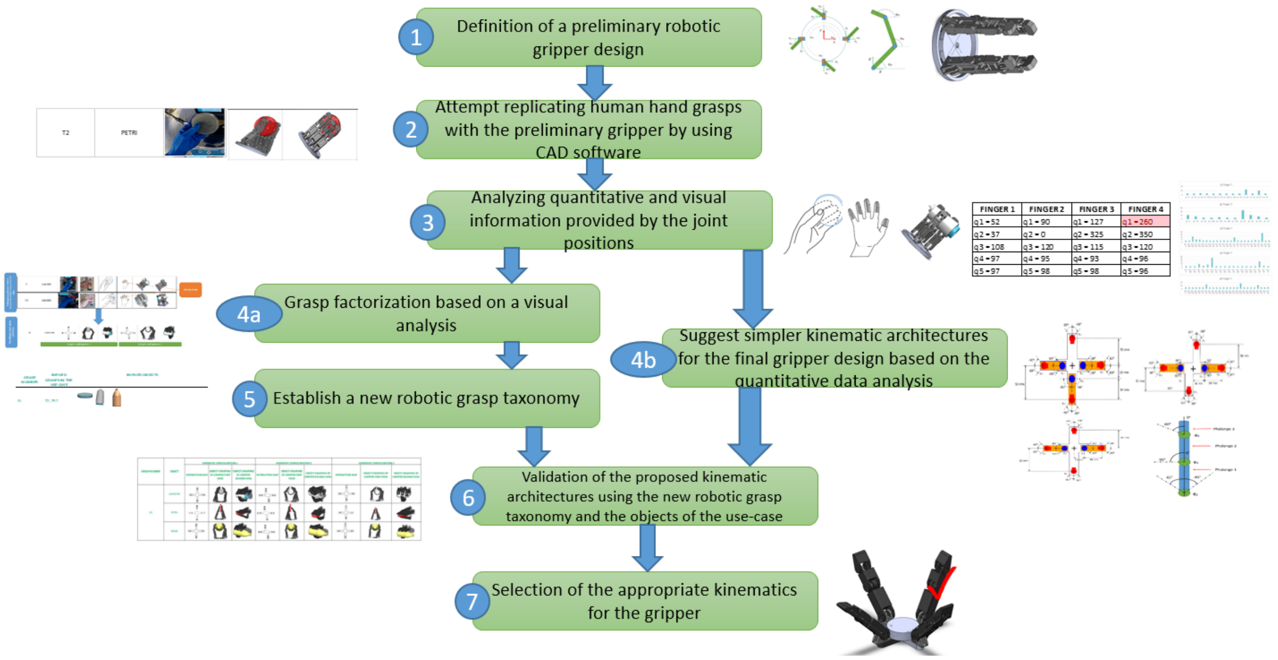

Figure 7.1: Summary of the rules for the kinematic architecture for the gripper.

These steps will provide us with criteria to define:

1. The final kinematic configuration for the gripper.

Horizon 2020

TraceBOT receives funding from the European Union's H2020-EU.2.1.1. INDUSTRIAL LEADERSHIP programme (grant agreement No 101017089)

2. The dimensions of the phalanges and the palm.
3. The regions where to place the tactile sensors in the fingers and the palm.

From mapping from human grasp to robotic grasp, let us consider Table 6.2 in section 6, which provides us insights about human grasps involved in the TraceBot use-case. This table presents 81 human hand grasps, resulting from 46 grasp patterns applied at least one time to one of the 15 objects of the use-case as is summarized 1n Table. 7.1.

7.2 Initial gripper configuration

In this subsection, we proposed an initial 20 degrees-of freedom gripper architecture in order to replicate the grasp patterns of the human hand. Four fingers (five degrees of freedom per finger) compose the preliminary gripper architecture. Figure 7.2 represents the preliminary kinematic configuration of the gripper used to replicate the human hand grasps involved in the use-case. The angles are measured from the horizontal axis of each local reference frame, as shown in the figure. The function of each joint is described as follows:

- q_{1i}, regulates the rotational motion of each finger around the palm.
- q_{2i}, is used to rotate each finger around z- axis.
- q_{3i}, performs the flexion-extension motion of the proximal phalange (P).
- q_{4i}, performs the flexion-extension motion of the intermediate phalange (I).
- q_{5i} performs the flexion-extension motion of the distal phalange (D).

For the palm, we set a circular design with 100 mm in diameter. We have selected this dimension taking into consideration the size of the base of the larger object used in the use-case, which is the Rinse glass, whose base has a radius of 97 mm.

The lengths of each phalange are established as follows:

- Proximal phalange: 62 mm
- Intermediate phalange: 37 mm
- Distal phalange: 28 mm

Moreover, the width of each phalanx was set at 27 mm. The proposed dimensions for the phalanges have a ratio of 1:1.5 with respect to the dimensions of the human hand. We consider this relationship because slightly larger phalanges to human ones will provide us with an increased contact surface

Horizon 2020

TraceBOT receives funding from the European Union's H2020-EU.2.1.1. INDUSTRIAL LEADERSHIP programme (grant agreement No 101017089)

with the object (ensuring better grasp stability), while providing also enough space to place tactile sensors and their corresponding electronics.

GRASP FRECUENCY BY OBJECT															
GRASP	PETRI	CANISTER	RINSE GLASS	MARKER	MARKER CAP	NEEDLE	NEEDLE CAP	TUBE CLAMP	TUBE	RED PLUG	YELLOW PLUG	KIT TAB	KIT	SCISSORS	GLASS VIAL
T2	■	■	■												
T3	■														
T4	■						■		■						
T7	■														
T8	■														
T9				■											
T10				■											
T13				■											
T16				■											
T17					■				■						
T18	■	■	■	■											
T21						■				■	■	■			
T22													■		
T23									■						
T24									■						
T26		■													
T27									■						
T28						■	■	■	■						
T29									■						
T30									■						
T33						■									
T34			■												
T35			■										■		
T38			■												
T39			■												
T45															■
T51			■												
T53					■										
T57		■													
T58			■												
T60						■									
T65								■							
T68														■	
T68_														■	
T69			■												
T70									■						
C1		■													
C2									■						
C6	■	■	■						■				■		
C7									■				■		
C8	■	■		■		■			■				■	■	
C11													■		
C12	■		■												
C14							■								
C16					■			■						■	
F17									■						
F26				■					■	■					
F28	■			■									■		

Table 7.1: Summary of human hand grasps involved on the TraceBot use-case.

Horizon 2020

TraceBOT receives funding from the European Union's H2020-EU.2.1.1. INDUSTRIAL LEADERSHIP programme (grant agreement No 101017089)

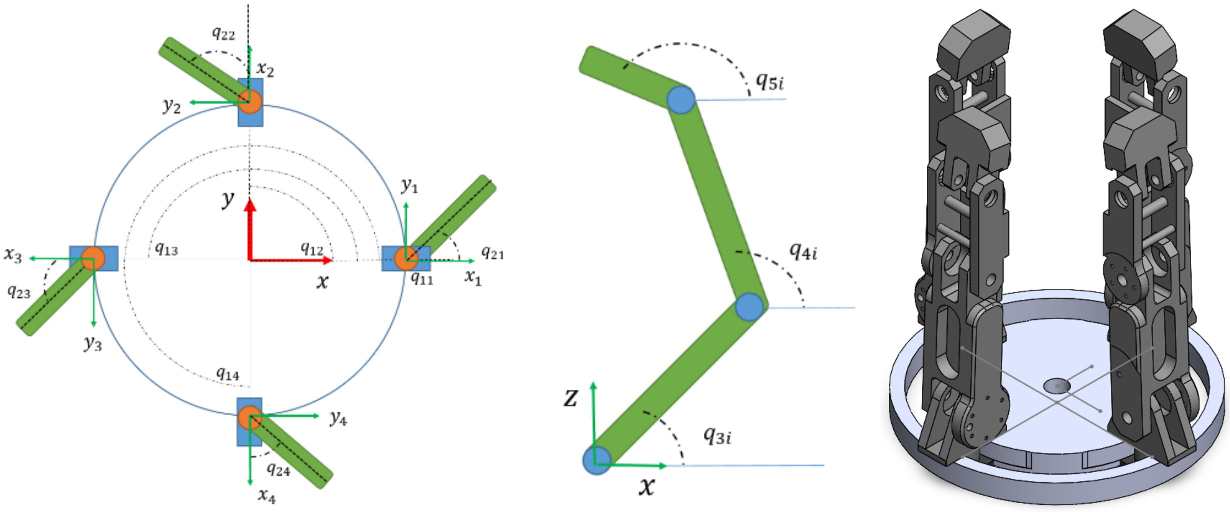

Figure 7.2: Scheme of the kinematics of the preliminary gripper design (left: configuration of the circular palm, middle: configuration of the fingers' phalanges, right: CAD illustration).

7.3 Mapping from human grasps to robotic grasps

In the following, the grasp patterns obtained with our proposed initial gripper kinematics are detailed, in attempting to replicate the grasps performed by the human hand in the use-case. These grasp patterns are provided in Table 7.2, whose columns organize the information in the following form:

1. Object involved in the analysis;
2. Name of the grasp based on Cutkosky's, Feix's, or TraceBot's taxonomy;
3. Visualization of the grasp performed by the gripper in CAD software;
4. Alternative visualization of the current grasp performed by the gripper in CAD software;
5. Location of the contact points in the object (where the red circles represent contact points viewed from the front, while the blue ones represent contact points viewed from the rear side);
6. Joint configuration of the gripper (providing the angular displacements[2] of the five revolute joints related to the four-fingered gripper).

[2] The joint angles are measured from the horizontal local axis of each joint as illustrated in Figure 7.2.

Horizon 2020

TraceBOT receives funding from the European Union's H2020-EU.2.1.1. INDUSTRIAL LEADERSHIP programme (grant agreement No 101017089)

The following exhaustive list that documents the mapping from human grasps to practical robotic grasps will provide us information about the minimum number of degrees of freedom to be considered in the final gripper design, as well as the required range of motion of each joint[3], to perform all the grasps. It guides CEA towards a gripper architecture, whose complexity in terms of kinematics and number of degrees-of-freedom is rationalized with respect to the targeted TraceBot grasp patterns. Indeed, considering complex kinematics embedding extra actuated degrees-of-freedom may imply more sophisticated designs leading to mechanical motor-to-joint transmissions that are difficult to achieve in practice, and to an increase volume and weight of the gripper.

[3] Thus, no restrictions on the range of displacement of the joints have been considered in the simulated grasps.

Horizon 2020

TraceBOT receives funding from the European Union's H2020-EU.2.1.1. INDUSTRIAL LEADERSHIP programme (grant agreement No 101017089)

Table 7.2: List of all mappings between object and gripper grasps involved in the use-case.

Object	Grasp name	Object grasped by gripper: First CAD visualization	Second CAD visualization	Location of contact points	Joint configuration of the gripper			
PETRI	T2	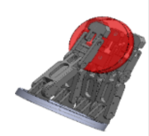	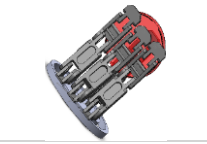	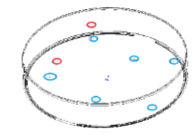	q1 = 52 q2 = 37 q3 = 108 q4 = 97 q5 = 97	q1 = 90 q2 = 0 q3 = 120 q4 = 95 q5 = 98	q1 = 127 q2 = 325 q3 = 115 q4 = 93 q5 = 98	q1 = 260 q2 = 350 q3 = 120 q4 = 96 q5 = 96
CANISTE R	T2	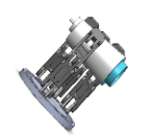	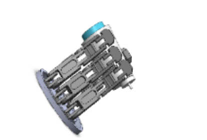	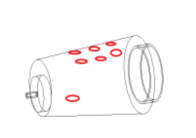	q1 = 52 q2 = 37 q3 = 108 q4 = 97 q5 = 97	q1 = 90 q2 = 0 q3 = 120 q4 = 95 q5 = 98	q1 = 127 q2 = 325 q3 = 115 q4 = 93 q5 = 98	q1 = 260 q2 = 350 q3 = 80 q4 = 96 q5 = 130
RINSE GLASS K	T2	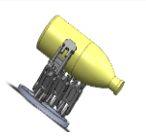	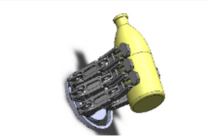	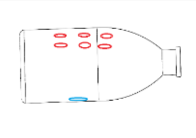	q1 = 52 q2 = 37 q3 = 108 q4 = 97 q5 = 97	q1 = 90 q2 = 0 q3 = 120 q4 = 95 q5 = 98	q1 = 127 q2 = 325 q3 = 115 q4 = 93 q5 = 98	q1 = 260 q2 = 350 q3 = 55 q4 = 96 q5 = 110
PETRI	T3		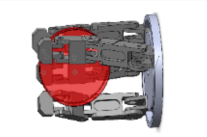	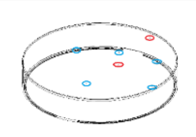	q1 = 45 q2 = 45 q3 = 100 q4 = 109 q5 = 90	q1 = 90 q2 = 0 q3 = 120 q4 = 95 q5 = 98	q1 = 150 q2 = 325 q3 = 85 q4 = 130 q5 = 96	q1 = 300 q2 = 220 q3 = 65 q4 = 86 q5 = 90
PETRI	T4		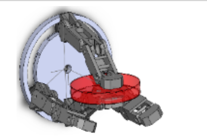	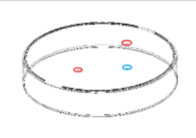	q1 = 30 q2 = 37 q3 = 85 q4 = 90 q5 = 90	q1 = 90 q2 = 0 q3 = 120 q4 = 95 q5 = 98	q1 = 150 q2 = 325 q3 = 80 q4 = 90 q5 = 90	q1 = 270 q2 = 0 q3 = 100 q4 = 130 q5 = 95
TUBE	T4		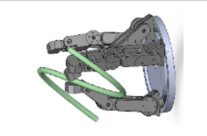	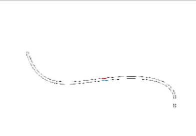	q1 = 30 q2 = 37 q3 = 85 q4 = 90 q5 = 90	q1 = 90 q2 = 0 q3 = 120 q4 = 95 q5 = 113	q1 = 150 q2 = 325 q3 = 80 q4 = 90 q5 = 90	q1 = 270 q2 = 0 q3 = 100 q4 = 130 q5 = 95
NEEDLE CAP	T4		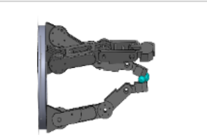	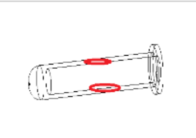	q1 = 30 q2 = 37 q3 = 85 q4 = 90 q5 = 90	q1 = 90 q2 = 0 q3 = 120 q4 = 95 q5 = 113	q1 = 150 q2 = 325 q3 = 80 q4 = 90 q5 = 90	q1 = 270 q2 = 0 q3 = 100 q4 = 130 q5 = 95
PETRI	T7		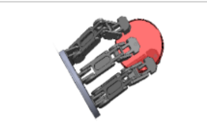	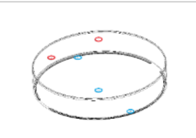	q1 = 30 q2 = 37 q3 = 73 q4 = 150 q5 = 90	q1 = 90 q2 = 0 q3 = 90 q4 = 160 q5 = 96	q1 = 150 q2 = 300 q3 = 75 q4 = 140 q5 = 90	q1 = 230 q2 = 320 q3 = 108 q4 = 90 q5 = 90
PETRI	T8			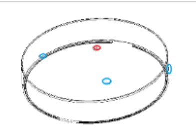	q1 = 0 q2 = 37 q3 = 73 q4 = 150 q5 = 160	q1 = 90 q2 = 0 q3 = 90 q4 = 160 q5 = 180	q1 = 150 q2 = 300 q3 = 60 q4 = 120 q5 = 150	q1 = 230 q2 = 350 q3 = 80 q4 = 160 q5 = 120
MARKER	T9		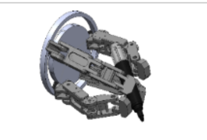	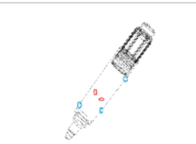	q1 = 30 q2 = 350 q3 = 120 q4 = 110 q5 = 130	q1 = 90 q2 = 310 q3 = 75 q4 = 135 q5 = 98	q1 = 150 q2 = 30 q3 = 65 q4 = 130 q5 = 115	q1 = 230 q2 = 0 q3 = 85 q4 = 130 q5 = 95

Horizon 2020

TraceBOT receives funding from the European Union's H2020-EU.2.1.1. INDUSTRIAL LEADERSHIP programme (grant agreement No 101017089)

MARKER	T10		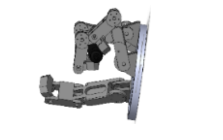	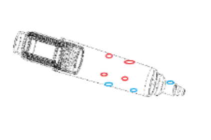	q1 = 20 q2 = 70 q3 = 20 q4 = 140 q5 = 225	q1 = 90 q2 = 0 q3 = 105 q4 = 180 q5 = 280	q1 = 135 q2 = 315 q3 = 85 q4 = 185 q5 = 266	q1 = 220 q2 = 0 q3 = 60 q4 = 90 q5 = 150
MARKER	T13			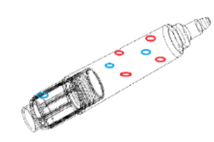	q1 = 321 q2 = 300 q3 = 60 q4 = 100 q5 = 180	q1 = 90 q2 = 25 q3 = 85 q4 = 185 q5 = 260	q1 = 150 q2 = 330 q3 = 85 q4 = 185 q5 = 266	q1 = 230 q2 = 90 q3 = 65 q4 = 185 q5 = 220
MARKER	T16		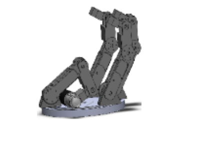	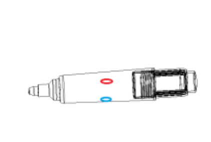	q1 = 330 q2 = 300 q3 = 60 q4 = 90 q5 = 150	q1 = 90 q2 = 0 q3 = 145 q4 = 250 q5 = 330	q1 = 220 q2 = 50 q3 = 75 q4 = 140 q5 = 90	q1 = 270 q2 = 0 q3 = 60 q4 = 90 q5 = 150
MARKER CAP	T17	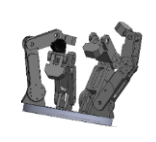		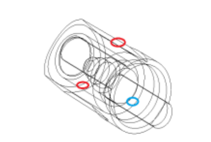	q1 = 46 q2 = 0 q3 = 65 q4 = 140 q5 = 225	q1 = 90 q2 = 338 q3 = 128 q4 = 180 q5 = 250	q1 = 180 q2 = 0 q3 = 75 q4 = 153 q5 = 185	q1 = 330 q2 = 0 q3 = 60 q4 = 90 q5 = 150
TUBE	T17	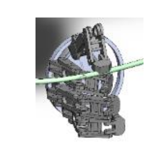	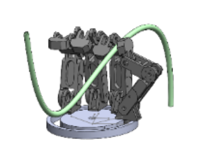		q1 = 45 q2 = 20 q3 = 90 q4 = 140 q5 = 225	q1 = 90 q2 = 345 q3 = 100 q4 = 130 q5 = 210	q1 = 135 q2 = 300 q3 = 75 q4 = 145 q5 = 180	q1 = 0 q2 = 15 q3 = 50 q4 = 160 q5 = 105
PETRI	T18	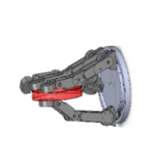		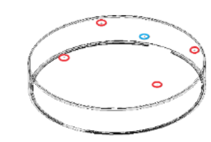	q1 = 60 q2 = 30 q3 = 110 q4 = 95 q5 = 98	q1 = 120 q2 = 330 q3 = 110 q4 = 95 q5 = 98	q1 = 180 q2 = 325 q3 = 70 q4 = 90 q5 = 90	q1 = 270 q2 = 0 q3 = 100 q4 = 130 q5 = 95
MARKER	T18		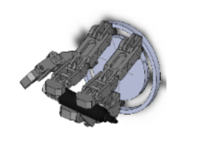	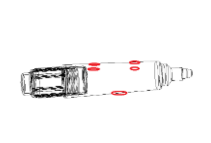	q1 = 60 q2 = 30 q3 = 110 q4 = 95 q5 = 98	q1 = 120 q2 = 330 q3 = 110 q4 = 95 q5 = 98	q1 = 180 q2 = 325 q3 = 70 q4 = 90 q5 = 90	q1 = 270 q2 = 0 q3 = 98 q4 = 130 q5 = 95
CANISTER	T18	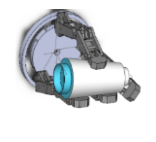		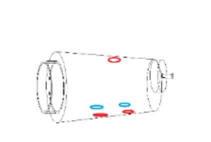	q1 = 60 q2 = 30 q3 = 110 q4 = 95 q5 = 98	q1 = 120 q2 = 330 q3 = 110 q4 = 95 q5 = 98	q1 = 180 q2 = 325 q3 = 70 q4 = 90 q5 = 90	q1 = 270 q2 = 0 q3 = 75 q4 = 115 q5 = 100
RINSE GLASS K	T18		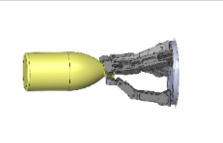	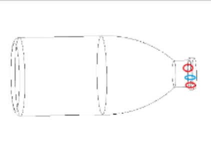	q1 = 45 q2 = 0 q3 = 110 q4 = 95 q5 = 98	q1 = 120 q2 = 350 q3 = 110 q4 = 95 q5 = 98	q1 = 180 q2 = 325 q3 = 70 q4 = 90 q5 = 90	q1 = 270 q2 = 0 q3 = 98 q4 = 130 q5 = 95
KIT TAB	T21	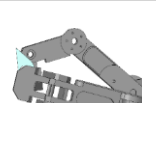		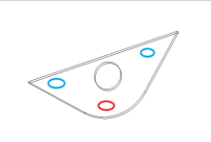	q1 = 40 q2 = 320 q3 = 87 q4 = 170 q5 = 90	q1 = 110 q2 = 340 q3 = 65 q4 = 120 q5 = 200	q1 = 180 q2 = 0 q3 = 75 q4 = 120 q5 = 120	q1 = 270 q2 = 0 q3 = 60 q4 = 90 q5 = 150
NEEDLE	T21	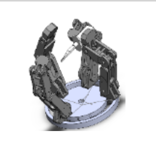		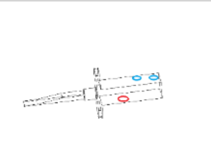	q1 = 40 q2 = 320 q3 = 75 q4 = 160 q5 = 90	q1 = 110 q2 = 340 q3 = 65 q4 = 120 q5 = 200	q1 = 180 q2 = 0 q3 = 75 q4 = 120 q5 = 120	q1 = 270 q2 = 0 q3 = 60 q4 = 90 q5 = 150

Horizon 2020

TraceBOT receives funding from the European Union's H2020-EU.2.1.1. INDUSTRIAL LEADERSHIP programme (grant agreement No 101017089)

YELLOW PLUG	T21	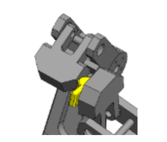	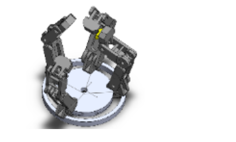	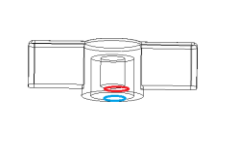	q1 = 40 q2 = 320 q3 = 77 q4 = 170 q5 = 95	q1 = 110 q2 = 340 q3 = 65 q4 = 120 q5 = 200	q1 = 180 q2 = 0 q3 = 75 q4 = 120 q5 = 120	q1 = 270 q2 = 0 q3 = 60 q4 = 90 q5 = 150
RED PLUG	T21	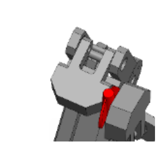	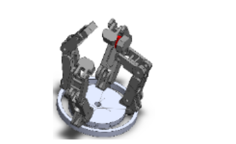	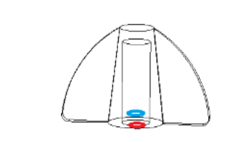	q1 = 40 q2 = 320 q3 = 80 q4 = 170 q5 = 95	q1 = 110 q2 = 340 q3 = 65 q4 = 120 q5 = 200	q1 = 180 q2 = 0 q3 = 75 q4 = 120 q5 = 120	q1 = 270 q2 = 0 q3 = 60 q4 = 90 q5 = 150
KIT	T22	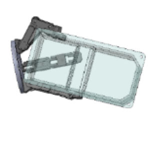	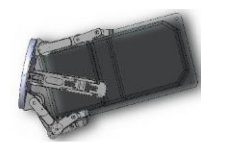	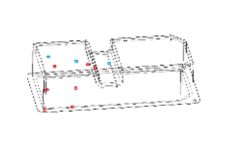	q1 = 330 q2 = 350 q3 = 39 q4 = 120 q5 = 110	q1 = 115 q2 = 10 q3 = 65 q4 = 60 q5 = 75	q1 = 220 q2 = 95 q3 = 95 q4 = 90 q5 = 90	q1 = 290 q2 = 55 q3 = 52 q4 = 135 q5 = 115
TUBE	T23	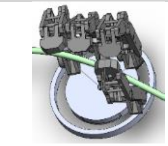	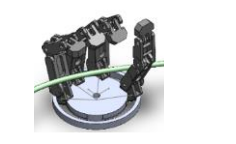		q1 = 45 q2 = 45 q3 = 90 q4 = 140 q5 = 225	q1 = 90 q2 = 0 q3 = 100 q4 = 130 q5 = 210	q1 = 135 q2 = 320 q3 = 75 q4 = 145 q5 = 180	q1 = 330 q2 = 60 q3 = 75 q4 = 90 q5 = 90
TUBE	T24	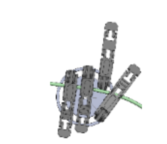	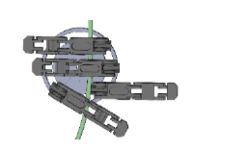	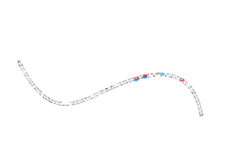	q1 = 45 q2 = 45 q3 = 0 q4 = 0 q5 = 0	q1 = 90 q2 = 0 q3 = 185 q4 = 185 q5 = 180	q1 = 135 q2 = 320 q3 = 185 q4 = 185 q5 = 180	q1 = 320 q2 = 80 q3 = 185 q4 = 185 q5 = 180
CANISTER	T26		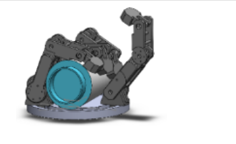	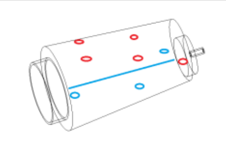	q1 = 45 q2 = 45 q3 = 120 q4 = 210 q5 = 250	q1 = 90 q2 = 0 q3 = 135 q4 = 175 q5 = 250	q1 = 135 q2 = 320 q3 = 110 q4 = 195 q5 = 215	q1 = 270 q2 = 0 q3 = 50 q4 = 90 q5 = 150
TUBE	T27	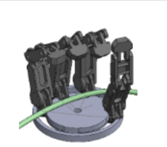	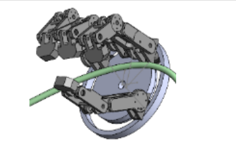	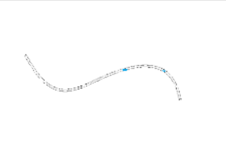	q1 = 45 q2 = 45 q3 = 90 q4 = 140 q5 = 225	q1 = 90 q2 = 0 q3 = 100 q4 = 130 q5 = 210	q1 = 135 q2 = 320 q3 = 75 q4 = 145 q5 = 180	q1 = 330 q2 = 60 q3 = 75 q4 = 90 q5 = 90
TUBE	T28	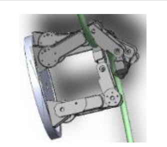	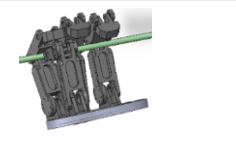	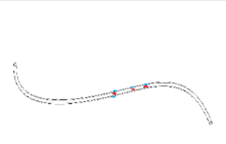	q1 = 45 q2 = 45 q3 = 90 q4 = 140 q5 = 225	q1 = 90 q2 = 0 q3 = 100 q4 = 130 q5 = 210	q1 = 135 q2 = 320 q3 = 75 q4 = 145 q5 = 180	q1 = 220 q2 = 320 q3 = 88 q4 = 185 q5 = 180
NEEDLE	T28			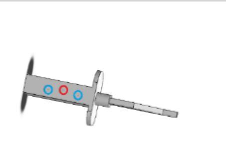	q1 = 45 q2 = 60 q3 = 90 q4 = 140 q5 = 225	q1 = 90 q2 = 15 q3 = 100 q4 = 130 q5 = 210	q1 = 135 q2 = 345 q3 = 75 q4 = 145 q5 = 180	q1 = 220 q2 = 275 q3 = 100 q4 = 185 q5 = 180
NEEDLE CAP	T28		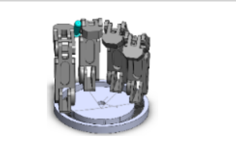	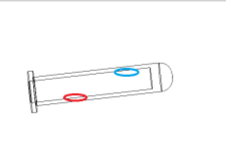	q1 = 45 q2 = 60 q3 = 90 q4 = 140 q5 = 225	q1 = 90 q2 = 15 q3 = 100 q4 = 130 q5 = 210	q1 = 135 q2 = 345 q3 = 75 q4 = 145 q5 = 180	q1 = 282 q2 = 275 q3 = 105 q4 = 185 q5 = 180
TUBE CLAMP	T28		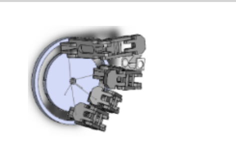	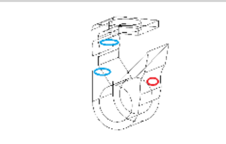	q1 = 45 q2 = 60 q3 = 90 q4 = 140 q5 = 225	q1 = 90 q2 = 15 q3 = 100 q4 = 130 q5 = 210	q1 = 135 q2 = 345 q3 = 75 q4 = 145 q5 = 180	q1 = 220 q2 = 270 q3 = 110 q4 = 185 q5 = 180

Horizon 2020

TraceBOT receives funding from the European Union's H2020-EU.2.1.1. INDUSTRIAL LEADERSHIP programme (grant agreement No 101017089)

TUBE	T29	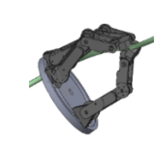	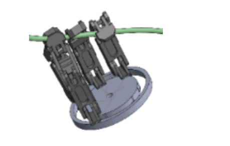	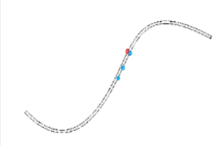	q1 = 45 q2 = 45 q3 = 90 q4 = 140 q5 = 225	q1 = 90 q2 = 0 q3 = 100 q4 = 130 q5 = 150	q1 = 135 q2 = 320 q3 = 75 q4 = 140 q5 = 110	q1 = 220 q2 = 320 q3 = 85 q4 = 140 q5 = 110
TUBE	T30	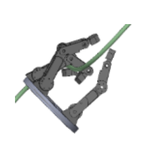		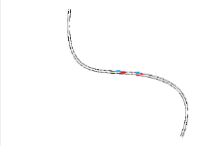	q1 = 45 q2 = 45 q3 = 90 q4 = 200 q5 = 310	q1 = 90 q2 = 0 q3 = 110 q4 = 170 q5 = 270	q1 = 135 q2 = 320 q3 = 75 q4 = 120 q5 = 110	q1 = 220 q2 = 320 q3 = 75 q4 = 120 q5 = 110
NEEDLE	T33			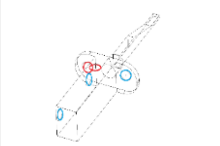	q1 = 45 q2 = 20 q3 = 90 q4 = 140 q5 = 225	q1 = 90 q2 = 345 q3 = 100 q4 = 130 q5 = 210	q1 = 135 q2 = 300 q3 = 75 q4 = 145 q5 = 180	q1 = 290 q2 = 100 q3 = 100 q4 = 185 q5 = 180
RINSE GLASS K	T34	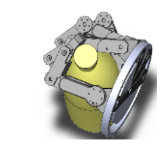	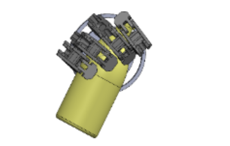	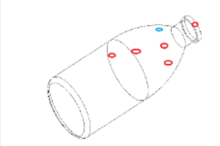	q1 = 45 q2 = 20 q3 = 110 q4 = 145 q5 = 227	q1 = 90 q2 = 345 q3 = 90 q4 = 150 q5 = 195	q1 = 135 q2 = 300 q3 = 50 q4 = 150 q5 = 170	q1 = 315 q2 = 73 q3 = 85 q4 = 185 q5 = 200
KIT	T35		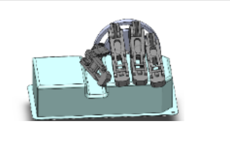	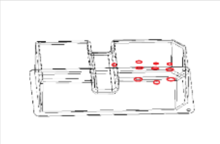	q1 = 45 q2 = 70 q3 = 96 q4 = 90 q5 = 100	q1 = 90 q2 = 15 q3 = 120 q4 = 90 q5 = 100	q1 = 135 q2 = 338 q3 = 115 q4 = 95 q5 = 95	q1 = 190 q2 = 25 q3 = 55 q4 = 130 q5 = 115
RINSE GLASS K	T35		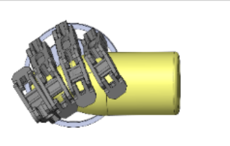	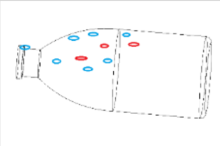	q1 = 45 q2 = 70 q3 = 98 q4 = 142 q5 = 205	q1 = 90 q2 = 15 q3 = 112 q4 = 143 q5 = 195	q1 = 135 q2 = 338 q3 = 110 q4 = 158 q5 = 220	q1 = 225 q2 = 291 q3 = 100 q4 = 185 q5 = 240
RINSE GLASS K	T38	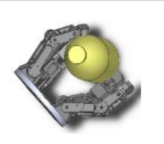		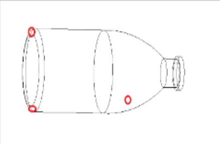	q1 = 0 q2 = 0 q3 = 45 q4 = 85 q5 = 90	q1 = 60 q2 = 15 q3 = 45 q4 = 85 q5 = 90	q1 = 135 q2 = 338 q3 = 45 q4 = 85 q5 = 90	q1 = 225 q2 = 0 q3 = 75 q4 = 118 q5 = 122
RINSE GLASS A	T39	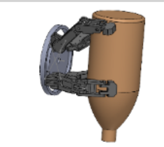	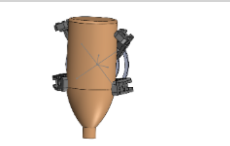	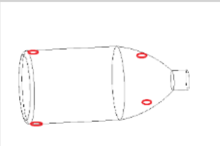	q1 = 320 q2 = 60 q3 = 45 q4 = 110 q5 = 90	q1 = 45 q2 = 15 q3 = 45 q4 = 85 q5 = 90	q1 = 142 q2 = 338 q3 = 45 q4 = 85 q5 = 90	q1 = 225 q2 = 30 q3 = 70 q4 = 110 q5 = 122
GLASS VIAL	T45		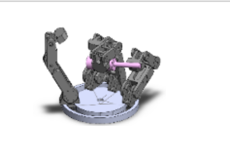	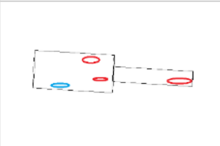	q1 = 30 q2 = 70 q3 = 25 q4 = 140 q5 = 210	q1 = 90 q2 = 0 q3 = 105 q4 = 180 q5 = 280	q1 = 135 q2 = 315 q3 = 25 q4 = 140 q5 = 180	q1 = 220 q2 = 0 q3 = 60 q4 = 90 q5 = 150
RINSE GLASS	T51	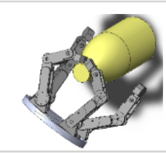		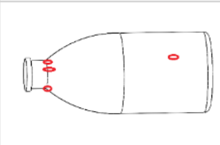	q1 = 330 q2 = 60 q3 = 90 q4 = 85 q5 = 90	q1 = 60 q2 = 300 q3 = 60 q4 = 130 q5 = 160	q1 = 135 q2 = 50 q3 = 75 q4 = 140 q5 = 160	q1 = 225 q2 = 45 q3 = 45 q4 = 90 q5 = 90
MARKER CAP	T53		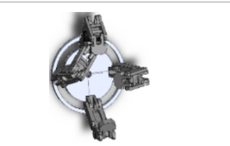	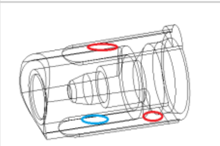	q1 = 0 q2 = 0 q3 = 65 q4 = 140 q5 = 225	q1 = 90 q2 = 0 q3 = 45 q4 = 120 q5 = 180	q1 = 175 q2 = 50 q3 = 110 q4 = 210 q5 = 185	q1 = 270 q2 = 0 q3 = 60 q4 = 90 q5 = 150

Horizon 2020

TraceBOT receives funding from the European Union's H2020-EU.2.1.1. INDUSTRIAL LEADERSHIP programme (grant agreement No 101017089)

CANISTER	T57			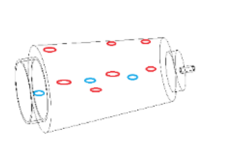	q1 = 45 q2 = 45 q3 = 90 q4 = 140 q5 = 225	q1 = 90 q2 = 0 q3 = 100 q4 = 130 q5 = 210	q1 = 135 q2 = 320 q3 = 75 q4 = 145 q5 = 180	q1 = 270 q2 = 0 q3 = 60 q4 = 160 q5 = 180
RINSE GLASS	T58			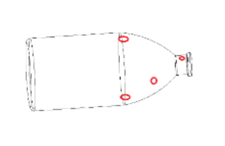	q1 = 330 q2 = 60 q3 = 90 q4 = 110 q5 = 150	q1 = 60 q2 = 0 q3 = 100 q4 = 120 q5 = 150	q1 = 135 q2 = 50 q3 = 55 q4 = 140 q5 = 160	q1 = 225 q2 = 45 q3 = 45 q4 = 100 q5 = 140
NEEDLE	T60	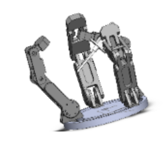	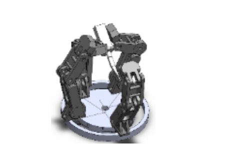	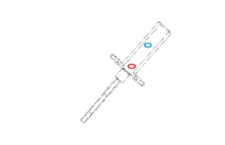	q1 = 40 q2 = 320 q3 = 70 q4 = 160 q5 = 105	q1 = 110 q2 = 340 q3 = 85 q4 = 120 q5 = 150	q1 = 180 q2 = 0 q3 = 75 q4 = 120 q5 = 120	q1 = 270 q2 = 0 q3 = 60 q4 = 90 q5 = 150
TUBE CLAMP	T65		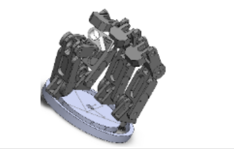	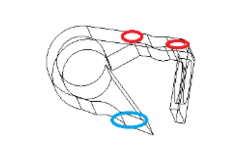	q1 = 45 q2 = 20 q3 = 90 q4 = 140 q5 = 225	q1 = 90 q2 = 345 q3 = 100 q4 = 130 q5 = 210	q1 = 135 q2 = 300 q3 = 75 q4 = 145 q5 = 180	q1 = 220 q2 = 320 q3 = 65 q4 = 185 q5 = 190
SCISSORS	T68	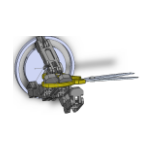	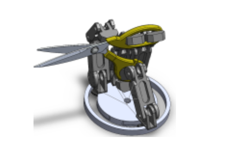	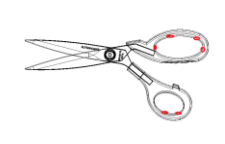	q1 = 55 q2 = 35 q3 = 100 q4 = 120 q5 = 150	q1 = 90 q2 = 0 q3 = 105 q4 = 120 q5 = 150	q1 = 125 q2 = 325 q3 = 65 q4 = 120 q5 = 180	q1 = 280 q2 = 0 q3 = 128 q4 = 220 q5 = 290
SCISSORS	T68_			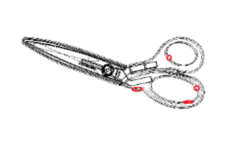	q1 = 30 q2 = 350 q3 = 120 q4 = 110 q5 = 130	q1 = 90 q2 = 310 q3 = 55 q4 = 135 q5 = 120	q1 = 170 q2 = 30 q3 = 65 q4 = 115 q5 = 115	q1 = 215 q2 = 0 q3 = 85 q4 = 130 q5 = 95
RINSE GLASS	T69	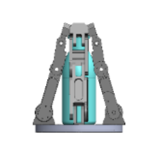	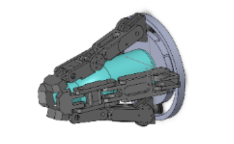	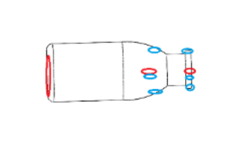	q1 = 0 q2 =0 q3 = 107 q4 = 100 q5 = 108	q1 = 90 q2 =0 q3 = 107 q4 = 100 q5 = 108	q1 = 180 q2 =0 q3 = 107 q4 = 100 q5 = 108	q1 = 270 q2 =0 q3 = 107 q4 = 100 q5 = 108
TUBE	T70	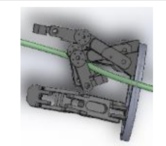		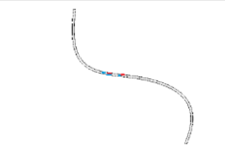	q1 = 45 q2 = 45 q3 = 70 q4 = 90 q5 = 90	q1 = 90 q2 = 0 q3 = 110 q4 = 210 q5 = 300	q1 = 135 q2 = 320 q3 = 90 q4 = 200 q5 = 310	q1 = 325 q2 = 320 q3 = 75 q4 = 120 q5 = 110
CANISTER	C1	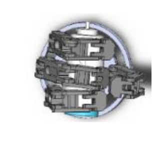	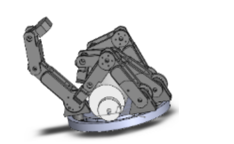	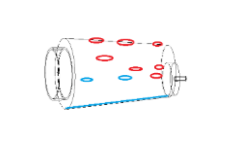	q1 = 45 q2 = 45 q3 = 120 q4 = 225 q5 = 220	q1 = 90 q2 = 0 q3 = 135 q4 = 175 q5 = 250	q1 = 135 q2 = 320 q3 = 110 q4 = 195 q5 = 215	q1 = 270 q2 = 0 q3 = 50 q4 = 90 q5 = 150
TUBE	C2	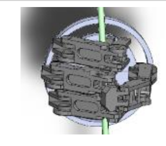	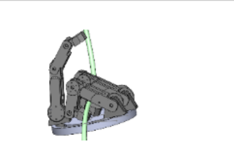	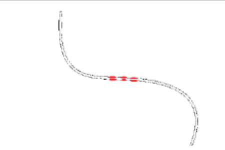	q1 = 52 q2 = 37 q3 = 145 q4 = 250 q5 = 330	q1 = 90 q2 = 0 q3 = 145 q4 = 250 q5 = 330	q1 = 127 q2 = 325 q3 = 145 q4 = 250 q5 = 330	q1 = 270 q2 = 0 q3 = 100 q4 = 130 q5 = 160
PETRI	C6	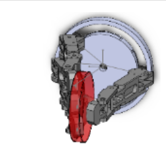	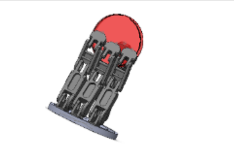	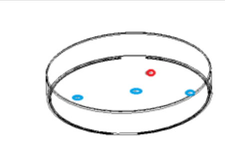	q1 = 52 q2 = 37 q3 = 108 q4 = 90 q5 = 115	q1 = 90 q2 = 0 q3 = 120 q4 = 85 q5 = 120	q1 = 127 q2 = 325 q3 = 115 q4 = 85 q5 = 120	q1 = 260 q2 = 350 q3 = 110 q4 = 96 q5 = 10

Horizon 2020

TraceBOT receives funding from the European Union's H2020-EU.2.1.1. INDUSTRIAL LEADERSHIP programme (grant agreement No 101017089)

KIT	C6	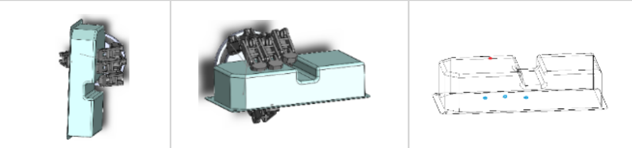	q1 = 52 q2 = 37 q3 = 65 q4 = 130 q5 = 115	q1 = 90 q2 = 0 q3 = 85 q4 = 125 q5 = 120	q1 = 127 q2 = 325 q3 = 75 q4 = 130 q5 = 120	q1 = 260 q2 = 350 q3 = 65 q4 = 115 q5 = 110
CANISTER	C6	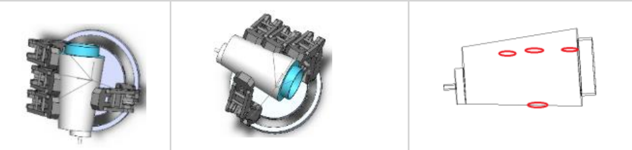	q1 = 52 q2 = 37 q3 = 65 q4 = 130 q5 = 115	q1 = 90 q2 = 0 q3 = 85 q4 = 125 q5 = 120	q1 = 127 q2 = 325 q3 = 75 q4 = 130 q5 = 120	q1 = 260 q2 = 350 q3 = 75 q4 = 125 q5 = 110
TUBE	C6	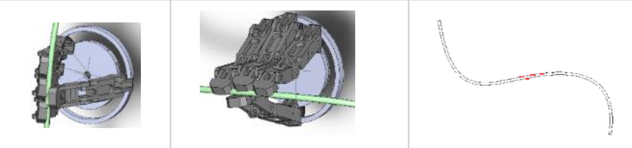	q1 = 52 q2 = 37 q3 = 108 q4 = 90 q5 = 115	q1 = 90 q2 = 0 q3 = 120 q4 = 85 q5 = 120	q1 = 127 q2 = 325 q3 = 115 q4 = 85 q5 = 120	q1 = 260 q2 = 350 q3 = 110 q4 = 120 q5 = 90
RINSE GLASS	C6	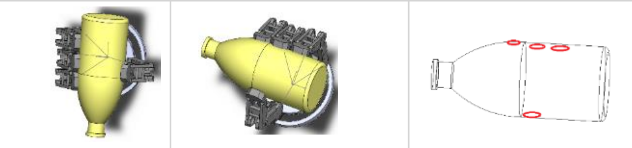	q1 = 52 q2 = 37 q3 = 70 q4 = 130 q5 = 120	q1 = 90 q2 = 0 q3 = 85 q4 = 125 q5 = 120	q1 = 127 q2 = 325 q3 = 75 q4 = 130 q5 = 120	q1 = 260 q2 = 350 q3 = 55 q4 = 125 q5 = 100
KIT	C7	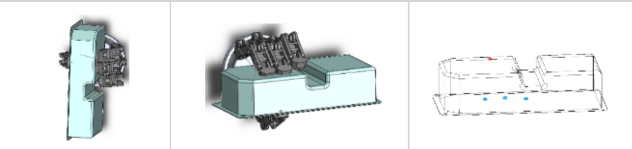	q1 = 52 q2 = 37 q3 = 65 q4 = 130 q5 = 115	q1 = 90 q2 = 0 q3 = 85 q4 = 125 q5 = 120	q1 = 127 q2 = 325 q3 = 75 q4 = 130 q5 = 120	q1 = 260 q2 = 350 q3 = 65 q4 = 115 q5 = 110
TUBE	C7	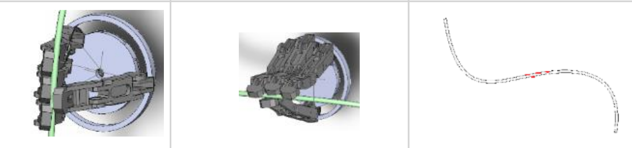	q1 = 52 q2 = 37 q3 = 108 q4 = 90 q5 = 115	q1 = 90 q2 = 0 q3 = 120 q4 = 85 q5 = 120	q1 = 127 q2 = 325 q3 = 115 q4 = 85 q5 = 120	q1 = 260 q2 = 350 q3 = 110 q4 = 120 q5 = 90
PETRI	C8	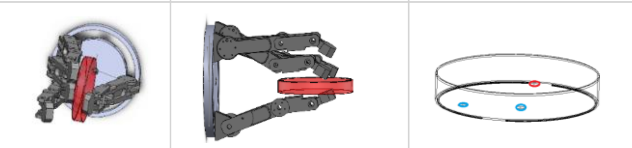	q1 = 52 q2 = 37 q3 = 108 q4 = 90 q5 = 115	q1 = 90 q2 = 0 q3 = 120 q4 = 85 q5 = 120	q1 = 127 q2 = 325 q3 = 85 q4 = 85 q5 = 120	q1 = 260 q2 = 350 q3 = 110 q4 = 96 q5 = 10
MARKER	C8	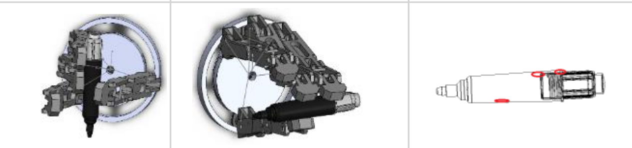	q1 = 52 q2 = 37 q3 = 108 q4 = 90 q5 = 115	q1 = 90 q2 = 0 q3 = 120 q4 = 85 q5 = 120	q1 = 127 q2 = 325 q3 = 85 q4 = 85 q5 = 120	q1 = 260 q2 = 350 q3 = 105 q4 = 96 q5 = 10
KIT	C8	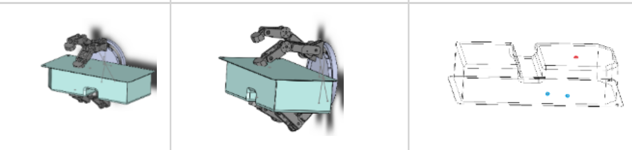	q1 = 52 q2 = 37 q3 = 65 q4 = 130 q5 = 115	q1 = 90 q2 = 0 q3 = 85 q4 = 125 q5 = 120	q1 = 127 q2 = 325 q3 = 55 q4 = 90 q5 = 120	q1 = 260 q2 = 350 q3 = 65 q4 = 115 q5 = 110
CANISTER	C8	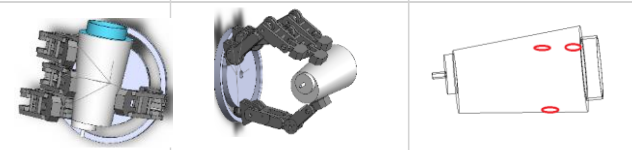	q1 = 52 q2 = 37 q3 = 65 q4 = 130 q5 = 115	q1 = 90 q2 = 0 q3 = 85 q4 = 125 q5 = 120	q1 = 127 q2 = 325 q3 = 55 q4 = 130 q5 = 120	q1 = 260 q2 = 350 q3 = 75 q4 = 125 q5 = 110
TUBE	C8	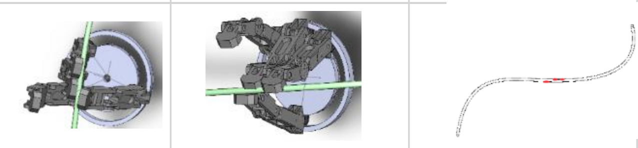	q1 = 52 q2 = 37 q3 = 108 q4 = 90 q5 = 115	q1 = 90 q2 = 0 q3 = 120 q4 = 85 q5 = 120	q1 = 127 q2 = 325 q3 = 65 q4 = 85 q5 = 120	q1 = 260 q2 = 350 q3 = 110 q4 = 120 q5 = 90

Horizon 2020

TraceBOT receives funding from the European Union's H2020-EU.2.1.1. INDUSTRIAL LEADERSHIP programme (grant agreement No 101017089)

NEEDLE	C8	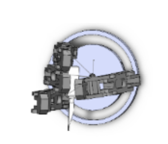	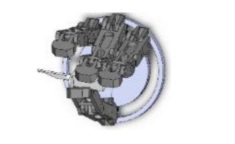	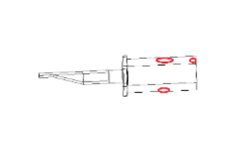	q1 = 52 q2 = 37 q3 = 108 q4 = 90 q5 = 115	q1 = 90 q2 = 0 q3 = 120 q4 = 85 q5 = 120	q1 = 127 q2 = 325 q3 = 85 q4 = 85 q5 = 120	q1 = 260 q2 = 350 q3 = 105 q4 = 125 q5 = 90
SCISSORS	C8	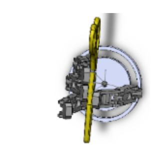	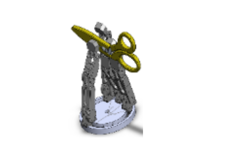	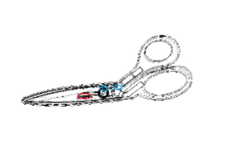	q1 = 52 q2 = 37 q3 = 108 q4 = 90 q5 = 115	q1 = 90 q2 = 0 q3 = 120 q4 = 85 q5 = 120	q1 = 127 q2 = 325 q3 = 85 q4 = 85 q5 = 120	q1 = 260 q2 = 350 q3 = 105 q4 = 125 q5 = 90
KIT	C11	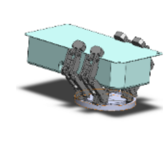	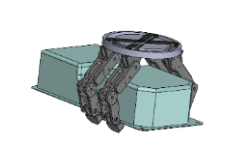	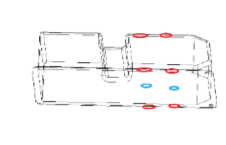	q1 = 60 q2 = 30 q3 = 45 q4 = 110 q5 = 130	q1 = 120 q2 = 330 q3 = 45 q4 = 110 q5 = 130	q1 = 240 q2 = 30 q3 = 45 q4 = 110 q5 = 130	q1 = 300 q2 = 30 q3 = 45 q4 = 110 q5 = 130
PETRI	C12	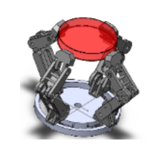	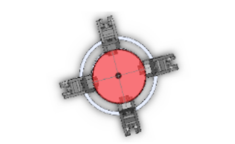	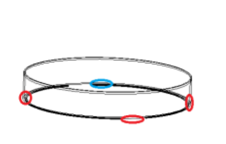	q1 = 0 q2 = 0 q3 = 55 q4 = 140 q5 = 108	q1 = 90 q2 = 0 q3 = 55 q4 = 140 q5 = 108	q1 = 180 q2 = 0 q3 = 55 q4 = 140 q5 = 108	q1 = 270 q2 = 0 q3 = 55 q4 = 140 q5 = 108
RINSE GLASS	C12			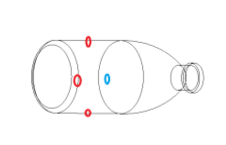	q1 = 0 q2 = 0 q3 = 65 q4 = 140 q5 = 98	q1 = 90 q2 = 0 q3 = 65 q4 = 140 q5 = 98	q1 = 180 q2 = 0 q3 = 65 q4 = 140 q5 = 98	q1 = 270 q2 = 0 q3 = 65 q4 = 140 q5 = 98
NEEDLE CAP	C14			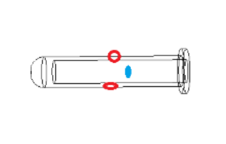	q1 = 310 q2 = 0 q3 = 140 q4 = 120 q5 = 95	q1 = 90 q2 = 300 q3 = 75 q4 = 135 q5 = 98	q1 = 150 q2 = 60 q3 = 68 q4 = 130 q5 = 125	q1 = 230 q2 = 0 q3 = 85 q4 = 130 q5 = 95
MARKER CAP	C16			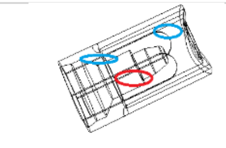	q1 = 45 q2 = 20 q3 = 90 q4 = 140 q5 = 225	q1 = 90 q2 = 345 q3 = 100 q4 = 130 q5 = 210	q1 = 135 q2 = 300 q3 = 75 q4 = 145 q5 = 180	q1 = 0 q2 = 15 q3 = 45 q4 = 140 q5 = 105
TUBE CLAMP	C16	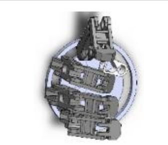	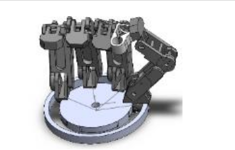	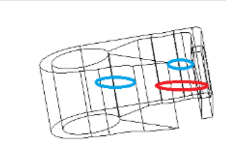	q1 = 45 q2 = 20 q3 = 90 q4 = 140 q5 = 225	q1 = 90 q2 = 345 q3 = 100 q4 = 130 q5 = 210	q1 = 135 q2 = 300 q3 = 75 q4 = 145 q5 = 180	q1 = 0 q2 = 15 q3 = 45 q4 = 140 q5 = 105
SCISSORS	C16		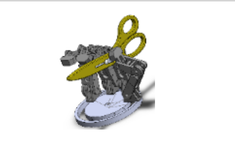	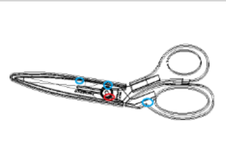	q1 = 45 q2 = 20 q3 = 90 q4 = 140 q5 = 225	q1 = 90 q2 = 345 q3 = 100 q4 = 130 q5 = 210	q1 = 135 q2 = 300 q3 = 75 q4 = 145 q5 = 180	q1 = 0 q2 = 15 q3 = 50 q4 = 160 q5 = 105
TUBE	F17		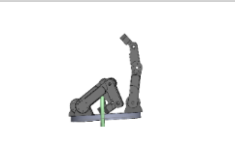		q1 = 52 q2 = 37 q3 = 145 q4 = 250 q5 = 330	q1 = 90 q2 = 0 q3 = 145 q4 = 250 q5 = 330	q1 = 127 q2 = 325 q3 = 145 q4 = 250 q5 = 330	q1 = 270 q2 = 0 q3 = 60 q4 = 90 q5 = 150
MARKER	F26	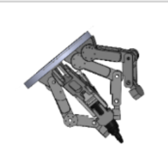		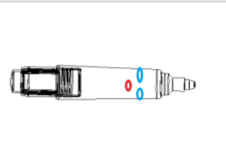	q1 = 310 q2 = 0 q3 = 140 q4 = 120 q5 = 95	q1 = 90 q2 = 300 q3 = 75 q4 = 135 q5 = 98	q1 = 150 q2 = 60 q3 = 60 q4 = 130 q5 = 125	q1 = 230 q2 = 0 q3 = 45 q4 = 130 q5 = 95

Horizon 2020

TraceBOT receives funding from the European Union's H2020-EU.2.1.1. INDUSTRIAL LEADERSHIP programme (grant agreement No 101017089)

TUBE	F26	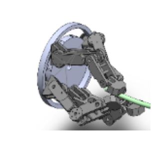	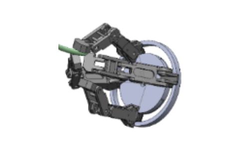		q1 = 340 q2 = 352 q3 = 130 q4 = 110 q5 = 140	q1 = 90 q2 = 310 q3 = 75 q4 = 135 q5 = 105	q1 = 150 q2 = 30 q3 = 65 q4 = 130 q5 = 130	q1 = 230 q2 = 0 q3 = 85 q4 = 130 q5 = 95
RED PLUG	F26		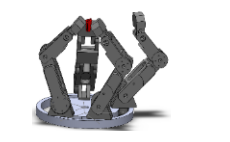	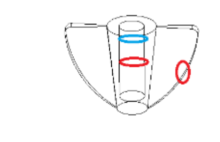	q1 = 310 q2 = 0 q3 = 140 q4 = 120 q5 = 120	q1 = 90 q2 = 300 q3 = 70 q4 = 135 q5 = 130	q1 = 150 q2 = 60 q3 = 60 q4 = 130 q5 = 125	q1 = 230 q2 = 0 q3 = 45 q4 = 130 q5 = 95
PETRI	F28			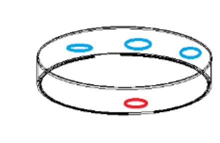	q1 = 45 q2 = 0 q3 = 55 q4 = 140 q5 = 108	q1 = 90 q2 = 0 q3 = 55 q4 = 140 q5 = 108	q1 = 135 q2 = 0 q3 = 55 q4 = 140 q5 = 108	q1 = 270 q2 = 0 q3 = 55 q4 = 140 q5 = 108
MARKER	F28			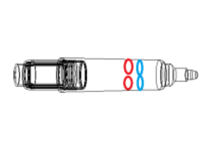	q1 = 0 q2 = 0 q3 = 85 q4 = 140 q5 = 112	q1 = 90 q2 = 0 q3 = 85 q4 = 140 q5 = 112	q1 = 180 q2 = 0 q3 = 85 q4 = 140 q5 = 112	q1 = 270 q2 = 0 q3 = 85 q4 = 140 q5 = 112
KIT	F28	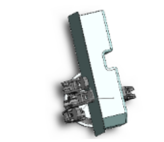	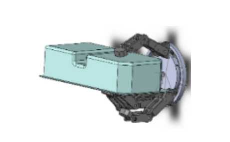	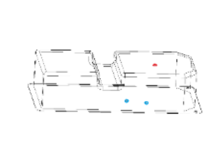	q1 = 52 q2 = 37 q3 = 65 q4 = 130 q5 = 115	q1 = 90 q2 = 0 q3 = 85 q4 = 125 q5 = 120	q1 = 127 q2 = 325 q3 = 55 q4 = 90 q5 = 120	q1 = 260 q2 = 350 q3 = 65 q4 = 115 q5 = 110

7.4 Alternative non human-inspired grasp strategies (for grasps requiring a huge amount of forces unavailable for the robotic gripper)

The proposed grasp alternatives presented in this subsection are hypotheses to perform the tasks described on Table 6.4, for which it is theoretically required to apply more than 20 N to deal with the external perturbations described in section 6. Table 7.3 depicts these alternative grasp patterns.

- Some of these alternative grasps are taken from the existing taxonomy given in Table 7.2:
    - For the "red plug" object, due to its small size, we consider grasp T4.
    - We suggest using the grasp C12 to pierce the Rinse with the needle and for recapping the marker cap (such grasp pattern, that provides four contact points on the object instead of only two contact points when considering T21, should guarantee better resistance against the described perturbations for the needle and marker cap).
- The other grasp patterns described in Table 7.3 are robotic-based grasps, which do not consider the human hand taxonomy. These grasp patterns are enumerated starting by the letter "R".
    - The first one appearing in this table is R24, which is proposed for inserting or removing the canister from its holder. Unlike C1, in R24, one finger exerts pressure on another to increase the amount of applied force over the canister.

Horizon 2020

TraceBOT receives funding from the European Union's H2020-EU.2.1.1. INDUSTRIAL LEADERSHIP programme (grant agreement No 101017089)

- Finally, we proposed the grasp R25 to resist to the perturbation when the other gripper opens the kit. This configuration provides three contact points in the three phalanges of each finger.

It should be mentioned that, in subsection 7.6, a complete list of robotic grasps is presented which are the result of a factorization given to the grasps based on human taxonomy. R24 and R25 are enumerated in this way because the list of robotic grasp patterns starts with the robotic grasps resulting from the factorization then those which are not inspired by the human hand taxonomy are included.

Table 7.3: Alternative grasps patterns for tasks where the amount of force of 20N is exceeded

Object	Original grasp	Alternative grasp	First view of the alternative grasp	Second view of the alternative grasp	Contact points in the object	Joint configuration of the gripper			
Red Plug	T21	T4	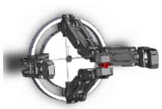	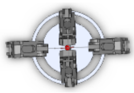	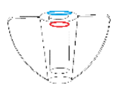	q1 = 0 q2 = 0 q3 = 45 q4 = 95 q5 = 100	q1 = 90 q2 = 0 q3 = 120 q4 = 95 q5 = 100	q1 = 180 q2 = 0 q3 = 45 q4 = 95 q5 = 100	q1 = 270 q2 = 0 q3 = 45 q4 = 95 q5 = 100
Canister	C1	R24	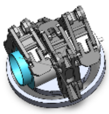	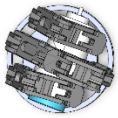	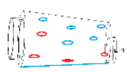	q1 = 52 q2 = 37 q3 = 137 q4 = 210 q5 = 270	q1 = 90 q2 = 0 q3 = 45 q4 = 95 q5 = 98	q1 = 127 q2 = 325 q3 = 115 q4 = 192 q5 = 25	q1 = 270 q2 = 0 q3 = 120 q4 = 200 q5 = 210
Needle	T21	C12	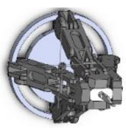	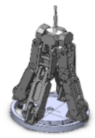	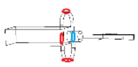	q1 = 0 q2 = 0 q3 = 117 q4 = 95 q5 = 100	q1 = 90 q2 = 0 q3 = 110 q4 = 95 q5 = 100	q1 = 180 q2 = 0 q3 = 117 q4 = 95 q5 = 100	q1 = 270 q2 = 0 q3 = 110 q4 = 95 q5 = 100
Kit	C11	R25	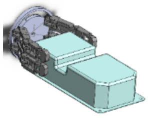	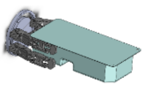	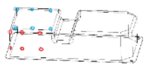	q1 = 70 q2 = 20 q3 = 60 q4 = 90 q5 = 95	q1 = 110 q2 = 340 q3 = 60 q4 = 90 q5 = 98	q1 = 230 q2 = 20 q3 = 80 q4 = 90 q5 = 95	q1 = 300 q2 = 30 q3 = 75 q4 = 90 q5 = 95
Marker Cap	C16	C12		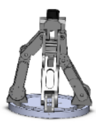	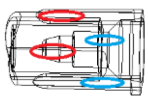	q1 = 0 q2 = 0 q3 = 100 q4 = 130 q5 = 90	q1 = 90 q2 = 0 q3 = 100 q4 = 130 q5 = 90	q1 = 180 q2 = 0 q3 = 100 q4 = 130 q5 = 90	q1 = 270 q2 = 0 q3 = 100 q4 = 130 q5 = 90
Canister	C1	R24	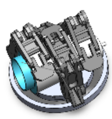	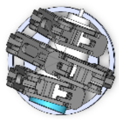	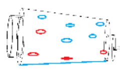	q1 = 52 q2 = 37 q3 = 137 q4 = 210 q5 = 270	q1 = 90 q2 = 0 q3 = 45 q4 = 95 q5 = 98	q1 = 127 q2 = 325 q3 = 115 q4 = 192 q5 = 25	q1 = 270 q2 = 0 q3 = 120 q4 = 200 q5 = 210

Horizon 2020

TraceBOT receives funding from the European Union's H2020-EU.2.1.1. INDUSTRIAL LEADERSHIP programme (grant agreement No 101017089)

7.5 Hypotheses for the final kinematic design of the gripper

The information presented for the angular displacements in Table 7.2 have been reorganized in a graph representation, which is given in Appendix. It gives the distribution of the angular values of all finger joints over all the grasps identified from the use-case. The grasps maps presented in Table 7.2, together with the graphs from the Appendix, provide us information to be used, so as to propose optimized gripper designs. The range of motion of certain joints is reduced in certain cases:

- the angle q_1 values reached by the second finger remain close to 90° in 87 % of all grasps.
- In 53% of the use-case, the angle q_2 value of the second finger is equal to 0°.
- The values q_1 of the fourth finger are comprised between 260° or 270° for more than 50% of all the grasp patterns.

This relevant information is considered in proposing simplified possible kinematics for gripper design in the following, while maintaining the capabilities of the gripper to perform the TraceBot tasks. At this point, we can establish several hypotheses for the kinematic configuration of the final gripper design, by eliminating one or two degrees of freedom from the initial architecture. Considering the angular displacements of Table 7.2, we firstly propose three configurations to compare themselves in terms of reachability to perform the grasp and in their kinematic simplicity. The palm configurations for the three-gripper architecture are summarized below. Each of the proposed kinematic configurations will be validated in replicating several grasp patterns via CAD modeling with the objects involved in the TraceBot use-case.

For the three phalanges of each finger, we established a range of motion resulting from an analysis of the joint positions given in Table 7.2.

7.5.1 Palm configuration 1

We first propose the following configuration for the translation motion around the palm (q_1):

- Finger 1 and 3 with a range of motion from -60° to 60°;
- Finger 4 with a range of motion from -90° to 90°;
- Finger 2 being fixed.

The four fingers have a rotation on their own axis (q_2) with a range of motion from -60° to 60°. Figure 7.3 represents this kinematic configuration of the palm.

Horizon 2020

TraceBOT receives funding from the European Union's H2020-EU.2.1.1. INDUSTRIAL LEADERSHIP programme (grant agreement No 101017089)

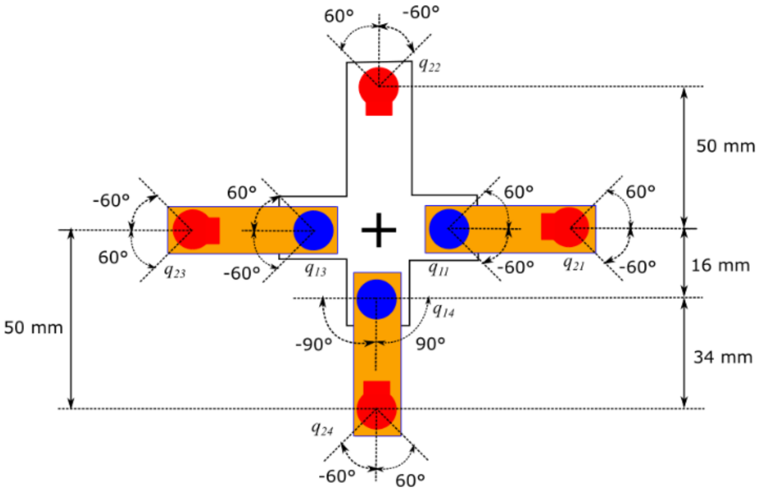

Figure 7.3: Kinematic configuration of the fist hypothesis for the palm.

7.5.2 Palm configuration 2

In this second hypothesis, we propose the following configuration for the translation motion around the palm (q_1):

- Finger 1 and 3 with a range of motion from -90° to 90°.
- Fingers 2 and 4 being fixed.

The four fingers have a rotation on their own axis (q_2) with a range of motion from -60° to 60°. Figure 7.4 represents the kinematic configuration of the second palm. In this configuration, the fingers that do not have rotational motion around the palm are positioned parallel to each other.

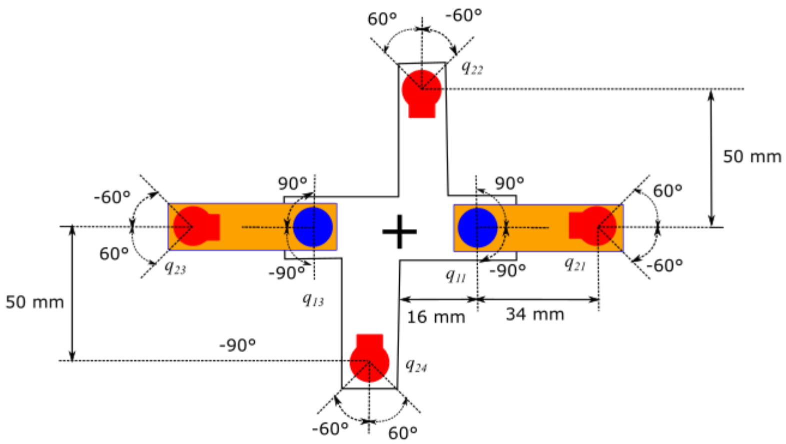

Figure 7.4: Kinematic configuration of the second hypothesis for the palm.

Horizon 2020

TraceBOT receives funding from the European Union's H2020-EU.2.1.1. INDUSTRIAL LEADERSHIP programme (grant agreement No 101017089)

7.5.3 Palm configuration 3

For this final hypothesis, we propose the following configuration for the translation motion around the palm (q_1):

- Finger 1 and 3 with a range of motion from -45° to 45°;
- Fingers 2 and 4 being fixed.

The four fingers have a rotation on their own axis (q_2) with a range of motion from -60° to 60°. Figure 7.5 represents the kinematic configuration of the third palm.

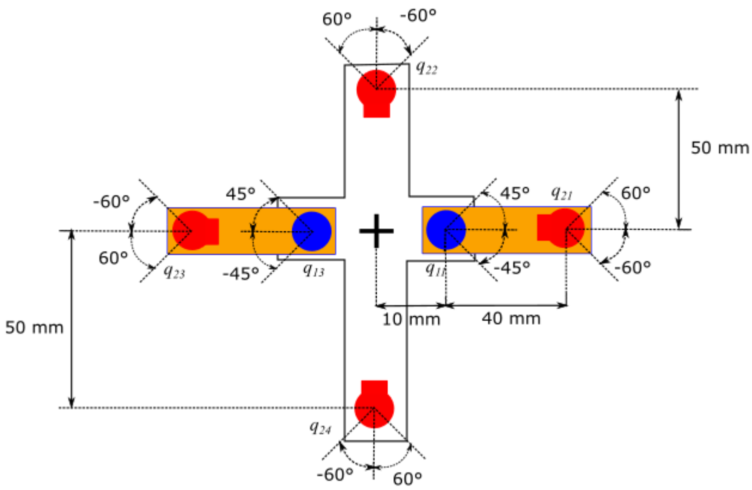

Figure 7.5: Kinematic configuration of the third hypothesis for the palm.

It is worth mentioning that the distances described in Figures 7.3, 7.4, and 7.5 were proposed to keep the diameter of the palm equal to 100mm.

7.5.4 Range of motion of fingers' phalanges

To establish an adequate range of motion for each phalanx, we have analyzed data provided by the joint values distribution provided in Appendix. Keeping the most frequently occurring values of those joint displacements leads to considering the ranges of motion for each phalange joint provided in Table 7.4.

Horizon 2020

TraceBOT receives funding from the European Union's H2020-EU.2.1.1. INDUSTRIAL LEADERSHIP programme (grant agreement No 101017089)

Table 7.4: Ranges of motion for the phalanges by using the information provided in Table 7.2

	Finger 1	Finger 2	Finger 3	Finger 4
Proximal (q_{3i})	65° to 108°	65° to 120°	65° to 115°	45° to 120°
Intermediate (q_{4i})	90° to 150°	85° to 135°	85° to 145°	90° to 185°
Distal (q_{5i})	90° to 225°	98° to 210°	90° to 180°	90° to 180°

Based on the resulting ranges of motion presented in Table 7.4, that do not differ much from one finger to an another one, and taking into account modularity finger design as well as practical mechanical constraints, we have defined the following reasonable ranges of motion for all the four fingers (Figure 7.6):

- Proximal joint (q_{3i}) from 45° to 135°;
- Intermediate joint (q_{4i}) from 90° to 180°;
- Distal joint (q_{5i}) from 90° to 225°.

This range of motion for the phalanges is repeated identically for the three configurations of the palm described beforehand.

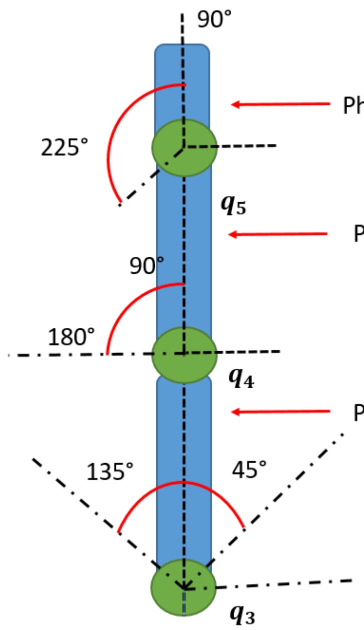

Figure 7.6: Range of motion for the proximal, intermediate and distal phalanges used in the three palm configurations

Horizon 2020
TraceBOT receives funding from the European Union's H2020-EU.2.1.1. INDUSTRIAL LEADERSHIP programme (grant agreement No 101017089)

7.5.5 Gripper workspace analysis

The computation of the workspace volume remains an important step for the gripper design to ensure that the contact areas of interest for all the objects are reachable, so as to be handled by the to-be-designed multifingered gripper. Considering dimensions of the objects involved in the use-case to determine an appropriate volume to grasp the objects. The workspace volume is defined by the fingertip positions in Cartesian space. Its determination relies on the computation of the forward kinematics model of the four fingers, together with their respective range of motion. As an example, the workspace of the gripper defined previously by the third configuration is represented in Figure 7.7.

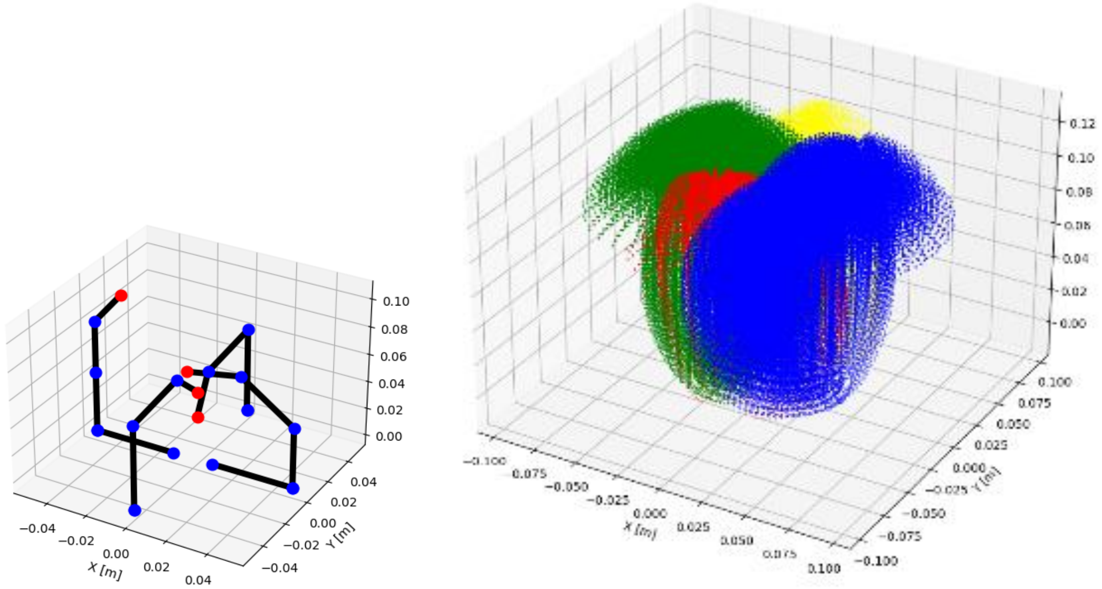

Figure 7.7: Kinematic configuration and workspace resulting from the third configuration (left: kinematic configuration of the fingers, right: resulting workspace).

Figure 7.8 presents additional perspectives of the gripper's workspace. Moreover, by superimposing all objects models involved in the use-case, we can see that all of them are contained in the workspace as illustrated in Figure 7.9. One can see that the maximum Cartesian distance between both pairs of opposite fingertips is about 190 mm. Such distance ensures to safely grasp the most bulky objects presented in the use-case such as the sterility kit, and the Rinse glasses.

Horizon 2020

TraceBOT receives funding from the European Union's H2020-EU.2.1.1. INDUSTRIAL LEADERSHIP programme (grant agreement No 101017089)

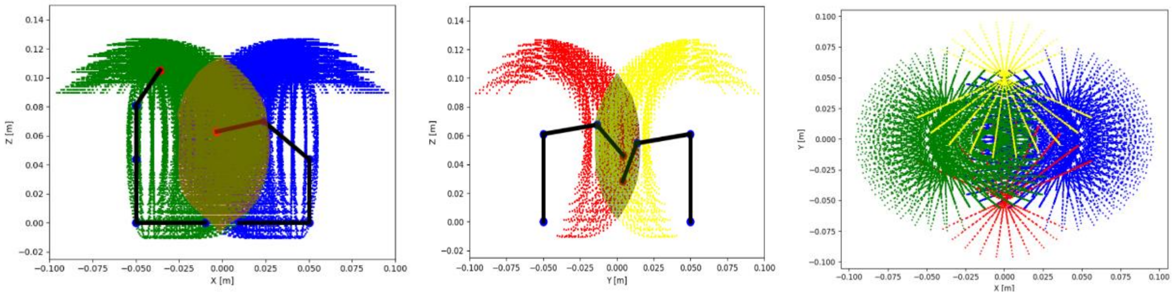

Figure 7.8: Perspectives of the gripper’s workspace.
Top-left xz plane, top-right yz plane, and bottom xy view.

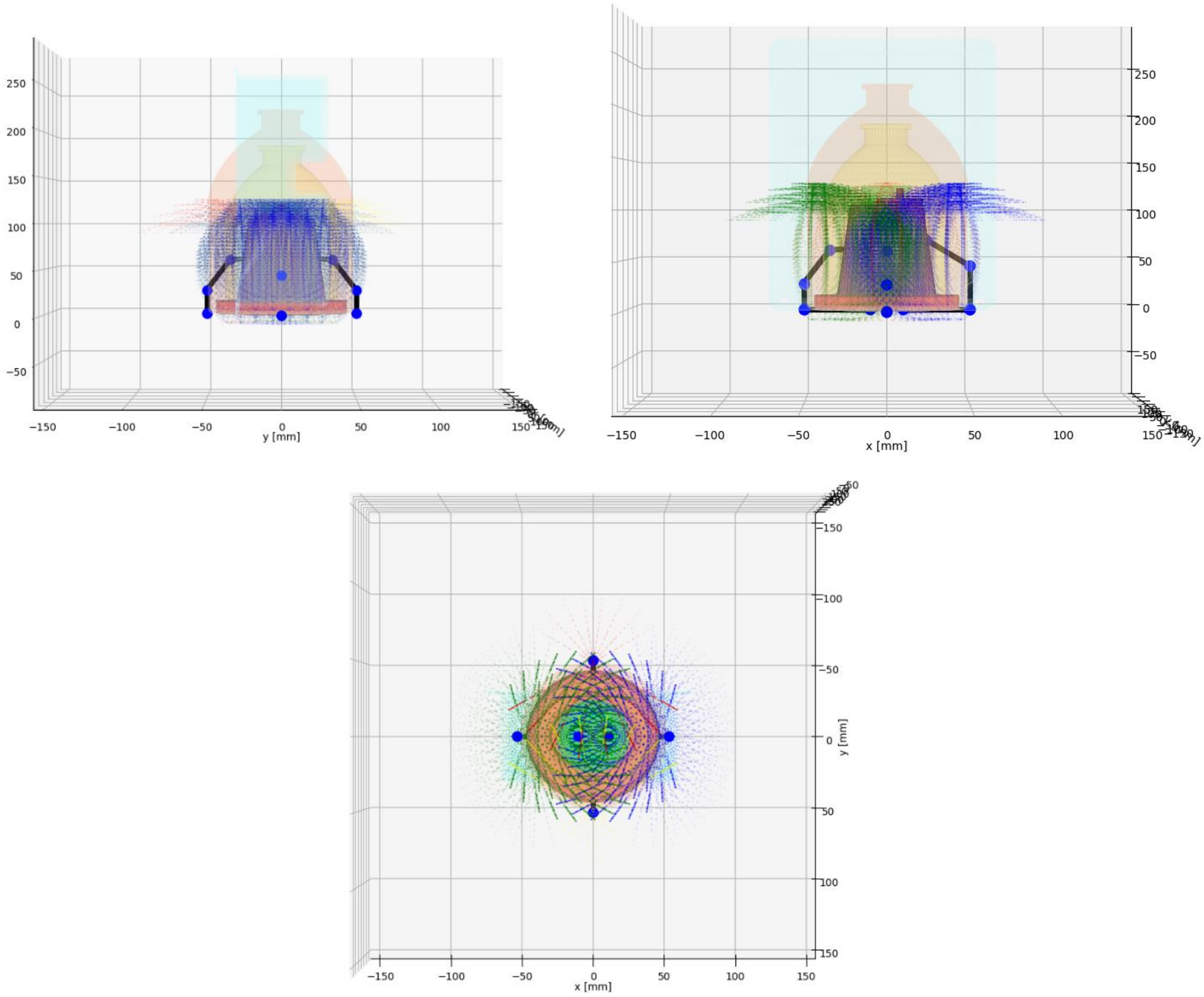

Figure 7.9: Perspectives of the gripper’s workspace including the objects of the use-case.
Top-left xz plane, top-right yz plane, and bottom xy view.

Horizon 2020
TraceBOT receives funding from the European Union's H2020-EU.2.1.1. INDUSTRIAL LEADERSHIP programme (grant agreement No 101017089)

7.6 Factorization of grasp patterns: from human hand to robotic gripper taxonomy

The previous table highlights that certain grasps performed by the gripper are similar to others owing to the absence of the fifth finger, unreachable workspace, or mechanical collisions due to practical design. It results that some of these grasp patterns can be factorized in a new robotic-oriented taxonomy. This aspect will be specifically addressed in the following.

From the pictures presented in Table 7.2, one can note that when mimicking the human grasps with the robotic gripper, some of them are quite similar. Analyzing the position of the fingers and contact points, we can deduce that the 81 grasps may be reduced if we make a factorization due to the following factors:

- Some grasps are the same due to the absence of one finger.
- Unreachable workspace due to the selected dimensions of the phalanges and the palm.
- Mechanical collisions between the fingers.

We thus propose factorizations following a visual analysis of the resulting grasps maps depicted in Tables 7.2 and 7.3. To illustrate some examples, let us consider the schemes presented on Figures 7.10 and 7.11.

If two or more grasp patterns are identical due to the absence of the fifth finger, we can group those grasp patterns to give rise to a new pattern based on the kinematics of the gripper instead of the human hand as is illustrated in Figure 7.10.

On the other hand, if replicating the current human grasp with the four-fingered gripper is not feasible in practice, due to mechanical collisions or unreachable workspace, we can propose similar grasps for which the gripper reaches the same contact zones discarding those regions that could not be reached.

Figure 7.11 illustrates three grasps taken from the human-based taxonomy that are quite similar in terms of patterns: T10, T13, and T16. Restricting the resulting grasps to contact zones only that can be reached by the gripper leads to a new factorization of grasps T10, T13 and T16 into one unique robotic grasp.

Considering these aspects, we conclude that the 81 grasps of the use case together with the alternative ones can be factorized, yielding 25 new robotic grasp patterns presented in Table 7.5.

Horizon 2020

TraceBOT receives funding from the European Union's H2020-EU.2.1.1. INDUSTRIAL LEADERSHIP programme (grant agreement No 101017089)

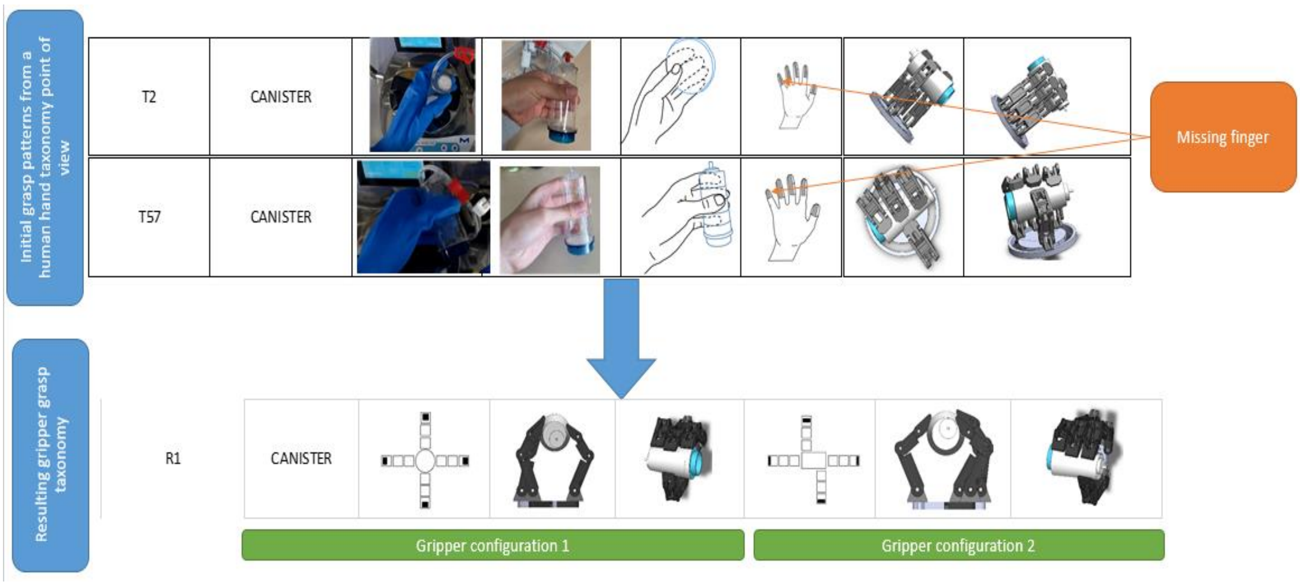

Figure 7.10: Exemplification of a grasp factorization where the fifth finger is missing.

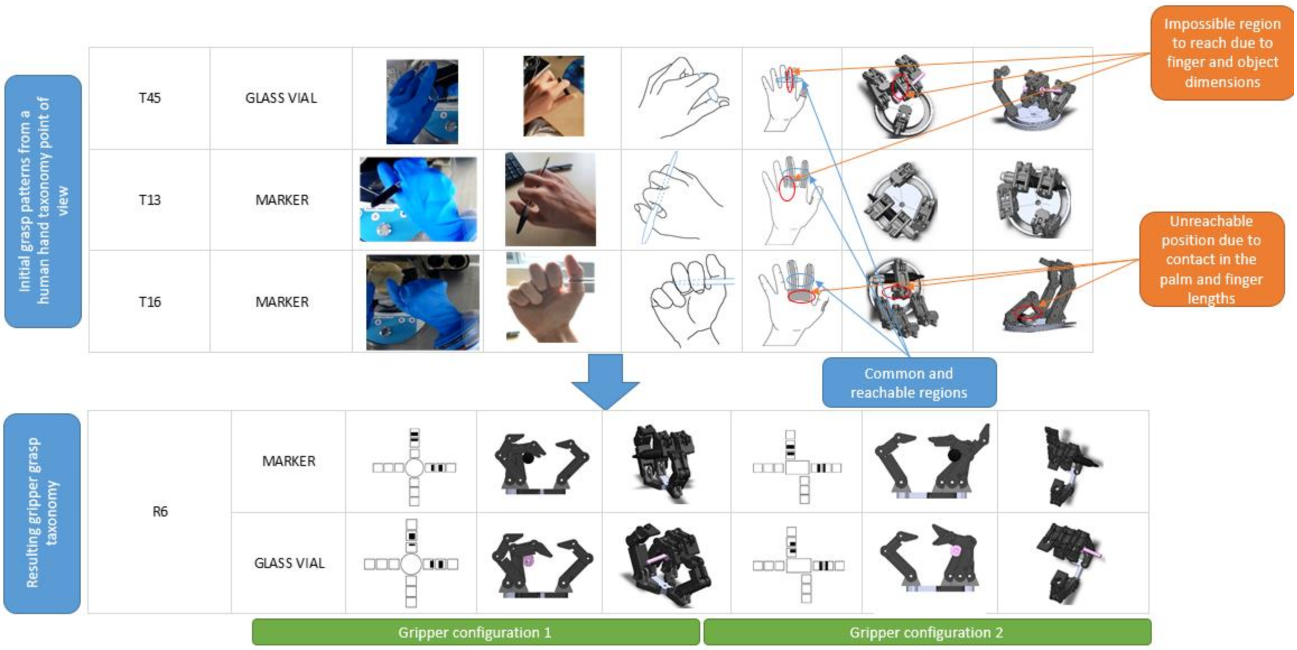

Figure 7.11: Exemplification of a grasp factorization
where mechanical collisions and workspace issues are present.

Horizon 2020
TraceBOT receives funding from the European Union's H2020-EU.2.1.1. INDUSTRIAL LEADERSHIP programme (grant agreement No 101017089)

Table 7.5: Robotic grasp patterns obtained from a factorization of human grasp of the use-case and alternative grasps.

Robotic-oriented grasp reference	Human-based grasp(s) covered by the robotic-oriented grasp reference	Objects of the use-case that are concerned by the grasp
R1	T2, T57	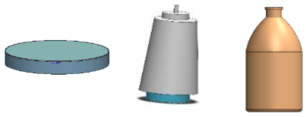
R2	T3	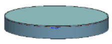
R3	T4	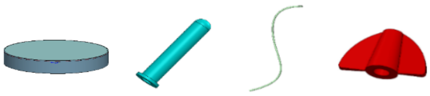
R4	T7, T8	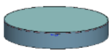
R5	T9	
R6	T10, T13, T16, T45,	
R7	T17, T21, C16, T60, T28, T33, T53	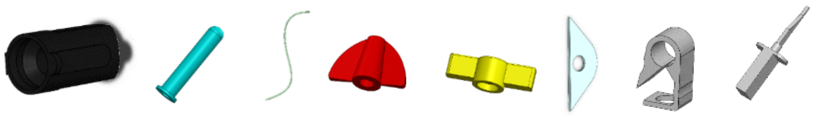
R8	T18	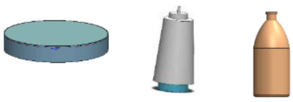
R9	T22	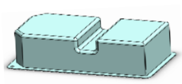
R10	T23, T27	
R11	T24	
R12	T29, T30	

Horizon 2020

TraceBOT receives funding from the European Union's H2020-EU.2.1.1. INDUSTRIAL LEADERSHIP programme (grant agreement No 101017089)

R13	T26, T35, C1, C2, F17	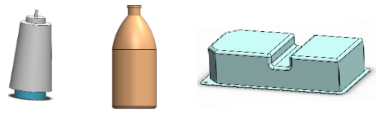
R14	T38	
R15	T39	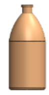
R16	T51	
R17	C6, C7	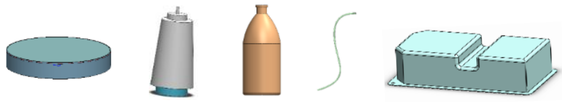
R18	T58	
R19	T68, T68_	
R20	T69, C12	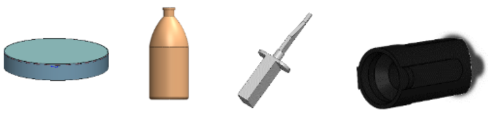
R21	T70	
R22	C8, C14	
R23	F26	
R24	ALTERNATIVE ROBOTIC GRASP 1	
R25	ALTERNATIVE ROBOTIC GRASP 2	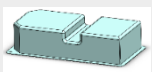

Horizon 2020

TraceBOT receives funding from the European Union's H2020-EU.2.1.1. INDUSTRIAL LEADERSHIP programme (grant agreement No 101017089)

7.7 Replicating grasps for validating the final four-fingered gripper architecture

Having defined the previous robotic grasp taxonomy based on the factorizations of the human-based grasps together with the alternative grasps, the final stage aims to verify if the three possible multi-fingered gripper architectures introduced previously in subsection 7.5 are well suited for replicating each grasp proposed in this taxonomy.

The resulting grasp maps using robotic-based taxonomy for each of the three gripper architectures are presented in Table 7.6. For the three alternatives, contact maps are also provided to indicate the contact areas of interests to select the appropriate placement for the integration of the tactile sensors in the phalanges and palm of the to-be-designed gripper.

A visual analysis of the robotic grasps presented in Table 7.6 proves that the three proposed architectures are able to replicate the 25 grasp patterns. Nevertheless, visual inspection tends to highlight the fact that some specific grasps are more stable for one particular architecture rather than another. For instance, grasp R25 is performed better with the second configuration due to the placement of the fixed parallel fingers. When performed by the first and third configurations, it is less stable because a finger makes contact with the edges and not with flat surfaces. On the other hand, some grasps, for example those related to R20, seem more stable with the first and third kinematic configurations than with the second one.

On the basis of all these particular points, the configuration chosen for further work is based on the third architecture. This configuration presents a reduced number of actuated degrees of freedom (compared to the other architectures), without limiting its grasping capabilities (all objects being graspable according to the taxonomy's grasp patterns). Thus, it brings a compromise between grasping capabilities and design complexity.

Horizon 2020

TraceBOT receives funding from the European Union's H2020-EU.2.1.1. INDUSTRIAL LEADERSHIP programme (grant agreement No 101017089)

Table 7.6: List of all mappings between object and factorized gripper grasps involved in the use-case

GRASP NUMBER	OBJECT	KINEMATIC CONFIGURATION 1			KINEMATIC CONFIGURATION 2			KINEMATIC CONFIGURATION 3		
		INTERACTION MAP	OBJECT GRASPING BY GRIPPER FIRST VIEW	OBJECT GRASPING BY GRIPPER SECOND	INTERACTION MAP	OBJECT GRASPING BY GRIPPER FIRST VIEW	OBJECT GRASPING BY GRIPPER SECOND VIEW	INTERACTION MAP	OBJECT GRASPING BY GRIPPER FIRST VIEW	OBJECT GRASPING BY GRIPPER SECOND VIEW
R1	CANISTER									
	PETRI									
	RINSE									
R2	PETRI									
R3	PETRI									
	NEEDLE CAP									
	TUBE	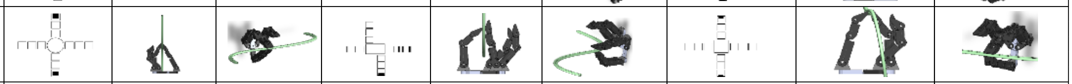								
	RED PLUG									
R4	PETRI	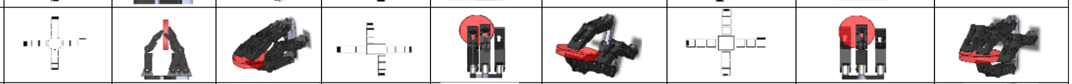								
R5	MARKER									
R6	MARKER									
	GLASS VIAL									
R7	MARKER CAP	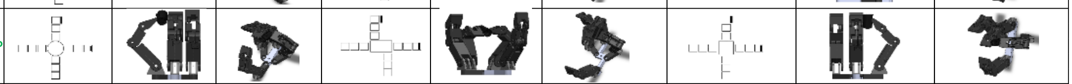								
	TUBE	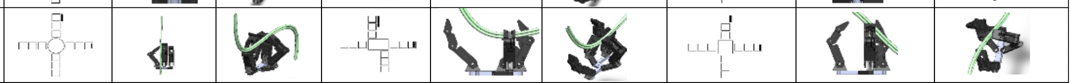								
	NEEDLE	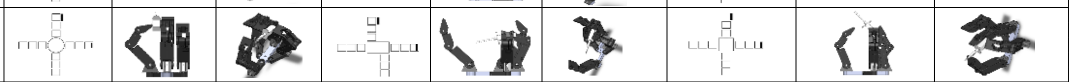								
	RED PLUG									
	YELLOW PLUG									
	KIT TAB									
	TUBE CLAMP									
	NEEDLE CAP									

Horizon 2020

TraceBOT receives funding from the European Union's H2020-EU.2.1.1. INDUSTRIAL LEADERSHIP programme (grant agreement No 101017089)

R8	PETRI
	MARKER
	CANISTER
	RINSE
R9	KIT
R10	TUBE
R11	TUBE
R12	TUBE
R13	CANISTER
	RINSE
	KIT
R14	RINSE
R15	RINSE
R16	RINSE
R17	PETRI
	CANISTER
	RINSE
	KIT
	TUBE
R18	RINSE
R19	SICCORS

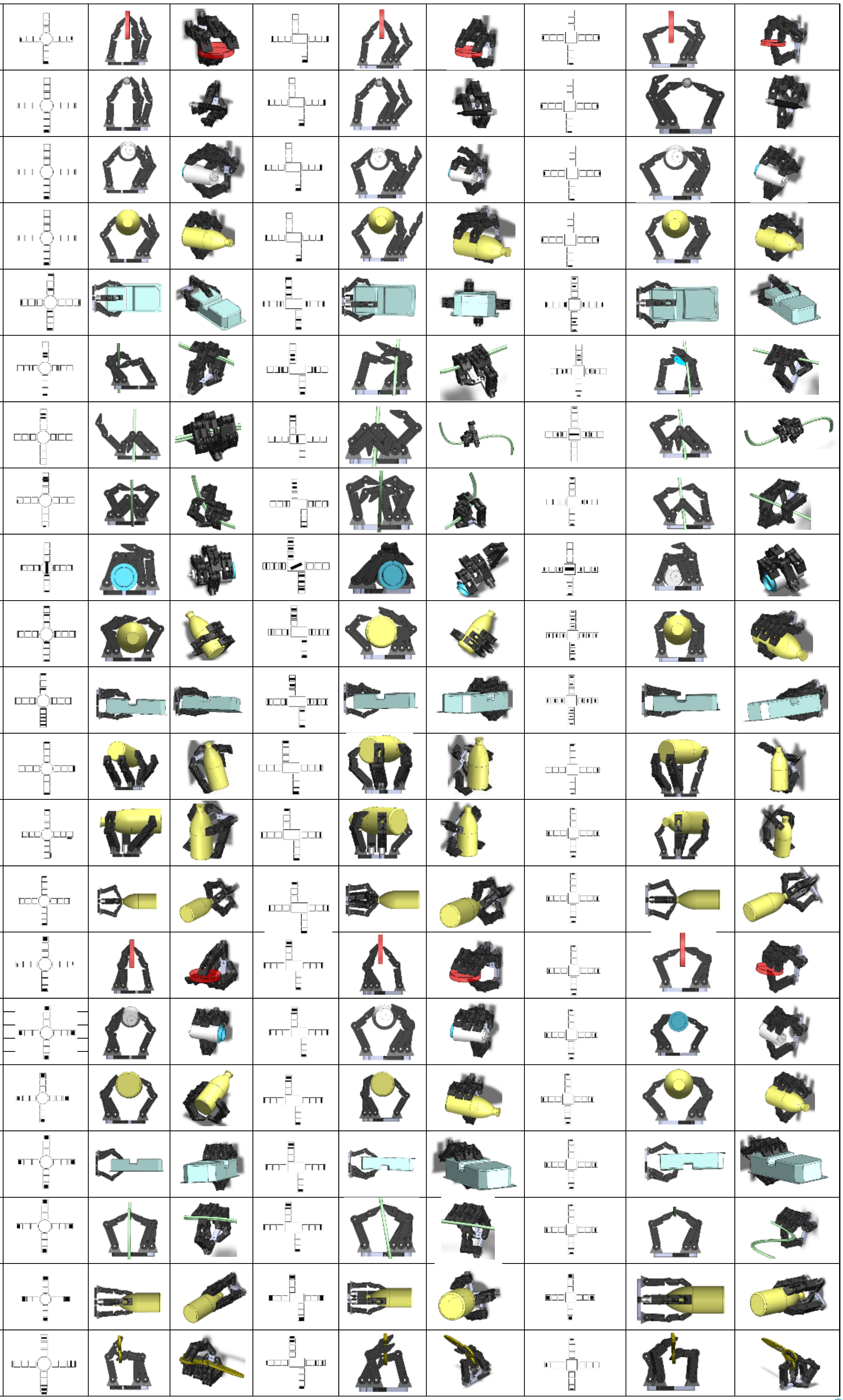

Horizon 2020

TraceBOT receives funding from the European Union's H2020-EU.2.1.1. INDUSTRIAL LEADERSHIP programme (grant agreement No 101017089)

R20	PETRI
	RINSE
	NEEDLE
	MARKER CAP
R21	TUBE
R22	PETRI
	NEEDLE CAP
	NEEDLE
	TUBE
	CANISTER
	KIT
	MARKER
	SCISSORS
R23	RED PLUG
	MARKER
R24	CANISTER
R25	KIT

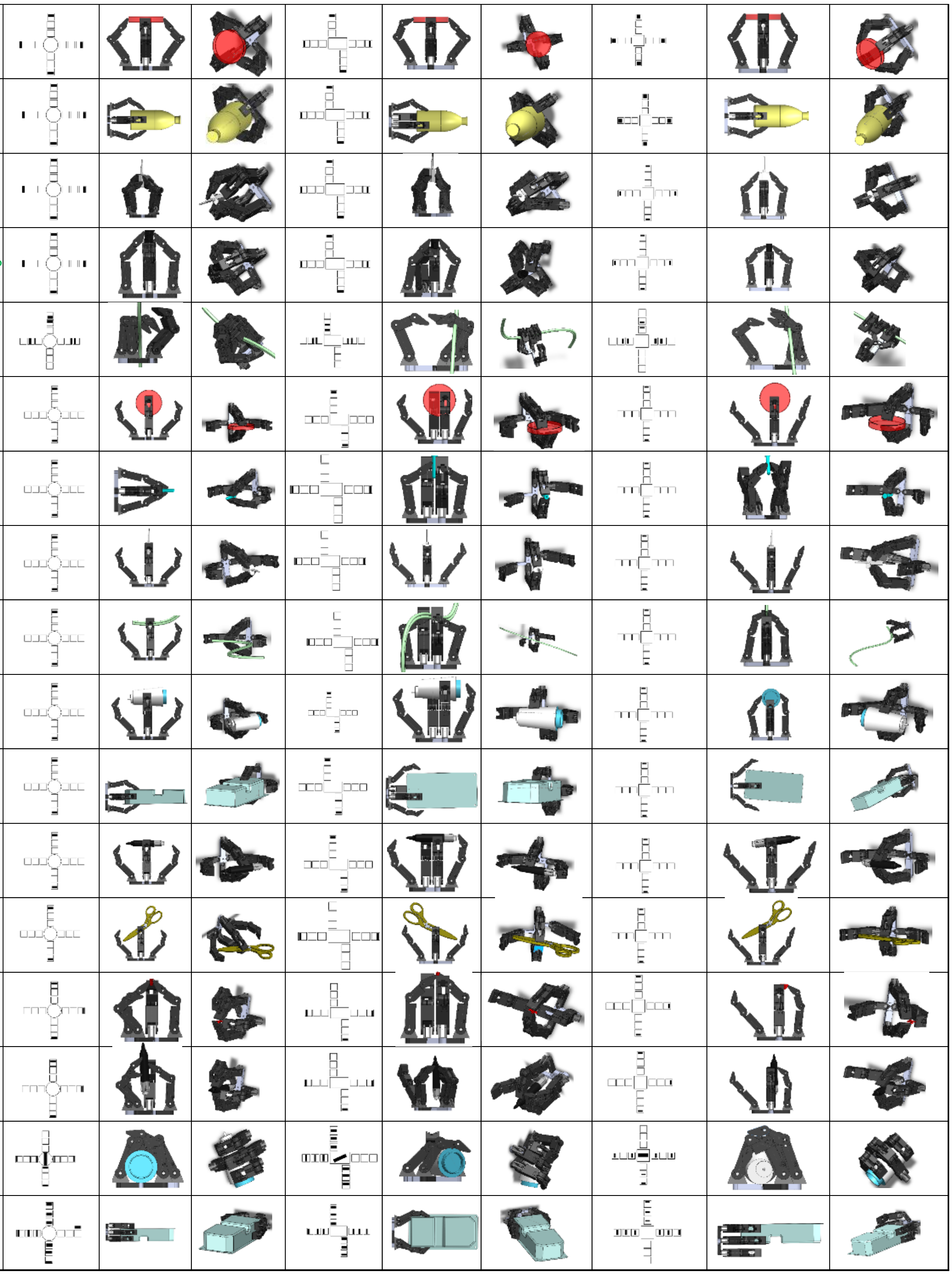

Horizon 2020

TraceBOT receives funding from the European Union's H2020-EU.2.1.1. INDUSTRIAL LEADERSHIP programme (grant agreement No 101017089)

8 Conclusion

The recommendations for the design of the multi-fingered robotic gripper presented in this deliverable result from an exhaustive study, starting from a gesture analysis of human handling the objects from the TraceBot sterility test process, up to proposing a gripper kinematic architecture capable to replicate the grasps involved in the TraceBot use-case. The technical specifications for the gripper design have been made following a multi-step procedure (including human-centered gesture analysis, force grasp stability analysis, and CAD-based kinematic design).

The human-centered gesture analysis starts with a thorough examination of the use-case videos. The human grasps involved in the sterility test process were classified in function of different taxonomies proposed by Cutkosky, Feix, and CEA for TraceBot use-case. Through the videos, at CEA we have identified 80 new grasp patterns not described in the existing literature. Each grasp is related to a hand-object contact area map providing useful information on the most used zones of the human hands, intending to generate interaction maps resulting by superimposing the contact areas. Moreover, the videos allow us to know how frequently each grasp is used in the whole sterility test process. A key point in this analysis based on the human hand is the calculation of efforts and their directions applied to each object. The applied efforts are considered as external disturbances, that the future gripper must be able to counteract. The first step is concluded with the generation of interaction maps (in *x, y* and *z* directions), which are the result of associating the inner contact surface of a given grasp pattern in a specified direction with their frequency of use. Looking at the interaction maps, one appreciates that the most requested direction is along the z-axis, which means normal to the skin.

The gesture analysis of the human hands provided input data such as human-hand grasp taxonomies, external efforts measurements, and their directions, that are useful for the force-based grasp stability analysis. In this analysis, all objects involved in the use-case were reconstructed in CAD modeling for numerical computations. Each pair of objects and grasps taken from the described human-hand taxonomies has been associated with some external force perturbations that may result from the weight of the object itself, and from task-oriented actions such as inserting, piercing, etc. Then, by relying on grasp quality metric tools, we have estimated the required theoretical amount of force to be applied by the gripper to counterbalance the external perturbations. A force threshold value of 20 N has been considered as an upper bound for the reachable amount of force that the future gripper may provide. From the considered set of tasks, this analysis concluded that few of them exceed the value of 20N, for which alternative non-human based grasps have been proposed so as to minimize the level of efforts at stake. Additionally, this analysis has allowed us to investigate the influence of

Horizon 2020

TraceBOT receives funding from the European Union's H2020-EU.2.1.1. INDUSTRIAL LEADERSHIP programme (grant agreement No 101017089)

certain kinematics related parameters (i.e. number of fingers, number of contact points) on the level of efforts. When considering four-fingered grasps, the obtained results demonstrate a reasonable increase between 0% and 15% of the required efforts to perform the tasks. Thanks to these results, a gripper formed by four fingers has been then considered as a potentially adequate solution to deal with the tasks involved in the TraceBot use-case.

Finally, a preliminary gripper kinematic architecture with 20 DoFs has been proposed to replicate the human-hand grasps described in section 6 using CAD software. This study resulted on the one hand in the creation of a new robotic grasp taxonomy, and on the other hand in the proposal of simpler kinematic architectures for the final gripper design. The quantitative data based on the joint positions of the preliminary gripper allowed us to reduce the number of degrees of freedom, and to establish an appropriate range of motion for the joints. Three kinematic architectures for the gripper have been investigated and validated by mapping the new robotic-based grasp patterns, concluding that the three architectures are able to map these grasp patterns.

Thus, our technical recommendation for the future gripper configuration is summarized in the following table.

Horizon 2020

TraceBOT receives funding from the European Union's H2020-EU.2.1.1. INDUSTRIAL LEADERSHIP programme (grant agreement No 101017089)

Required grasp types	• Precision grasp • Intermediate grasp • Power grasp • Non prehensile grasp
Controllable normal force component to be applied at each fingertip through joint actuation system	20 N
Number of controlled Cartesian DoFs per fingertip	3 DoFs on each fingertip (x,y,z) axes
Number of DoFs per gripper	Expecting 18 DoFs
Kinematic configuration of the gripper (third configuration selected)	Kinematics of the DoFs involved in the palm • Rotational motion around the palm (q_{1i}) performed by two fingers located in opposite side, whose range of motion vary form -45° to 45° • Rotational motion around the z_i-axis of all fingers (q_{2i}), whose range of motion vary form -60° to 60° Kinematics of the DoFs involved in the phalanges • Proximal phalange joint q_{3i} range of motion from 45° to 135° • Intermediate phalange joint q_{4i} range of motion from 90° to 180° • Distal phalange joint q_{5i} range of motion from 90° to 225°
Dimensions of the palm	Circular palm with 100 mm of diameter 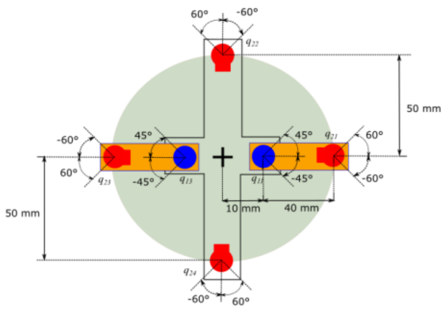
Dimensions of the phalanges of each finger	• Proximal phalange: 62 mm • Intermediate phalange: 37 mm • Distal phalange: 28 mm • Width of each phalange: 27 mm 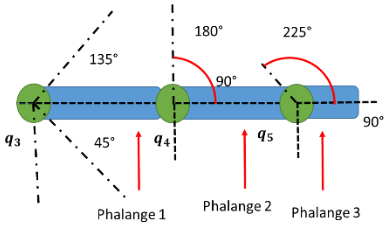
Cartesian distance between both pairs of opposite fingertips	196 mm
Weight	Be compatible with the payload of the robot arm (UR10), including the weight of the handled object
Location map to place the tactile sensors	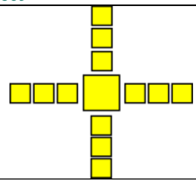
Possible CAD representation of the gripper's kinematics	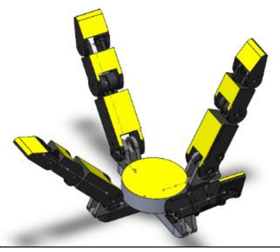

Horizon 2020

TraceBOT receives funding from the European Union's H2020-EU.2.1.1. INDUSTRIAL LEADERSHIP programme (grant agreement No 101017089)

9 Appendix

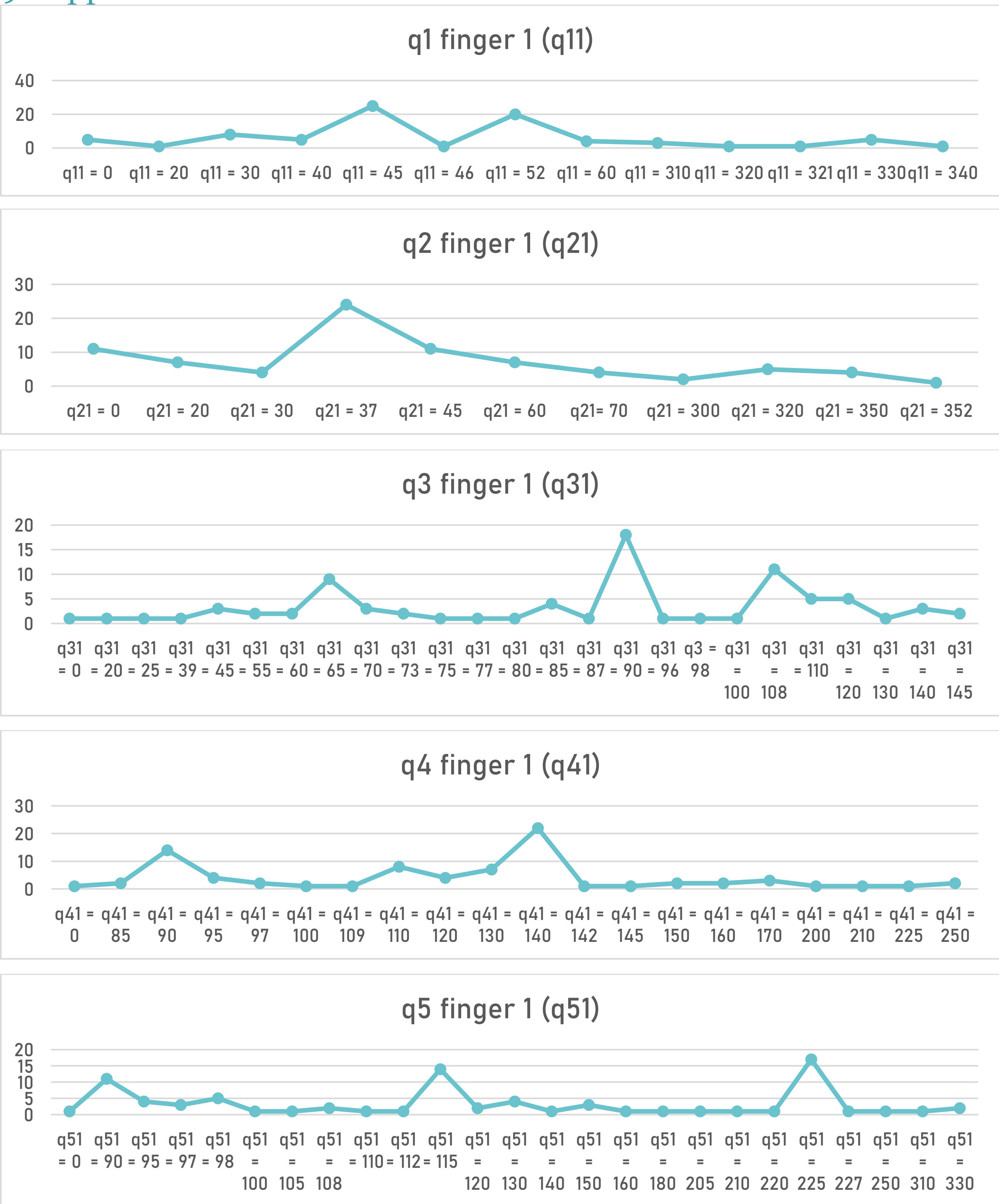

Figure A.1: Graphs of the joint positions of finger 1
used to map the 81 grasp patterns of the use-case.

Horizon 2020

TraceBOT receives funding from the European Union's H2020-EU.2.1.1. INDUSTRIAL LEADERSHIP programme (grant agreement No 101017089)

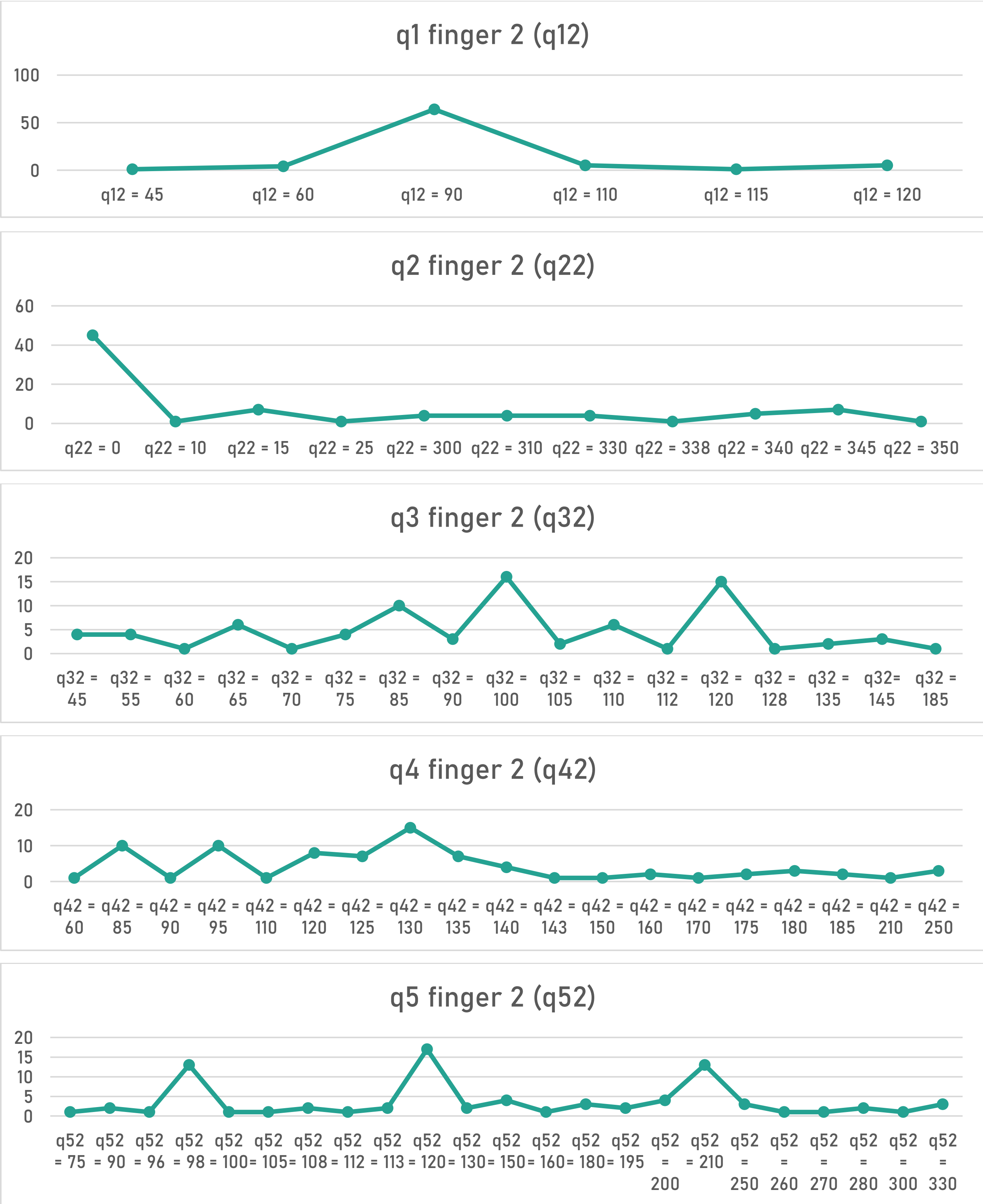

Figure A.2: Graphs of the joint positions of finger 2
used to map the 81 grasp patterns of the use-case.

Horizon 2020

TraceBOT receives funding from the European Union's H2020-EU.2.1.1. INDUSTRIAL LEADERSHIP programme (grant agreement No 101017089)

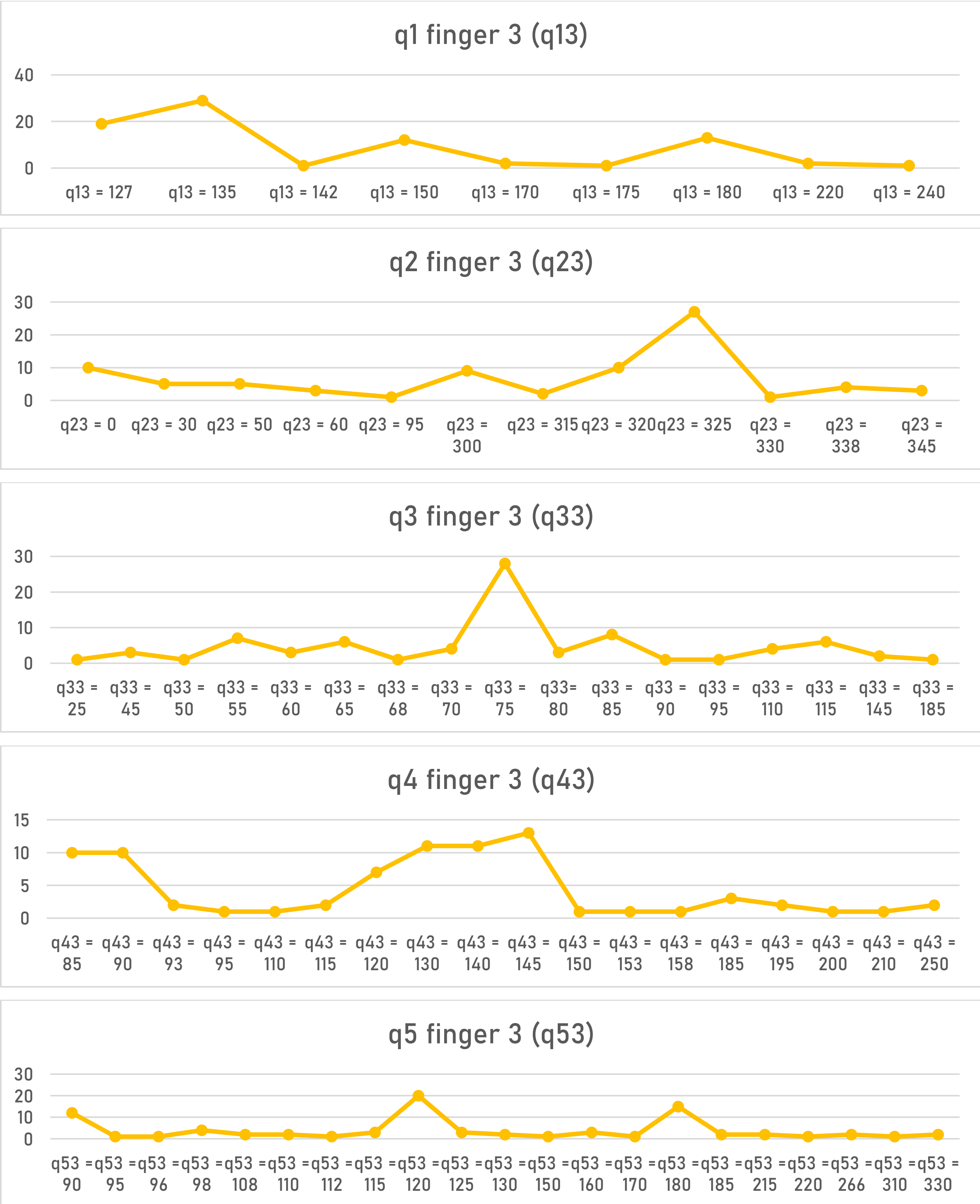

Figure A.3: Graphs of the joint positions of finger 3
used to map the 81 grasp patterns of the use-case.

Horizon 2020

TraceBOT receives funding from the European Union's H2020-EU.2.1.1. INDUSTRIAL LEADERSHIP programme (grant agreement No 101017089)

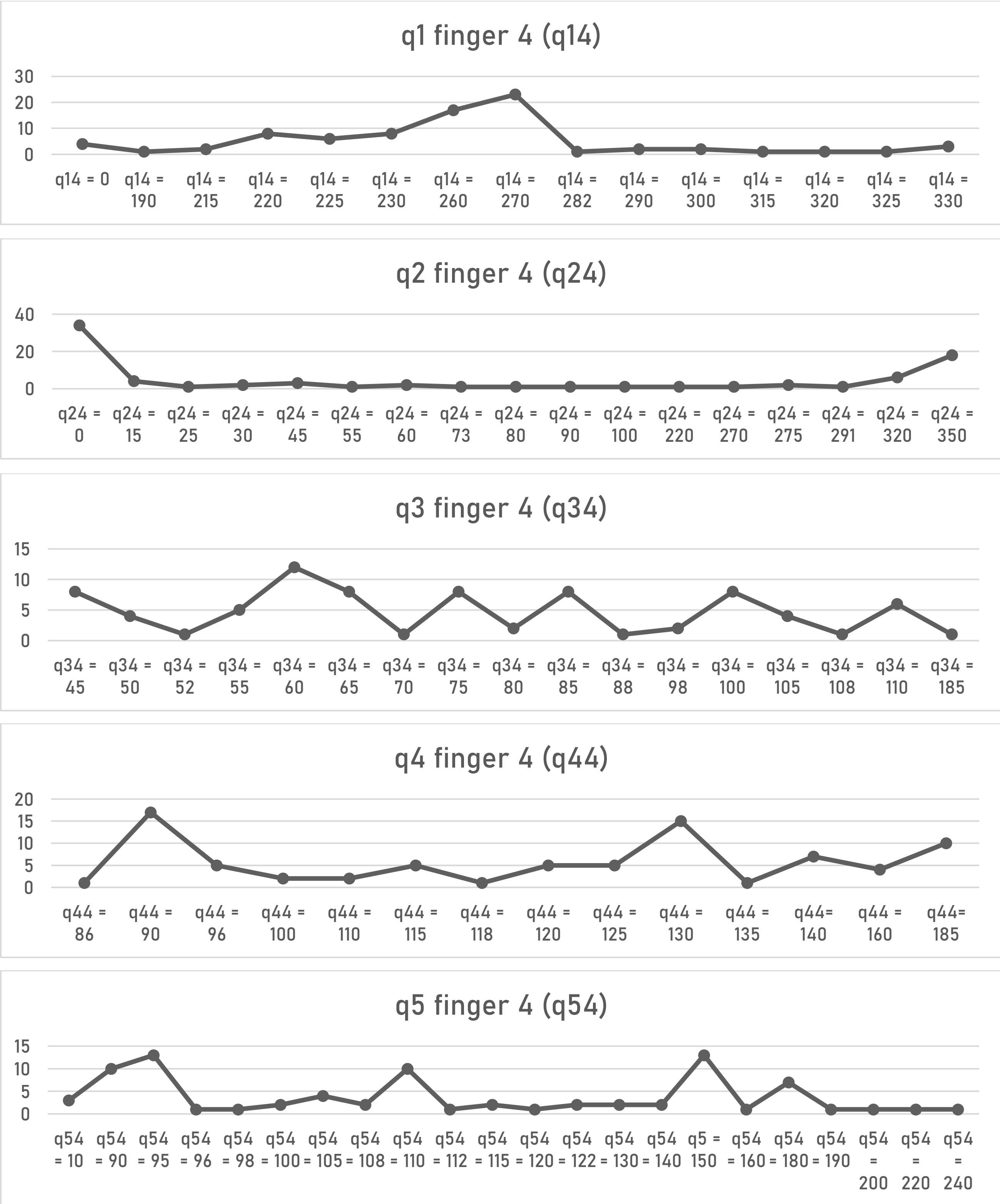

Figure A.4: Graphs of the joint positions of finger 4
used to map the 81 grasp patterns of the use-case.

Horizon 2020

TraceBOT receives funding from the European Union's H2020-EU.2.1.1. INDUSTRIAL LEADERSHIP programme (grant agreement No 101017089)

10 References

[Chabrier et al. 2015] A. Chabrier, F. Gonzalez, F. Gosselin, W. Bachta, 'Analysis of the Directions in which Forces are Applied on the Hand During Manual Manipulation and Exploration', Proc. IEEE World Haptics Conf., 2015, pp. 280-285.

[Cutkosky 1989] M. Cutkosky, 'On grasp choice, grasp models, and the design of hands for manufacturing tasks', IEEE Trans. on Robotics and Automation, 5(3), 1989, pp. 269–279.

[ElKoura et al. 2003] ElKoura, G., Singh, K. 'Handrix: animating the human hand'. In Proceedings of the 2003 ACM SIGGRAPH/Eurographics symposium on Computer animation, 2003, pp. 110-119.

[Feix et al. 2009] T. Feix, R. Pawlik, H. Schmiedmayer, X. Romero, D. Kragic, 'A comprehensive grasp taxonomy', Proc. Robotics, Science and Systems Conf., Workshop Understanding Human Hand Adv. Robot. Manipulation, 2009, available at grasp.xief.net.

[Gonzalez et al. 2013] F. Gonzalez, F. Gosselin, W. Bachta, 'A Framework for the Classification of Dexterous Haptic Interfaces Based on the Identification of the Most Frequently Used Hand Contact Areas', Proc. IEEE World Haptics Conf., 2013, pp. 461-466.

[Gonzalez et al. 2014] F. Gonzalez, F. Gosselin, W. Bachta, 'Analysis of Hand Contact Areas and Interaction Capabilities During Manipulation and Exploration', IEEE Trans. on Haptics, 7(4), 2014, pp. 415-429.

[Jones and Lederman 2006] L. Jones, S. Lederman, 'Human Hand Function', Oxford Univ. Press, 2006.

[Lederman and Klatzky 2009] S. Lederman, R. Klatzky, 'Haptic perception: A tutorial', Attention, Percept. Psychophys., 71(7), 2009, pp. 1439–1459.

[Prattichizzo et al. 2008]. D. Prattichizzo, J. C. Trinkle, 'Grasping. In Springer Handbook of Robotics', Springer Berlin Heidelberg, 2008, pp. 671-700.

[Zheng et al. 2011] J. Zheng, S. De La Rosa, A. Dollar, 'An investigation of grasp type and frequency in daily household and machine shop tasks', Proc. IEEE Int. Conf. on Robotics and Automation, 2011, pp. 4169–4175.

Horizon 2020

TraceBOT receives funding from the European Union's H2020-EU.2.1.1. INDUSTRIAL LEADERSHIP programme (grant agreement No 101017089)